Electronic Supplementary Information

"Clicking" trimeric peptides onto hybrid T_8POSS nanocages and identifying synthesis limitations

Lewis R. Anderson,[a,e] Ann P. Hunter,[b] Matthew Kershaw,[c] Sergey Y. Bylikin,[c] James Bowen,[d] Peter G. Taylor,[c] Martin A. Birchall,[a] and Nazia Mehrban*[e]

[a.] *University College London - Ear Institute, 332 Grays Inn Rd, London WC1X 8EE, UK*
[b.] *National Mass Spectroscopy Facility (NMSF), Swansea University Medical School, Singleton Park, Swansea, SA2 8PP, UK*
[c.] *The Open University, School of Life, Health & Chemical Sciences, Walton Hall, Kents Hill, Milton Keynes MK7 6AA, UK*
[d.] *The Open University, School of Engineering & Innovation, Walton Hall, Kents Hill, Milton Keynes MK7 6AA, UK*
[e.] *University of Bath, Department of Life Sciences, Claverton Down, Bath BA2 7AX, UK*

Contents

1. Synthesis of triglycine methyl ester hydrochloride (1a) - (Figures S1-S4)

yield: 81% , Analysis Calculated for $C_7H_{13}N_3O$: C, 41.38; N, 20.68, Found C, 41.02; N, 20.46.

NMR: The full ^1H and ^{13}C NMR spectra of the esterified triglycine compound (**1a**) are displayed in **Figures S1** and **S2**, respectively.

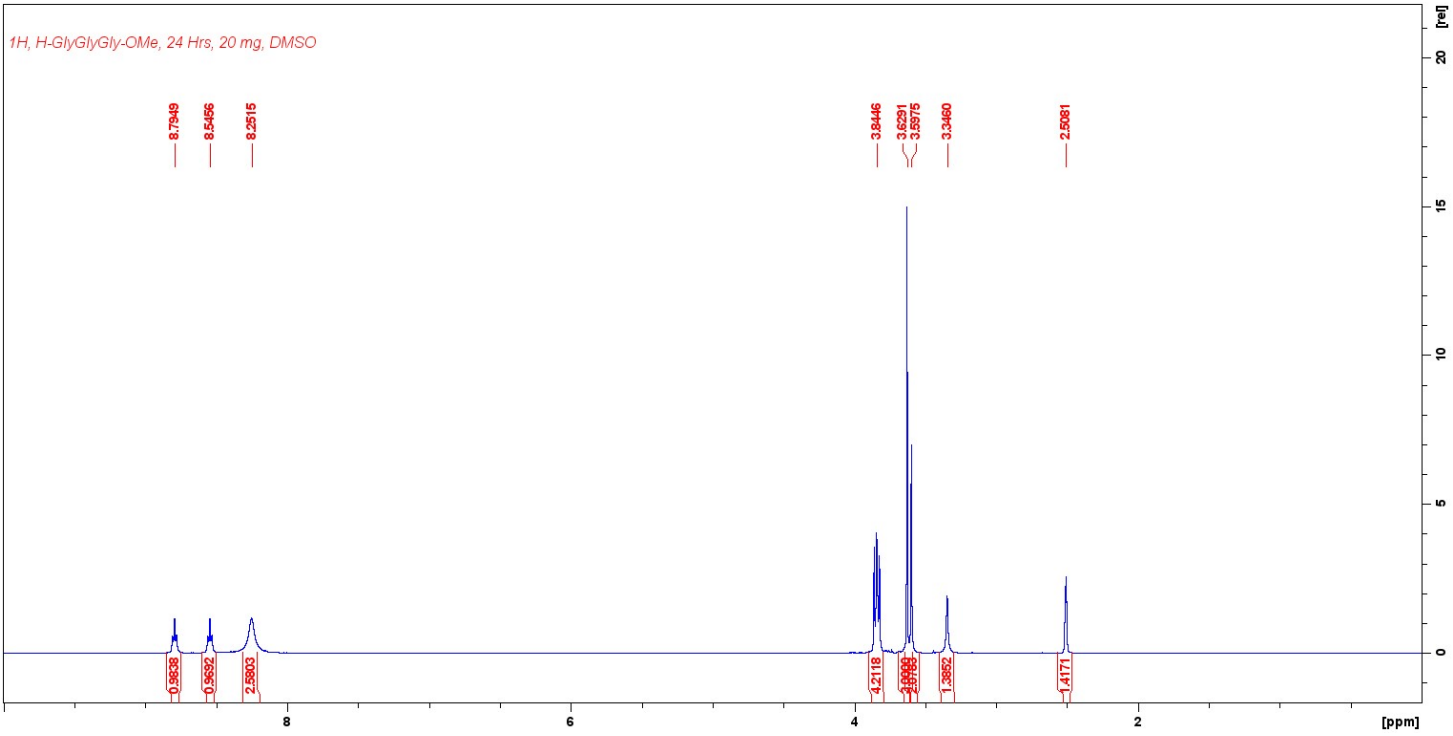

Figure S1 – ^1H NMR of triglycine methyl ester (**1a**). ^1H NMR (400 MHz, DMSO-d^6, δ, ppm): 8.79 (t, 1 H, R-**NH**-CH_2-C(=O)-OMe), 8.55 (t, 1 H, NH_2-CH_2-C(=O)-**NH**-R), 8.25 (s, 2 H, **NH_2**-R), 3.84 (m, 4 H, NH_2-CH_2-C(=O)-NH-**CH_2**-C(=O)-NH-**CH_2**-C(=O)-OMe), 3.63 (s, 3 H, R-O-**CH_3**), 3.60 (s, 2 H, NH_2-**CH_2**-C(=O)-NH-CH_2-C(=O)-NH-CH_2-C(=O)-OMe), 2.51 (DMSO).

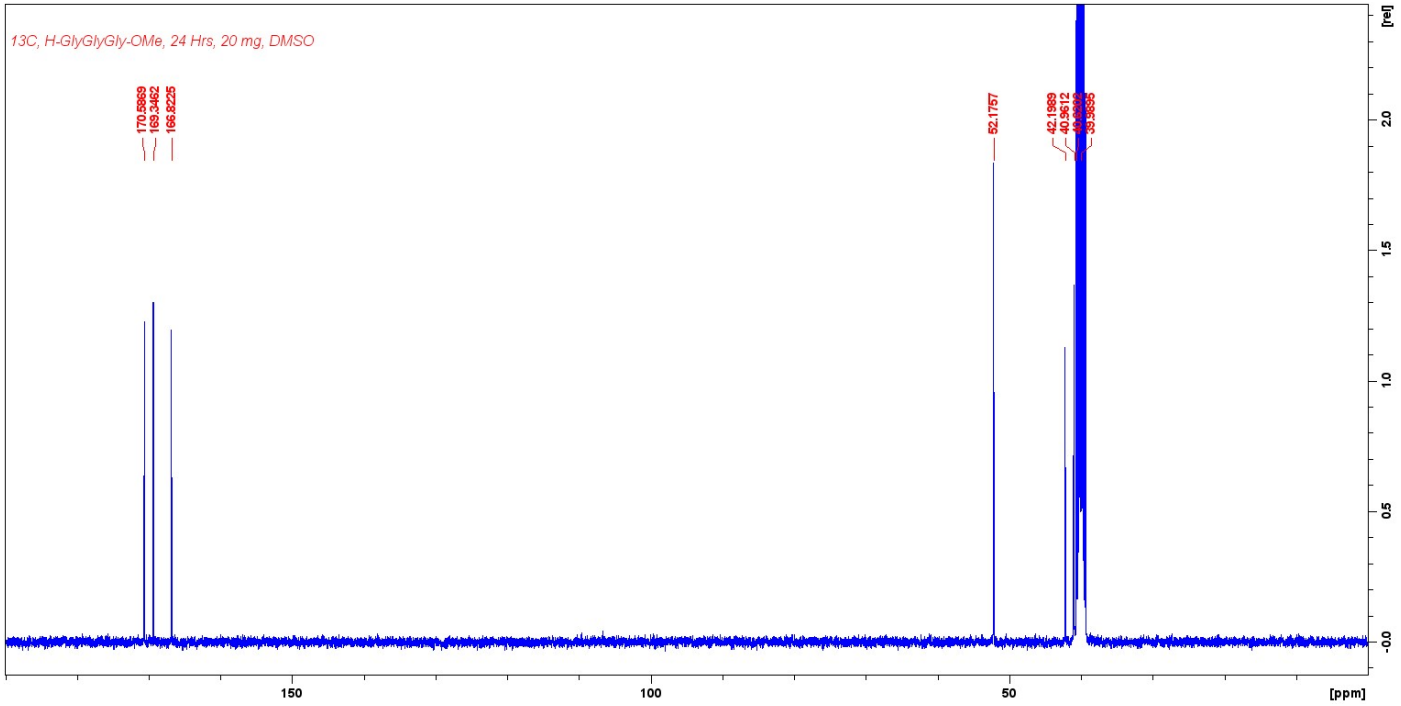

Figure S2 – ^{13}C NMR of NMR of triglycine methyl ester (**1a**). NMR ^{13}C (100 MHz, DMSO-d^6, δ, ppm): 170.59 (s, NH_2-gly-gly-NH-CH_2-**C**(=O)-OMe), 169.35 (s, NH_2-gly-NH-CH_2-**C**(=O)-NH-gly-OMe), 166.82 (s, NH_2-CH_2-**C**(=O)-NH-gly-gly-OMe), 52.18 (s, NH_2-gly-gly-gly-O**Me**), 42.20 (s, NH_2-gly-gly-NH-**C**H_2-C(=O)-OMe), 40.96 (s, NH_2-gly-NH-**C**H_2-C(=O)-NH-gly-OMe), 40.62 (s, NH_2-**C**H_2-C(=O)-NH-gly-gly-OMe).

ESI-MS for triglycine methyl ester (1a): calculated (M+H)/z: 204.20, found: (M+H)/z: 204.08 as seen in **Figure S3**.

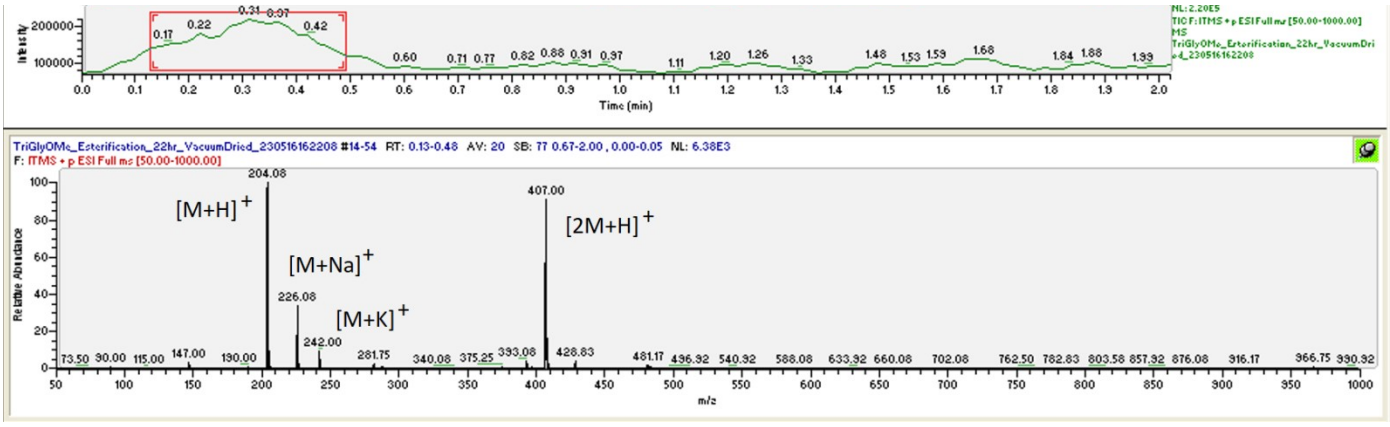

Figure S3 – ESI-MS of triglycine methyl ester (**1a**).

FTIR: The FTIR for triglycine and triglycine methyl ester (**1a**) are shown in **Figure S4a** and **S4b**, respectively. The introduction of a band at 2979.35 indicates the addition of the methyl group following esterification.

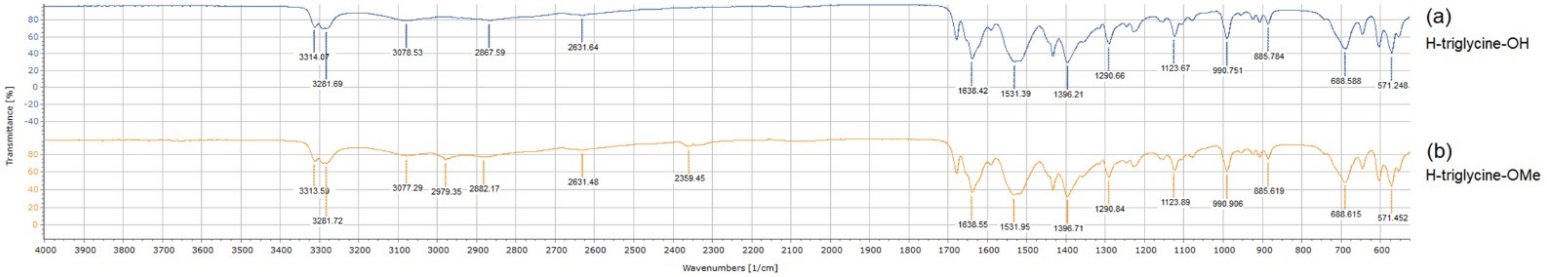

Figure S4 - FTIR for triglycine (a) and triglycine methyl ester (**1a**) (b).

2. Synthesis of 6-azidohexanoyl-triglycine methyl ester (2a) – (Figures S5-S10),

Yield: 87%, Analysis Calculated for $C_{13}H_{22}N_6O_5$: C, 45.61; N, 24.55, Found C, 45.55; N, 24.05.

Figure S5 and **S6** present the ^{1}H and ^{13}C NMR, respectively, of the azido-triglycine methyl ester product and its precursor materials. The successful esterification reaction of turning triglycine to triglycine methyl ester is observed through the appearance of ^{1}H NMR singlet at 3.84 ppm of the triglycine methyl ester precursor material spectra (**Figure S5** (**b**), location 'g'), and is further confirmed with the appearance of a ^{13}C NMR peak at 52.18 ppm (**Figure S6** (**b**), location 'g').

Confirmation of 6-azido hexanoic acid coupling with the triglycine methyl ester N-terminus is validated with a loss of the carboxylic acid's ^{1}H NMR peak at 11.99 ppm (**Figure S5** (**c**), location 'm') against that of the N_3-triglycine methyl ester (**2a**) product (**Figure S5** (**d**)), alongside the change of the triglycine N-terminus primary amide singlet at 8.25 ppm (**Figure S5** (**b**), location 'a') to a secondary amide triplet at 8.09 ppm (**Figure S5** (**d**), location 'a'). Additionally, all ^{13}C NMR peaks 'a' to 'm' are allocated within the azido-triglycine methyl ester product (**Figure S6** (**d**)).

The full ^{1}H and ^{13}C NMR spectra of (**2a**) are displayed in **Figures S7** and **S8**, respectively.

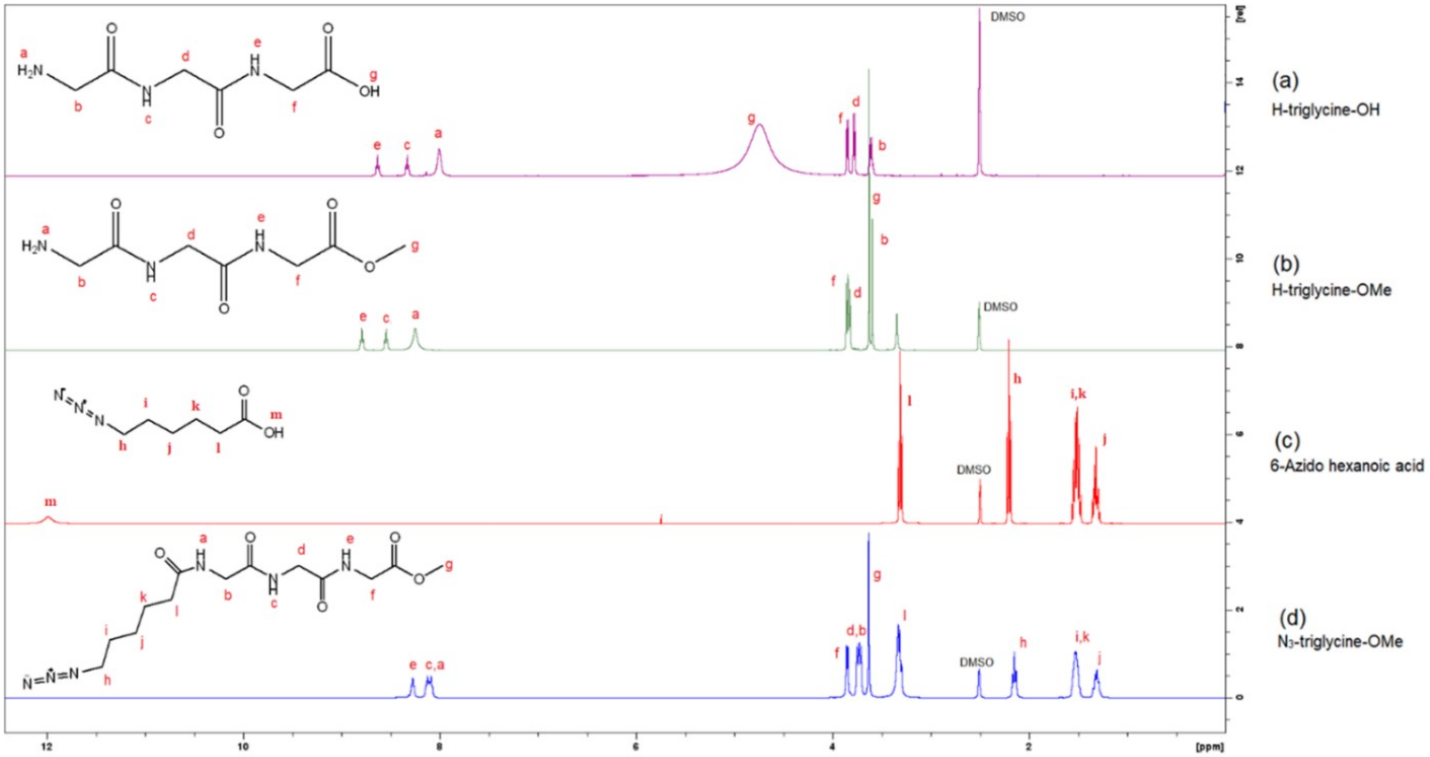

Figure S5 - ^{1}H NMR of triglycine starting material (spectra a), triglycine methyl ester following esterification (**1a**) (spectra b), 6-azidohexanoic acid (spectra c) and azido N-terminus modified triglycine methyl ester (**2a**) (spectra d) following coupling reaction between 6-azidohexanoic acid and triglycine methyl ester.

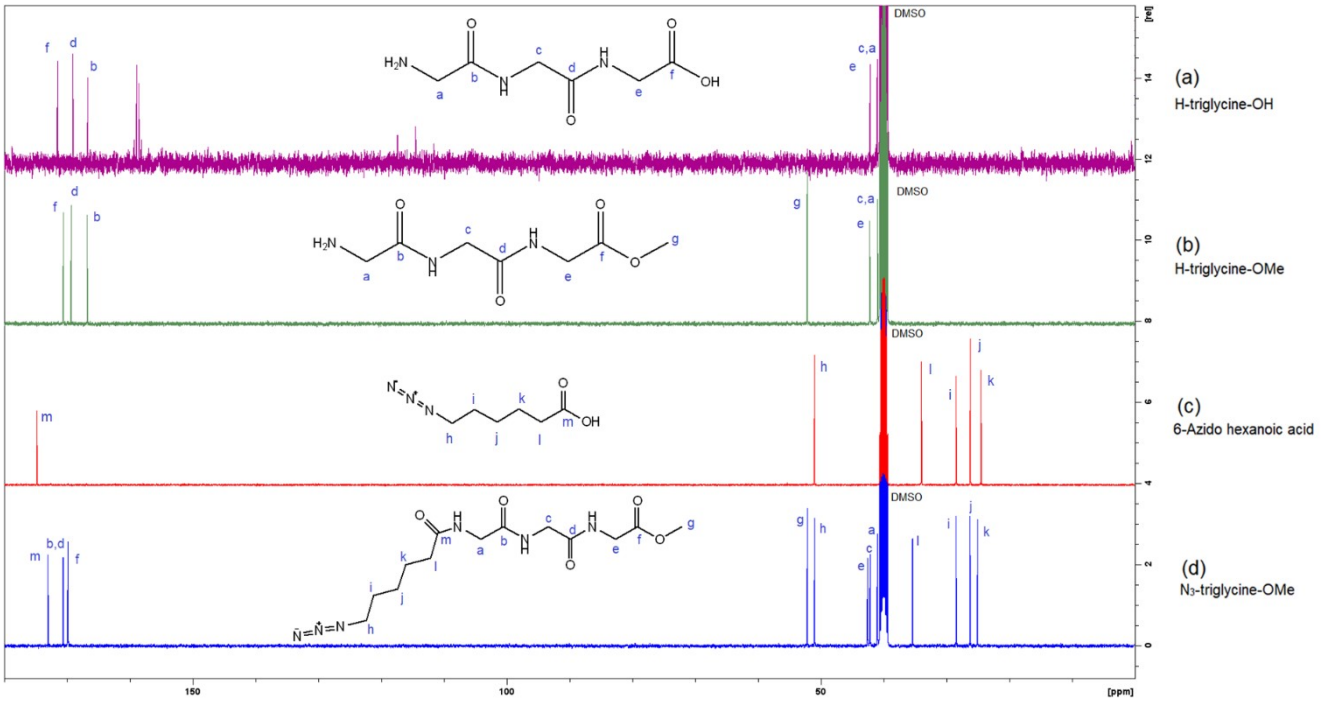

Figure S6 - ^{13}C NMR of triglycine starting material (spectra a), triglycine methyl ester following esterification (**1a**) (spectra b), 6-azidohexanoic acid (spectra c) and azido N-terminus modified triglycine methyl ester (**2a**) (spectra d) following coupling reaction between 6-azidohexanoic acid and triglycine methyl ester.

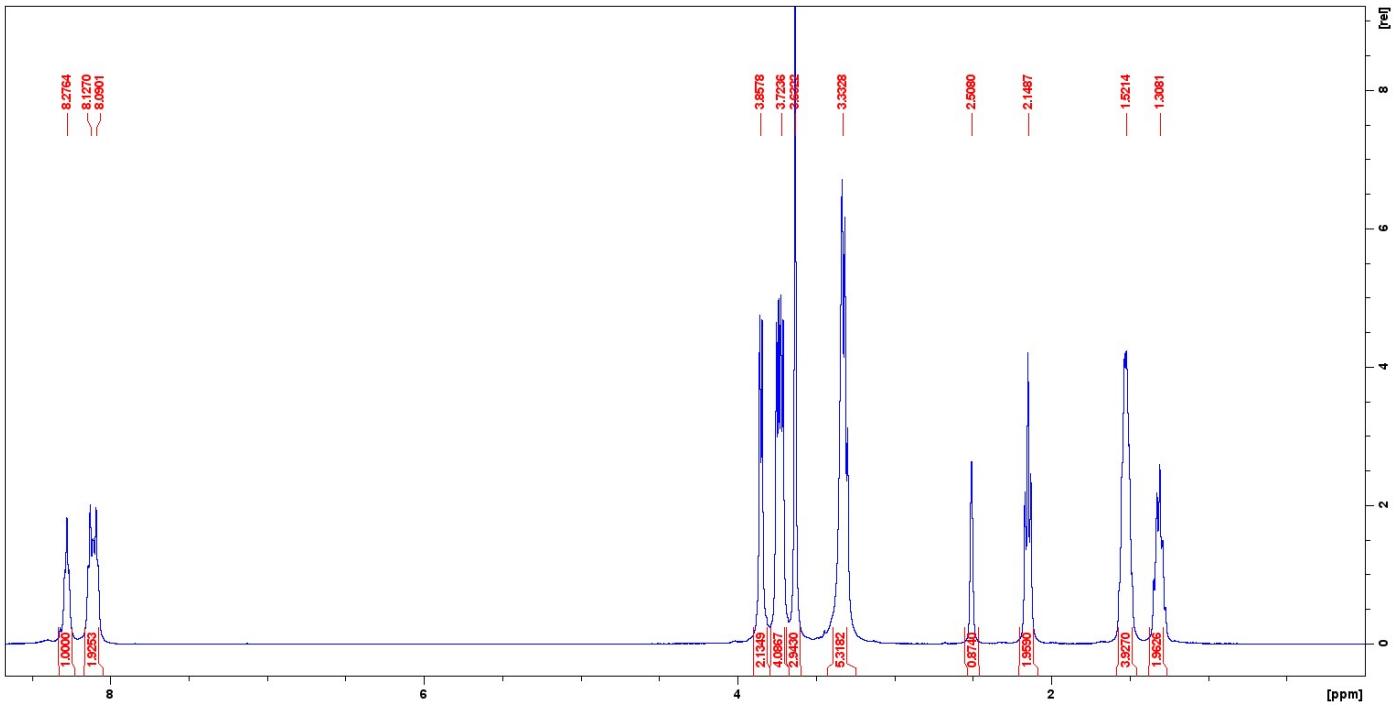

Figure 7 - NMR ^{1}H of 6-azidohexanoyl-triglycine methyl ester (**2a**) (400 MHz, DMSO-d^6, δ, ppm): 8.28 (t, 1 H, N_3-Hex-gly-gly-**NH**-CH_2-C(=O)-OMe), 8.13-8.09 (m, 2 x 1 H, N_3-Hex-**NH**-CH_2-C(=O)-**NH**-CH_2-C(=O)-gly-OMe), 3.86 (d, 2 H, N_3-Hex-gly-gly-NH-**CH_2**-C(=O)-OMe), 3.72 (m, 2 x 2 H, N_3-Hex-NH-**CH_2**-C(=O)-NH-**CH_2**-C(=O)-gly-OMe), 3.63 (s, 3 H, N_3-Hex-gly-gly-gly-O-**CH_3**), 3.33 (t, 2 H, N_3-$(CH_2)_4$-**CH_2**-C(=O)-gly-gly-gly-OMe), 2.15 (t, 2 H, N_3-**CH_2**-$(CH_2)_4$-C(=O)-gly-gly-gly-OMe), 1.52 (m, 2 x 2 H, N_3-CH_2-**CH_2**-CH_2-**CH_2**-CH_2-C(=O)-gly-gly-gly-OMe), 1.31 (t, 2 H, N_3-$(CH_2)_2$-**CH_2**-$(CH_2)_2$-C(=O)-gly-gly-gly-OMe).

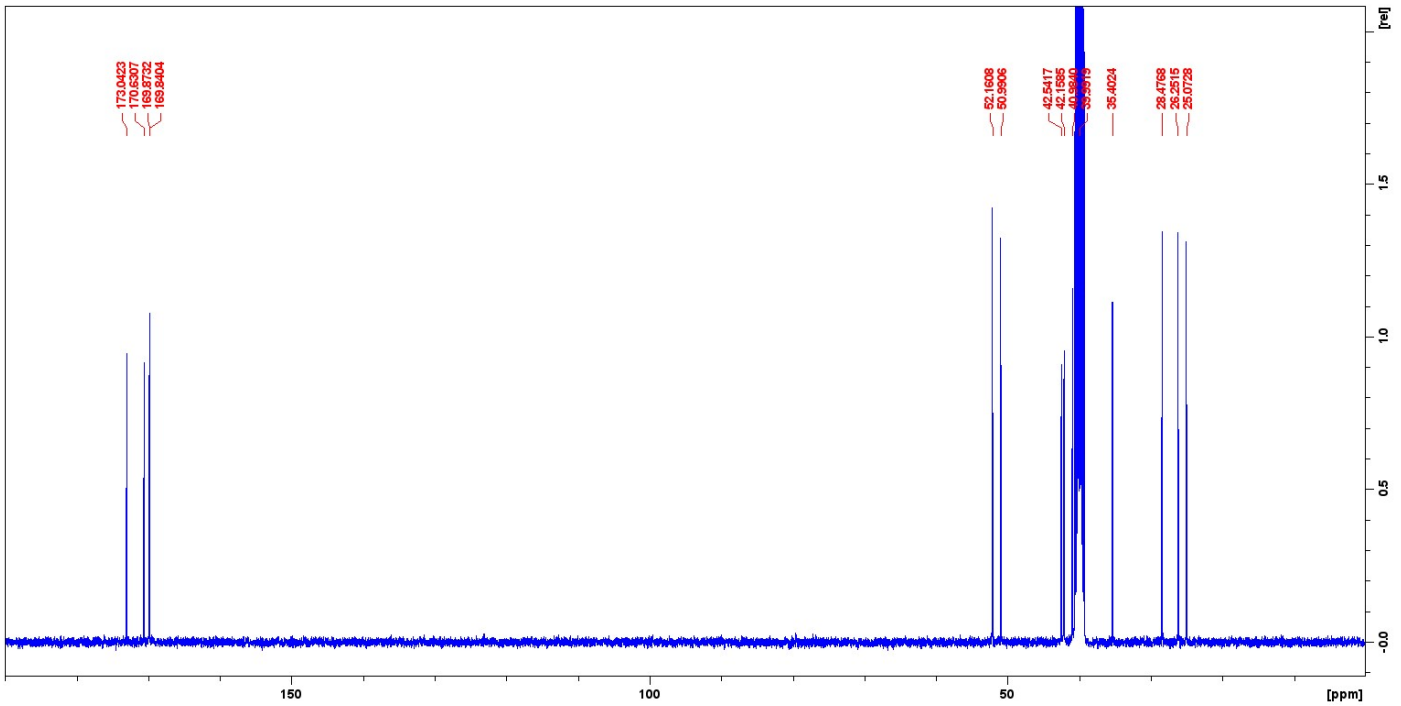

Figure 8 - NMR ^{13}C of 6-azidohexanoyl-triglycine methyl ester (**2a**) (100 MHz, DMSO-d^6, δ, ppm): 173.04 (s, N_3-$(CH_2)_5$ -**C**(=O)-gly-gly-gly-OMe), 170.63 (s, N_3-Hex-NH-CH_2-**C**(=O)-gly-gly-OMe), 169.87 (s, N_3-Hex-gly-NH-CH_2-**C**(=O)-gly-OMe), 169.84 (s, N_3-Hex-gly-gly-NH-CH_2-**C**(=O)-OMe), 52.16 (s, N_3-Hex-gly-gly-gly-O-**C**H_3), 50.99 (s, N_3-**C**H_2-$(CH_2)_4$-C(=O)-gly-gly-gly-OMe), 42.54 (s, N_3-Hex-gly-gly-NH-**C**H_2-C(=O)-OMe), 42.16 (s, 40.62 (s, N_3-Hex-gly-NH-**C**H_2-C(=O)-gly-OMe), 40.98 (s, N_3-Hex-NH-**C**H_2-C(=O)-gly-gly-OMe), 35.40 (s, N_3-$(CH_2)_4$-**C**H_2-C(=O)-gly-gly-gly-OMe), 28.48 (s, N_3-CH_2-**C**H_2-$(CH_2)_3$-C(=O)-gly-gly-gly-OMe), 26.25 (s, N_3-$(CH_2)_2$-**C**H_2-$(CH_2)_2$-C(=O)-gly-gly-gly-OMe), 25.07 (s, N_3-$(CH_2)_3$-**C**H_2-CH_2-C(=O)-gly-gly-gly-OMe).

ESI-MS for 6-azidohexanoyl-triglycine methyl ester (2a): calculated (M+H)/z: 343.36, found: (M+H)/z: 343.17 as seen in **Figure S9**.

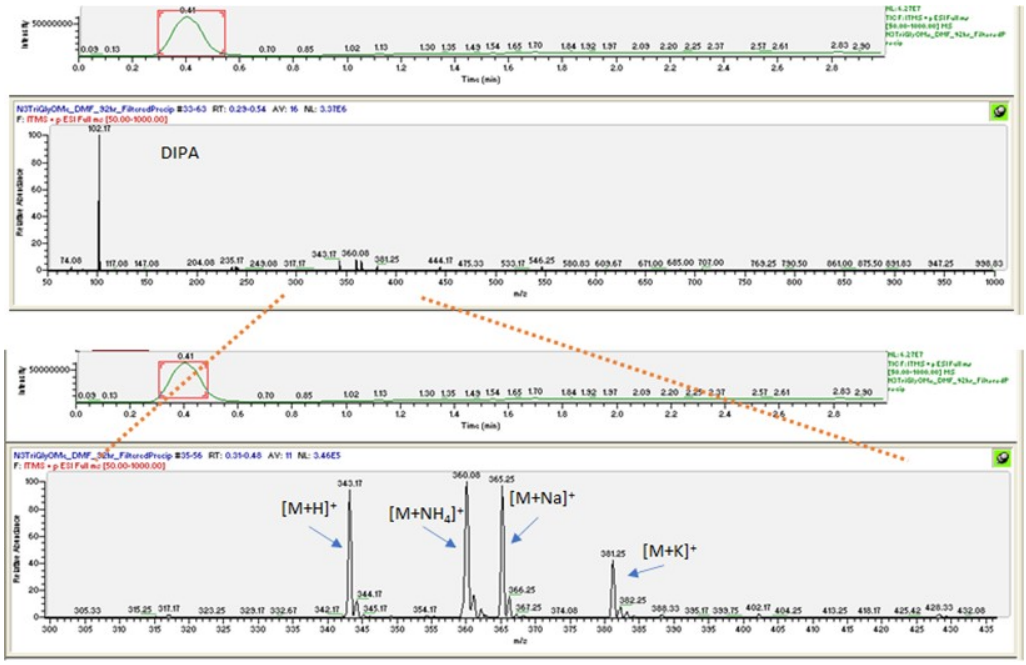

Figure S9 – ESI-MS of 6-azidohexanoyl-triglycine methyl ester (**2a**)

FTIR: **Figure S10** displays the FTIR spectra of the 6-azidohexanoyl-triglycine methyl ester (**2a**)

The presence of the azido antisymmetric stretch band at 2088 cm^{-1} within the product (**Figure S10** (**d**)), alongside the absence of N-H primary amine stretching at circa. 3314 cm^{-1}, indicates successful azido-modification to the triglycine methyl ester N-terminus through the coupling of 6-azido hexanoic acid with triglycine methyl ester using solution phase peptide synthesis methodology.

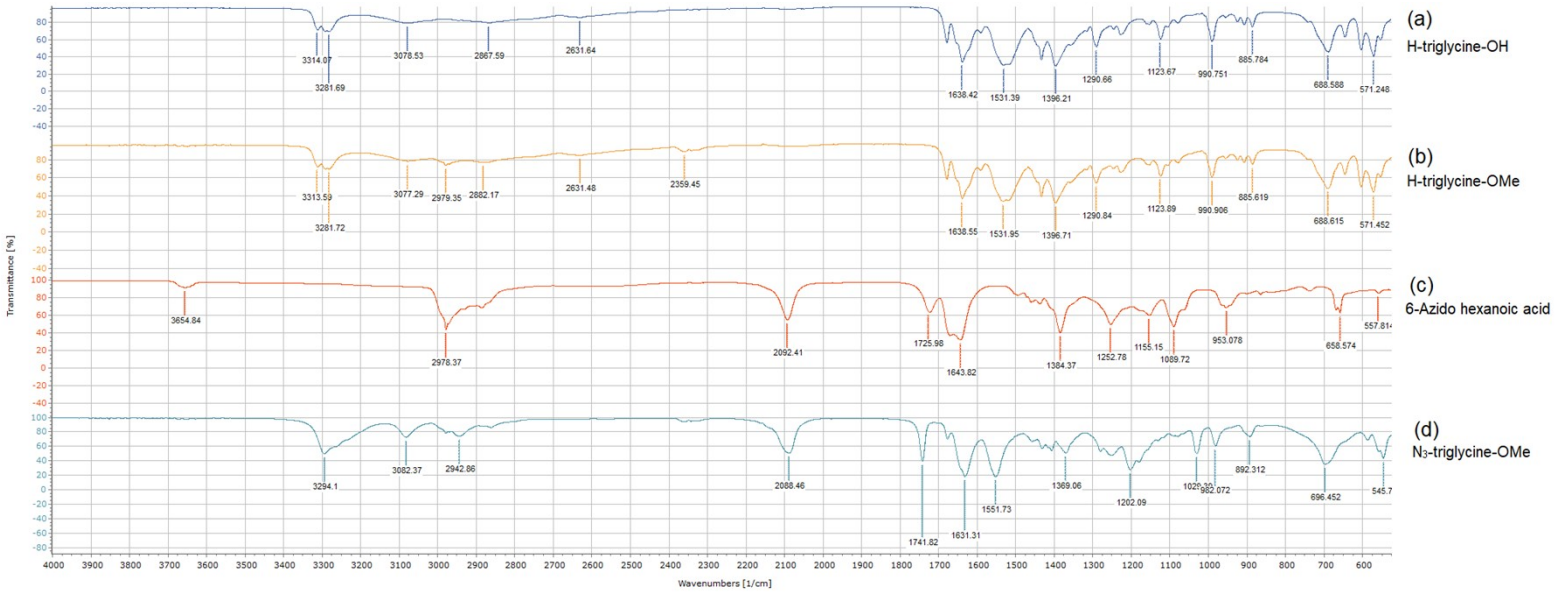

Figure S10 - FTIR of triglycine starting material (a), triglycine methyl ester following esterification (**1a**) (b), 6-azidohexanoic acid (c) and azido N-terminus modified 6-azidohexanoyl-triglycine methyl ester (**2a**) (d).

3. Synthesis of 6-azidohexanoyl-trialanine methyl ester (2b) – (Figures S11-S16)

Yield: 76%, Analysis Calculated for $C_{16}H_{28}N_6O_5$: C, 49.99; N, 21.86, Found C, 50.16; N, 22.31.

NMR: **Figure S11** and **S12** present the ^{1}H and ^{13}C NMR, respectively, of the azido-trialanine methyl ester product and its precursor materials. Confirmation of 6-azidohexanoic acid (**3**) coupling with the trialanine methyl ester N-terminus is validated with a loss of the carboxylic acid's ^{1}H NMR peak at 11.99 ppm (**Figure S11** (**b**), location 'p') against that of (**2b**) (**Figure S11** (**c**)), alongside the change of the trialanine N-terminus primary amide singlet at 8.12 ppm (**Figure S11**(**a**), location 'a') to a secondary amide triplet at 8.22 ppm (**Figure S11** (**C**), location 'a'). Additionally, all ^{13}C NMR peaks 'a' to 'o' are allocated within the azido-trialanine methyl ester product (**Figure S12**(**c**)).

The full NMR ^{1}H and ^{13}C are shown for 6-azidohexanoyl-trialanine methyl ester (**2b**) in **Figures S13** and **S14**, respectively.

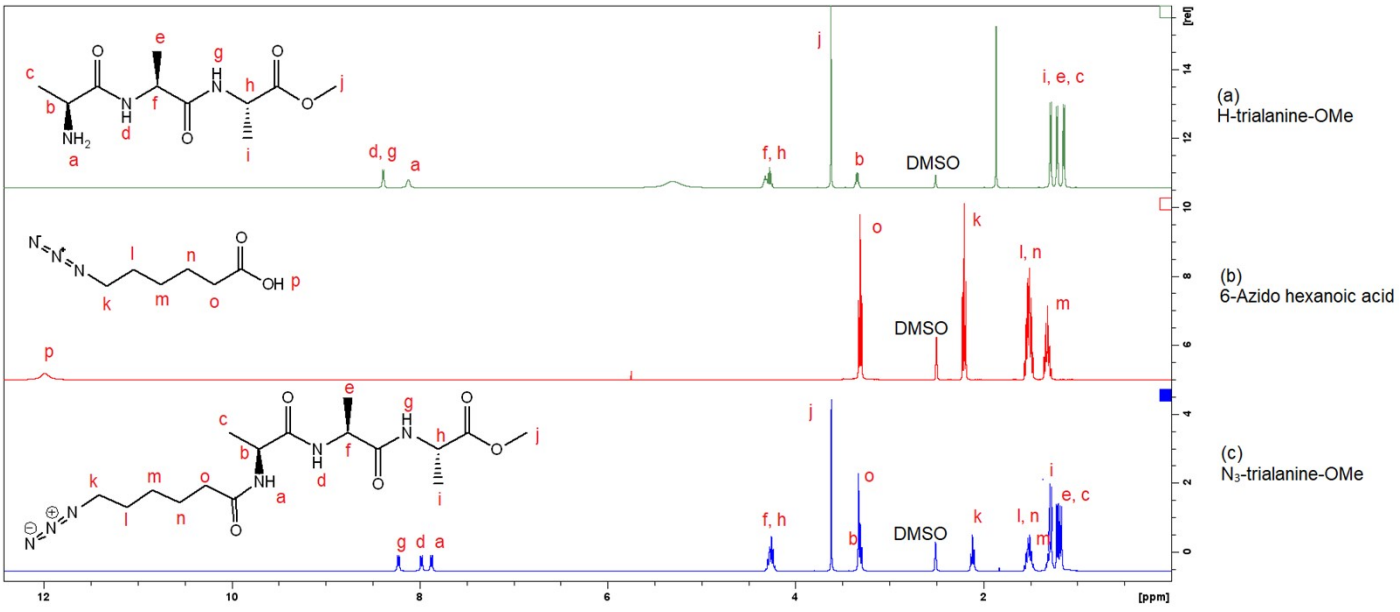

Figure S11 - ^{1}H NMR of trialanine methyl ester starting material (**1a**) (spectra a), 6-azidohexanoic acid (spectra b) and azido N-terminus modified trialanine methyl ester (**2b**) (spectra c).

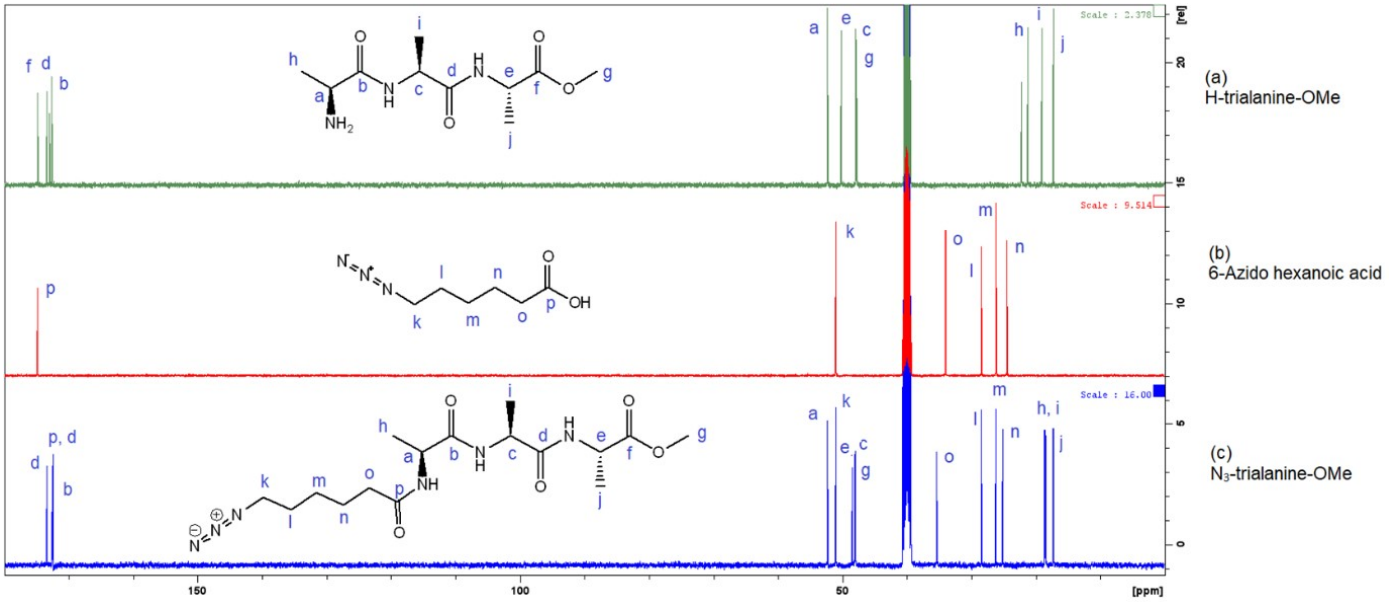

Figure S12 – ^{13}C NMR of trialanine methyl ester starting material (**1a**) (spectra a), 6-azidohexanoic acid (spectra b) and azido N-terminus modified trialanine methyl ester (**2b**) (spectra c).

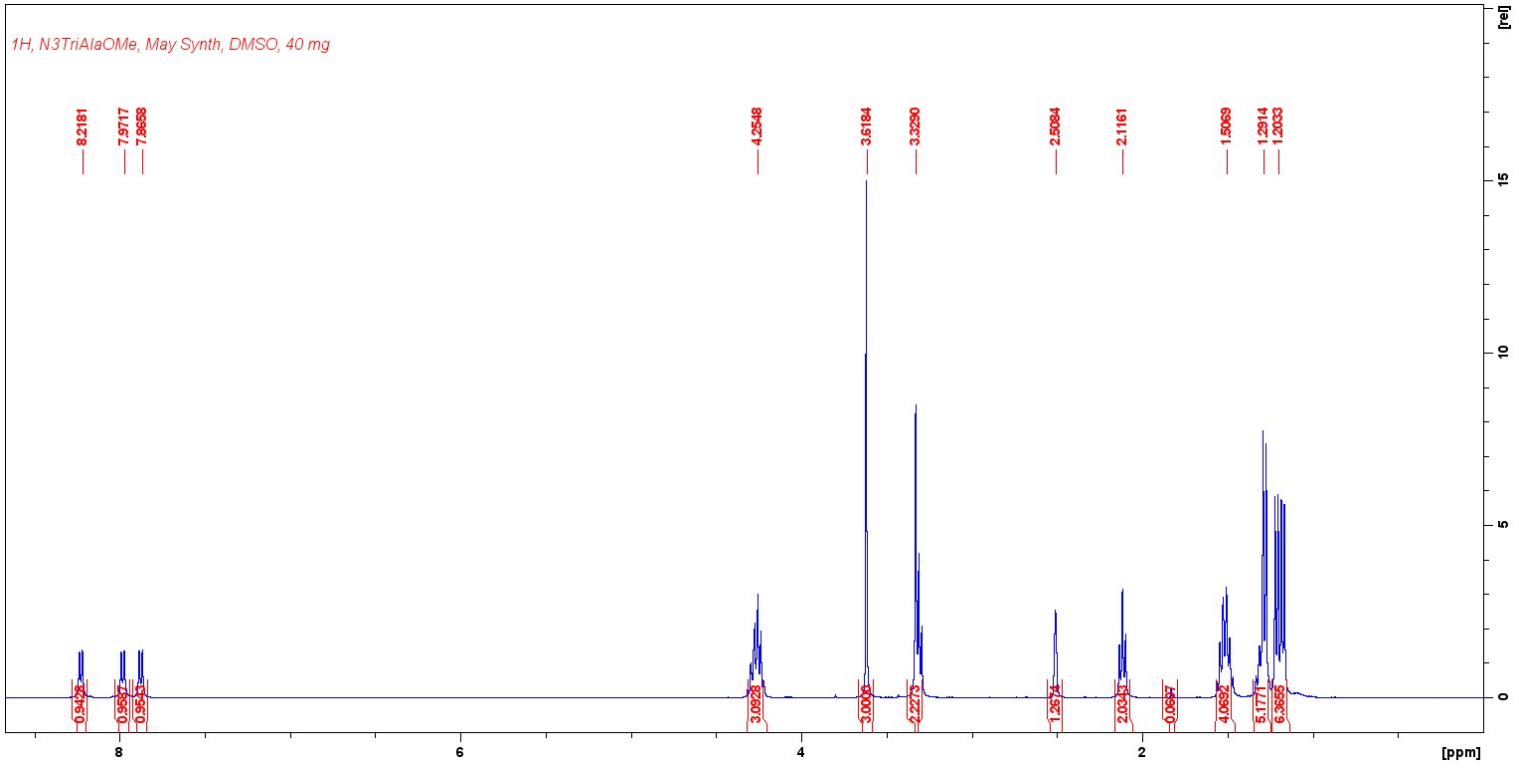

Figure S13 - NMR ^{1}H of 6-azidohexanoyl-trialanine methyl ester (**2b**) (400 MHz, DMSO-d^6, δ, ppm): 8.22 (d, 1 H, N_3-Hex-ala-ala-**NH**-CH_2-C(=O)-OMe), 7.97 (d, 1 H, N_3-Hex-ala-**NH**-CH_2-C(=O)-ala-OMe), 7.87 (d, 1 H, N_3-Hex-**NH**-CH_2-C(=O)-ala-ala-OMe), 4.25 (m, 3 H, N_3-Hex-NH-**CH**(CH_3)-C(=O)-NH-**CH**(CH_3)-C(=O)-NH-**CH**(CH_3)-C(=O)-OMe), 3.62 (s, 3 H, N_3-Hex-ala-ala-ala-O-**CH_3**), 3.63 (s, 3 H, N_3-Hex-ala-ala-ala-O-**CH_3**), 3.33 (t, 2 H, N_3-$(CH_2)_4$-**CH_2**-C(=O)-ala-ala-ala-OMe), 2.12 (t, 2 H, N_3-**CH_2**-$(CH_2)_4$-C(=O)-ala-ala-ala-OMe), 1.51 (m, 4 H, N_3-CH_2-**CH_2**-CH_2-**CH_2**-CH_2-C(=O)-ala-ala-ala-OMe), 1.29 (m, 5 H, N_3-$(CH_2)_2$-**CH_2**-$(CH_2)_2$-C(=O)-NH-CH(**CH_3**)-C(=O)-ala-ala-OMe), 1.20 (m, 4 H, N_3-Hex-ala-NH-CH(**CH_3**)-C(=O)-NH-CH(**CH_3**)-C(=O)-OMe).

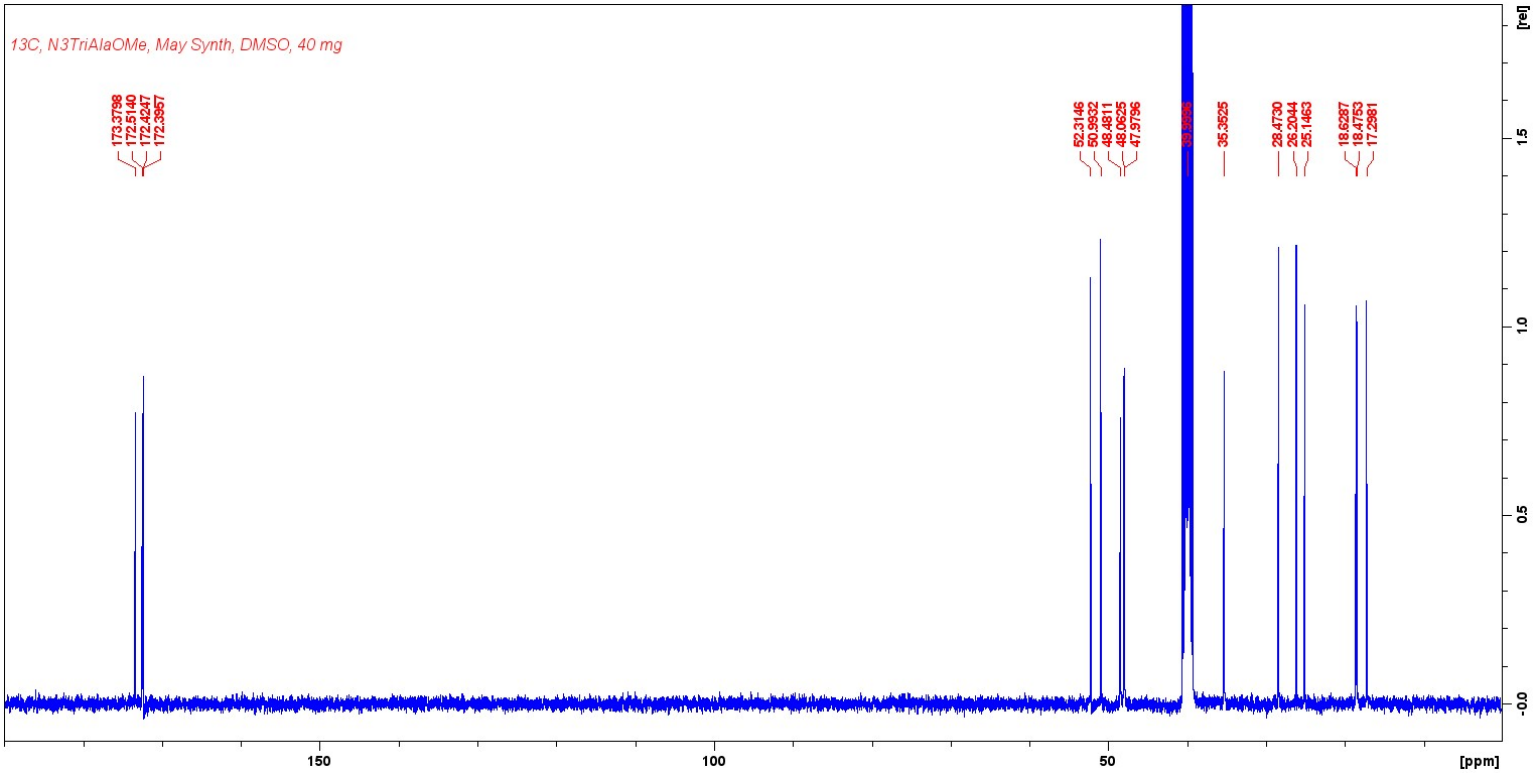

Figure S14 - NMR ^{13}C of 6-azidohexanoyl-trialanine methyl ester (**2b**) (100 MHz, DMSO-d^6, δ, ppm): 173.38 (s, N_3-$(CH_2)_5$ -**C**(=O)-ala-ala-ala-OMe), 172.51 (s, N_3-Hex-ala-ala-NH-CH(CH_3)-**C**(=O)-OMe), 172.42 (s, N_3-Hex-NH-CH(CH_3)-**C**(=O)-ala-ala-OMe), 172.40 (s, N_3-Hex-ala-NH-CH(CH_3)-**C**(=O)-ala-OMe), 52.31 (s, N_3-Hex-NH-**C**H(CH_3)-C(=O)-ala-ala-OMe), 50.99 (s, N_3-Hex-ala-NH-**C**H(CH_3)-C(=O)-ala-OMe), 48.48 (s, N_3-Hex-ala-ala-NH-**C**H(CH_3)-C(=O)-OMe), 48.06 (s, N_3-Hex-ala-ala-ala-O-**C**H_3), 47.98 (s, N_3-**C**H_2-$(CH_2)_4$-C(=O)-ala-ala-ala-OMe), 35.35 (s, N_3-$(CH_2)_4$-**C**H_2-C(=O)-ala-ala-ala-OMe), 28.47 (s, N_3-CH_2-**C**H_2-$(CH_2)_3$-C(=O)-ala-ala-ala-OMe), 26.20 (s, N_3-$(CH_2)_2$-**C**H_2-$(CH_2)_2$-C(=O)-ala-ala-ala-OMe), 25.15 (s, N_3-$(CH_2)_3$-**C**H_2-CH_2-C(=O)-ala-ala-ala-OMe), 18.63 (s, N_3-Hex-NH-CH(**C**H_3)-C(=O)-ala-ala-OMe), 18.48 (s, N_3-Hex-ala-NH-CH(**C**H_3)-C(=O)-ala-OMe), 17.30 (s, N_3-Hex-ala-ala-NH-CH(**C**H_3)-C(=O)-OMe).

ESI-MS: 6-azidohexanoyl-trialanine methyl ester (**2b**) calculated (M+H)/z: 385.44, found: (M+H)/z: 385.17 as found in **Figure S15**.

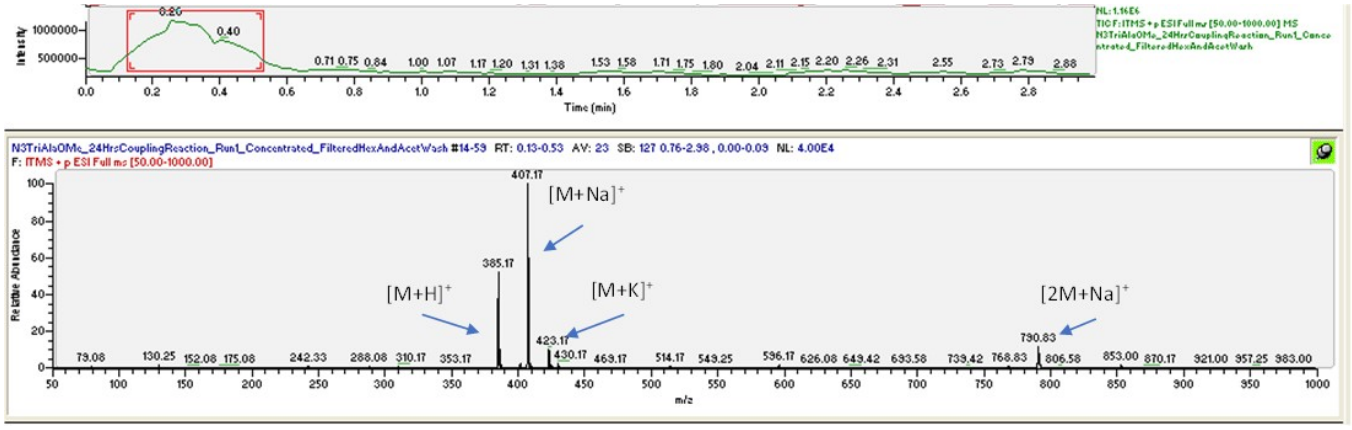

Figure S15 – ESI-MS of 6-azidohexanoyl-trialanine methyl ester (**2b**)

FTIR: **Figure S16** displays the FTIR spectra of the 6-azidohexanoyl-trialanine methyl ester (**2b**)

The presence of the azido antisymmetric stretch band at 2092.26 cm^{-1} within the product (**Figure S16**), alongside the absence of N-H primary amine stretching at circa. 3314 cm^{-1}, indicates successful azido-modification to the trialanine methyl ester N-terminus through the coupling of 6-azidohexanoic acid with trialanine methyl ester (**1a**) using solution phase peptide synthesis.

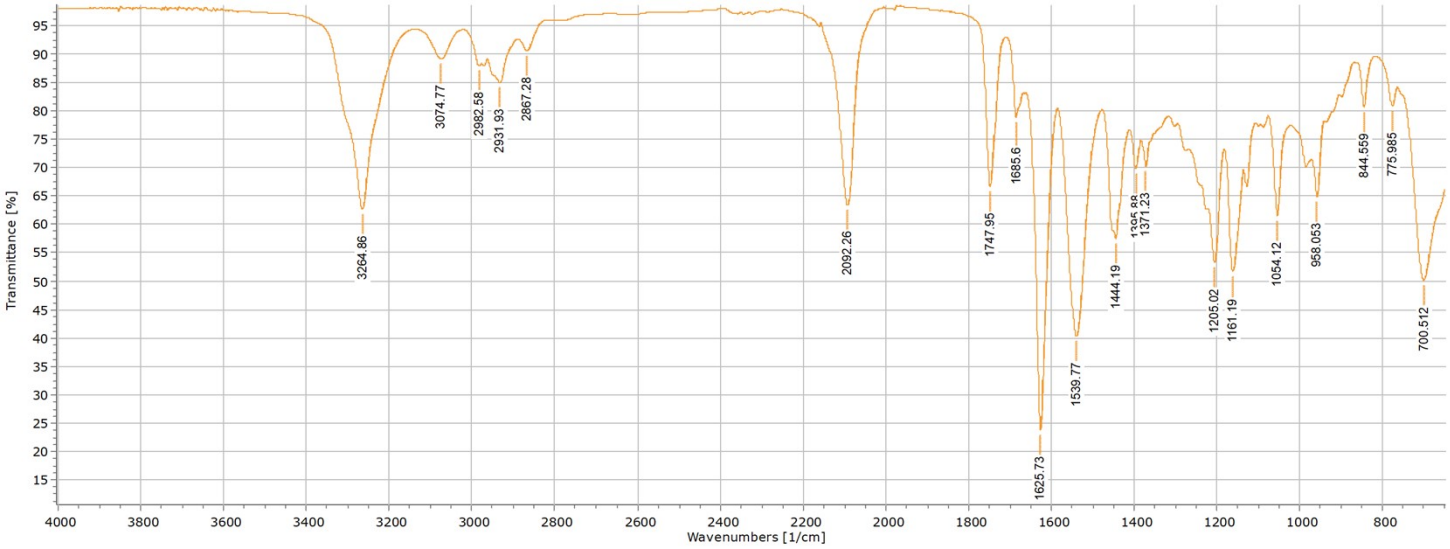

Figure S16 - FTIR of 6-azidohexanoyl-trialanine methyl ester (**2b**)

4. Synthesis of T_8[3-aminopropyl]$_8$ – (Figures S17-S19)

Yield: 87%

NMR: Confirmation of T_8[3-aminopropyl]$_8$ synthesis was established through NMR ^{1}H, ^{13}C, and ^{29}Si IG (Inverse Gated decoupling) relating to that reported by Szafert. S, et al (**Figure S17**(**a**), (**b**) & (**c**), respectively).

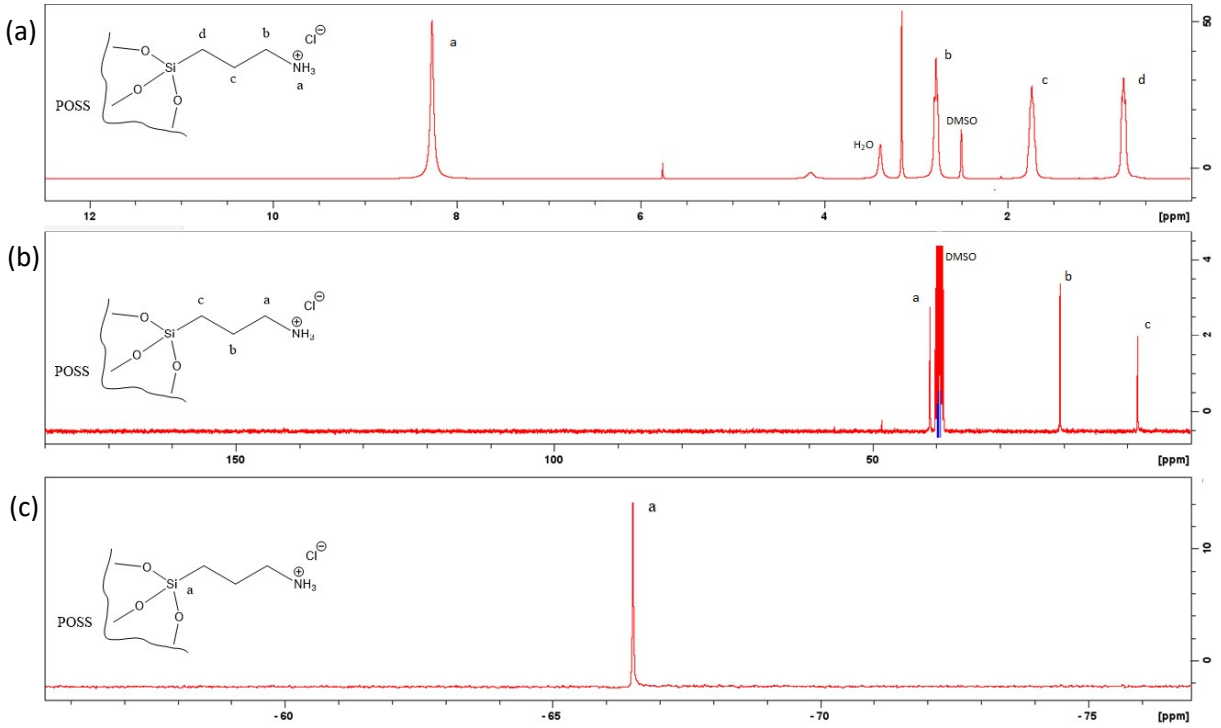

Figure S17. (a) NMR ^{1}H (400 MHz, DMSO-d^6, δ, ppm): 8.27 (s, 24 H, Si-R-**NH$_3^+$**), 2.78 (t, 16 H, Si-R-**CH$_2$**.NH$_3^+$), 1.74 (m, 16 H, Si-CH$_2$-**CH$_2$**-CH$_2$-NH$_3^+$) and 0.74 (t, 16 H, Si-CH$_2$-R), (b) NMR ^{13}C (100 MHz, DMSO-d^6, δ, ppm): 41.46 (s, Si-CH$_2$-CH$_2$-**C**H$_2$-NH$_3^+$), 21.05 (s, Si-CH$_2$-**C**H$_2$-CH$_2$-NH$_3^+$) and 8.87 (s, Si-**C**H$_2$-CH$_2$-CH$_2$-NH$_3$) and (c) NMR ^{29}Si-IG (105.7 MHz, DMSO-d^6, δ, ppm): -66.50, suggesting the full formation of Si-O-Si POSS cage with one type of Si environment reflective of the symmetrical single peak.

ESI-MS-ToF: T_8[3-aminopropyl]$_8$ calculated (M+H)/z: 881.28, found: (M+H)/z: 881.29 as shown in **Figure S18**.

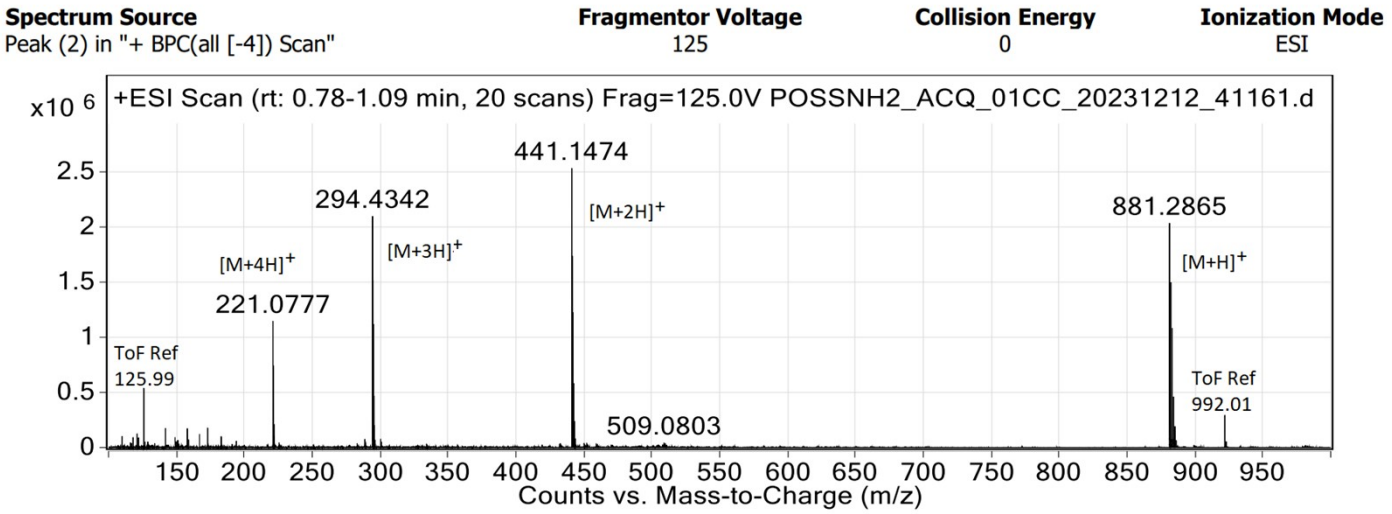

Figure S18 – ESI-TOF MS of T_8[3-aminopropyl]$_8$ (**3**)

FTIR: analysis of T_8[3-aminopropyl]$_8$ (**Figure S19**) confirms the presence of the POSS cage with a strong Si-O-Si stretching peak located at 1080.68 cm^{-1}, alongside Si-C stretching, ν_{as} and ν_{sym}, at 1222.49 and 699.12 cm^{-1}, respectively. The presence of N-H and C-H stretching at 2965.02 and 2890.09 cm^{-1}, alongside N-H and C-H bending at 1605.41 and 1499.14 cm^{-1}, respectively, shows successful addition of the propyl ammonium chloride to the POSS cage Si vertices.

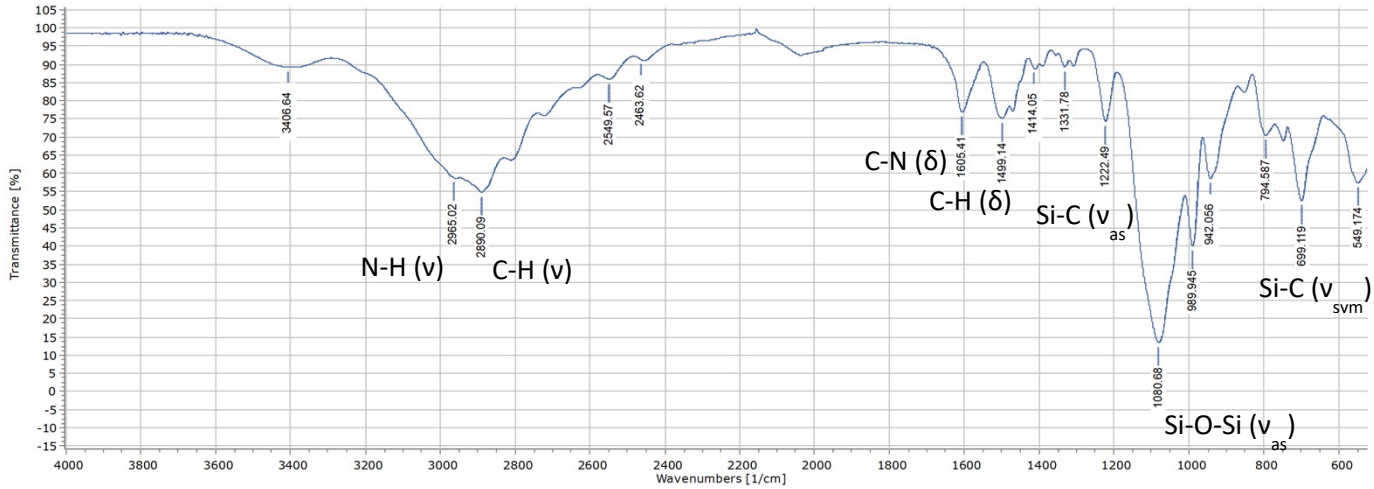

Figure S19 - FTIR spectra of T_8[3-aminopropyl]$_8$ (**3**)

5. Synthesis of T_8[N-propyl-hex-5-ynamide]$_8$ (4) – (Figures S20-S24)

Yield: 84%

NMR: Comparatively to the reported analysis of El Aziz, Y, *et al*. (**4**), confirmation of T_8[N-propyl-hex-5-ynamide]$_8$ synthesis was established through ^{1}H, ^{13}C, and ^{29}Si IG **Figure S20**-**S22**, respectively):

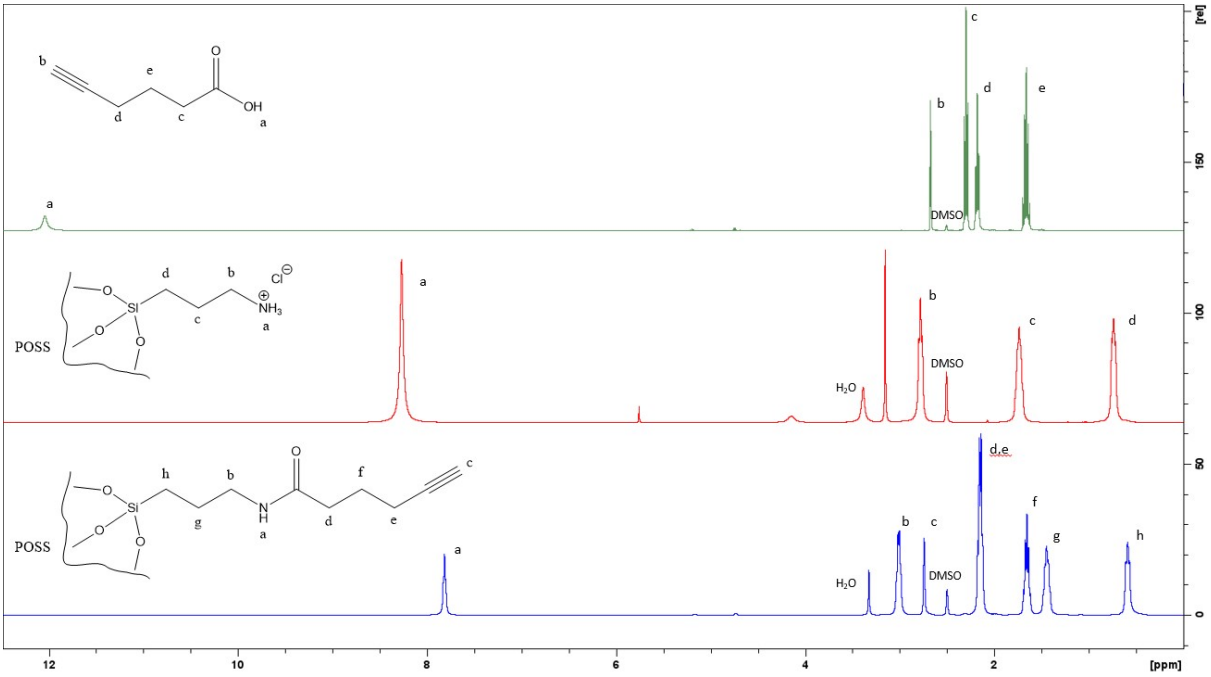

Figure S20 - Stacked ^{1}H NMR of reactants 5-hexynoic acid (green) and T_8[3-aminopropyl]$_8$ (**3**) (red) corresponding to T_8[N-propyl-hex-5-ynamide]$_8$ **(4)** product (blue). NMR ^{1}H of T_8[N-propyl-hex-5-ynamide]$_8$ (400 MHz, DMSO-d^6, δ, ppm): 7.82 (s, 8H, NH), 3.00 (m, 16H, NCH_2), 2.74 (s, 8H, C≡CH), 2.1-2.2 (m, 32H, (O)CCH_2 + CH_2C≡C), 1.65 (m, 16H, (O)$CCH_2C\mathbf{H_2}$), 1.45 (m, 16H, $SiCH_2C\mathbf{H_2}$), 0.59 (t, 16H, $SiCH_2$). NMR ^{29}Si (105.7 MHz, DMSO-d^6, δ, ppm): -66.50.

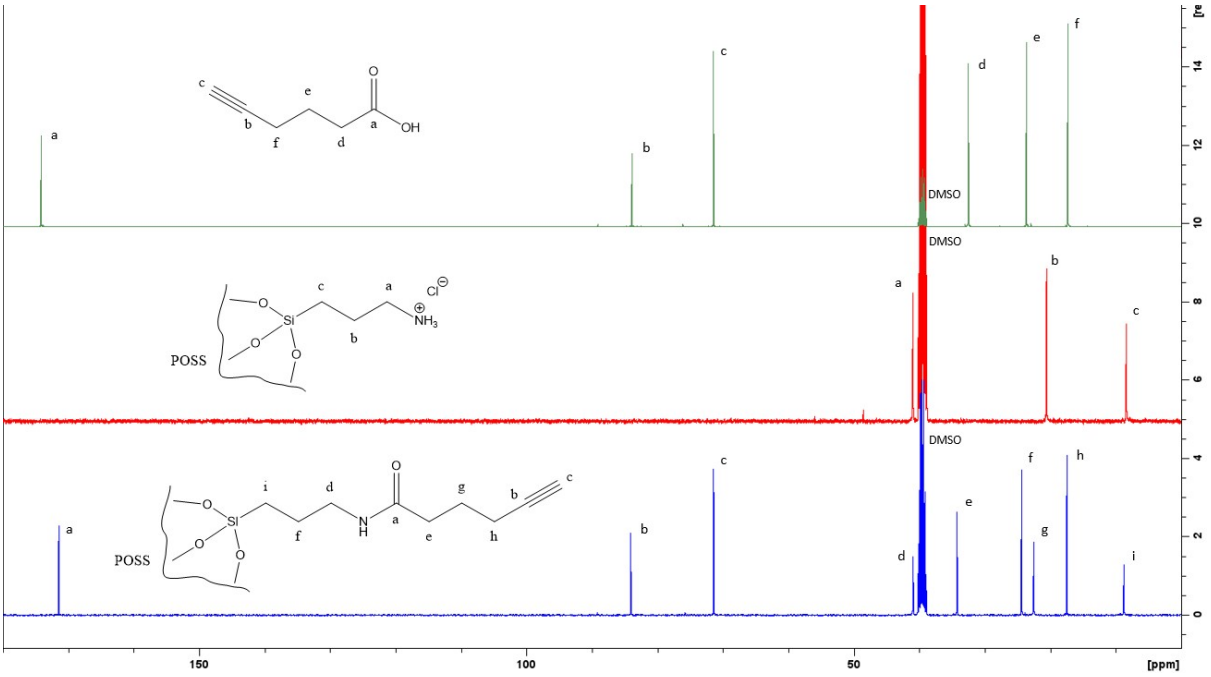

Figure S21 - Stacked ^{13}C NMR of reactants 5-hexynoic acid (green) and T_8[3-aminopropyl]$_8$ (**3**) (red) corresponding to T_8[N-propyl-hex-5-ynamide]$_8$ product (**4**) (blue). NMR ^{13}C of T_8[N-propyl-hex-5-ynamide]$_8$ (100 MHz, DMSO-d^6, δ, ppm): 171.86 (s, R-**C**(=O)-R), 84.50 (s, R-**C**≡CH), 71.82 (s, R-C≡**C**H), 41.38 (s, R-**C**H$_2$-NH-R), 34.66 (s, R-C(=O)-**C**H$_2$-R), 24.78 (s, Si-CH$_2$-**C**H$_2$-R), 22.92 (s, R-C(=O)-CH$_2$-**C**H$_2$-R), 17.88 (s, R-**C**H$_2$C≡C), 9.18 (s, Si-**C**H$_2$-R).

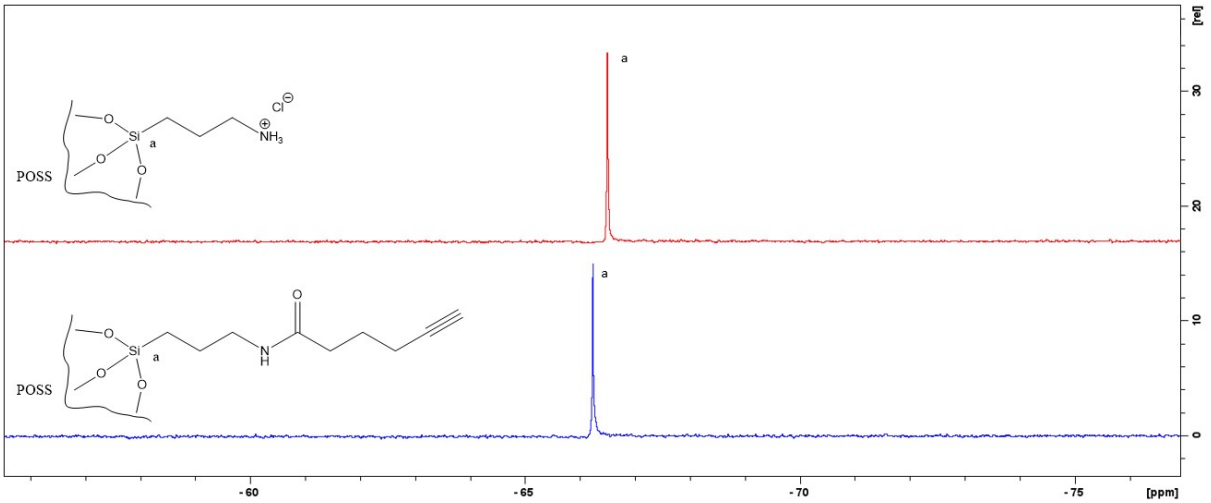

Figure S22 - Stacked ^{29}Si NMR of reactants T_8[3-aminopropyl]$_8$ (**3**) (red) corresponding to T_8[N-propyl-hex-5-ynamide]$_8$ product (**4**) (blue). NMR ^{29}Si of T_8[N-propyl-hex-5-ynamide]$_8$ (105.7 MHz, DMSO-d^6, δ, ppm): -66.50.

ESI MS: T_8[N-propyl-hex-5-ynamide]$_8$ calculated (M+H)/z: 1633.62, found: (M+H)/z: 1634.75 as found in **Figure S23**, alongside adducts $[M+Na]^+$ and $[M+K]^+$ at m/z 1656.67 and 1674.67, respectively.

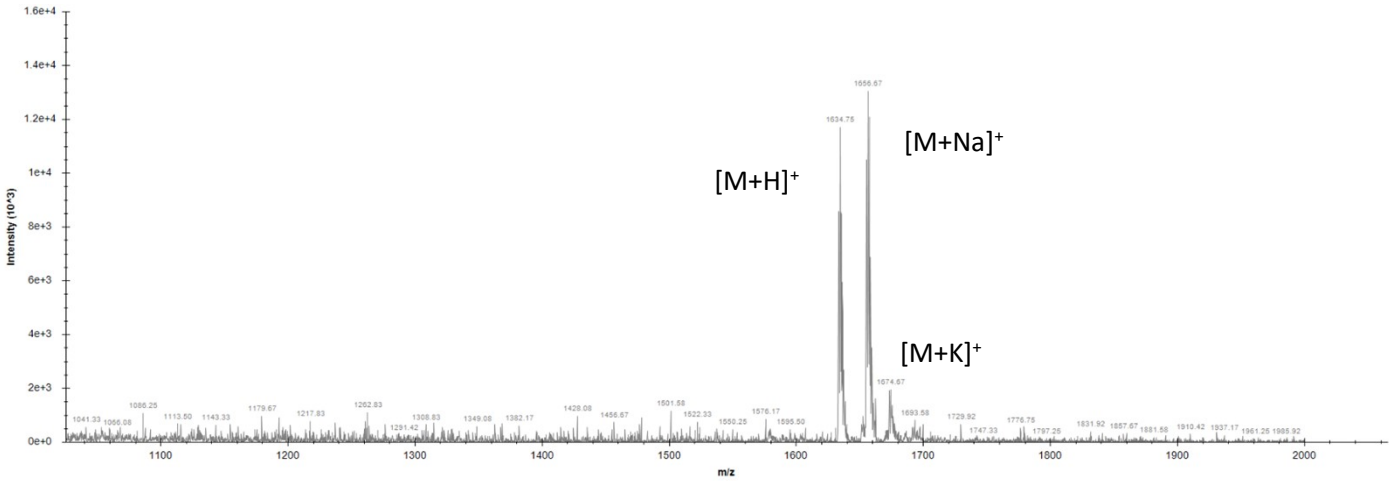

Figure S23 - ESI MS of T_8[N-propyl-hex-5-ynamide]$_8$ (**4**)

FTIR: Analysis confirms the successful production of alkyne modification of POSS-octa-NH_2 to POSS-octa-Alkyne. FT-IR of 5-heynoic acid (**Figure S6** (**a**)) measures peaks at 3290.23 cm^{-1} for ν(CH) of the terminal alkyne carbon (C≡**C-H**), 2116.49 cm^{-1} of ν_{as}(C≡C) and 1701.64 cm^{-1} of ν(C=O), with these peaks centred in the POSS-Alkyne product (**Figure S6** (**c**)) at 3286.66, 2111.67 and 1635.04 cm^{-1}, respectively. The ν(Si-O-Si) centred at 1080.68 cm^{-1} and both ν_{as} and ν_{sym}(Si-C) at 1222.49 and 699.12 cm^{-1} of POSS-NH_2, respectively, are measured in the POSS-Alkyne product at 1093.44, 1196.27 and 687.98 cm^{-1}, respectively.

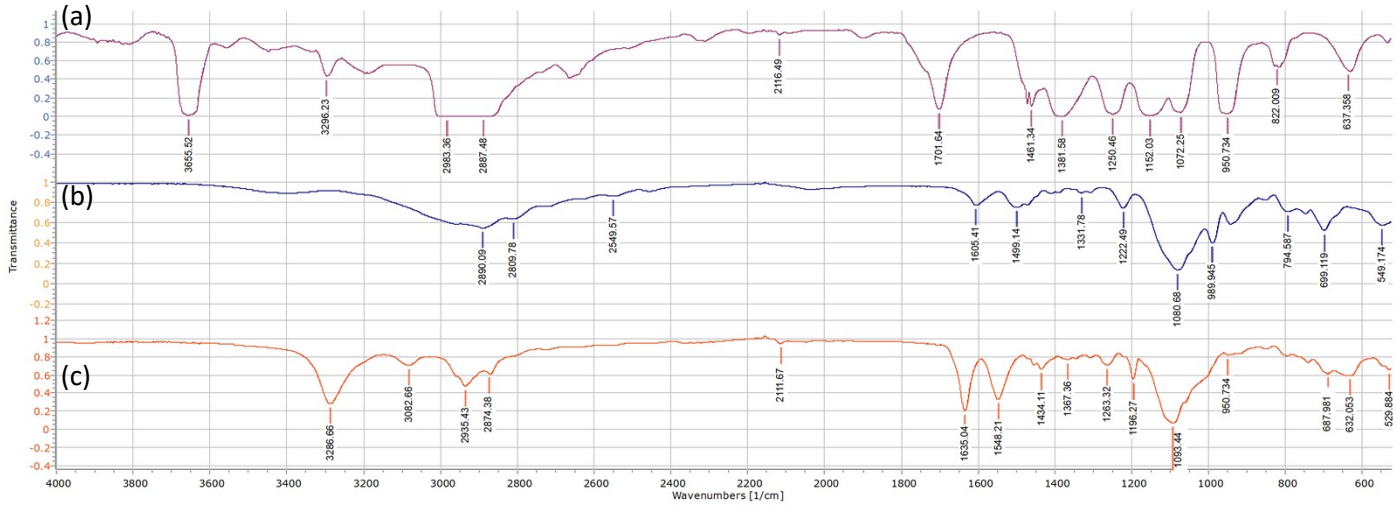

Figure S24 - FTIR spectra of 5-hexynoic acid (a), T_8[3-aminopropyl]$_8$ (**3**)(b) and T_8[N-propyl-hex-5-ynamide]$_8$ (**4**) (c).

6. Synthesis of POSS-octa-triglycine methyl ester (T_8[(6-(4-(4-oxo-4-(propylamino)butyl)-1H-1,2,3-triazol-1-yl)hexanoyl)triglycine methyl ester]$_8$) nanocages through CuAAC "click" reaction (5a) – (Figures S25-S28)

NMR: Confirmation of T_8[(6-(4-(4-oxo-4-(propylamino)butyl)-1H-1,2,3-triazol-1-yl)hexanoyl)triglycine methyl ester]$_8$ ("POSS-octa-triglycine methyl ester") (**5a**) synthesis was established through NMR ^{1}H, ^{13}C and ^{29}Si IG, Figures 25-27, respectively. For ^{13}C and ^{29}Si NMR, HFIP solvent was used to dissolve (**5a**) (6.0 mg mL^{-1}) before addition of 50.0 µL DMSO-d^6 NMR solvent. ^{1}H NMR samples were prepared by addition of (**5a**) (1.2 mg) in to DMSO-d^6 (1.0 mL).

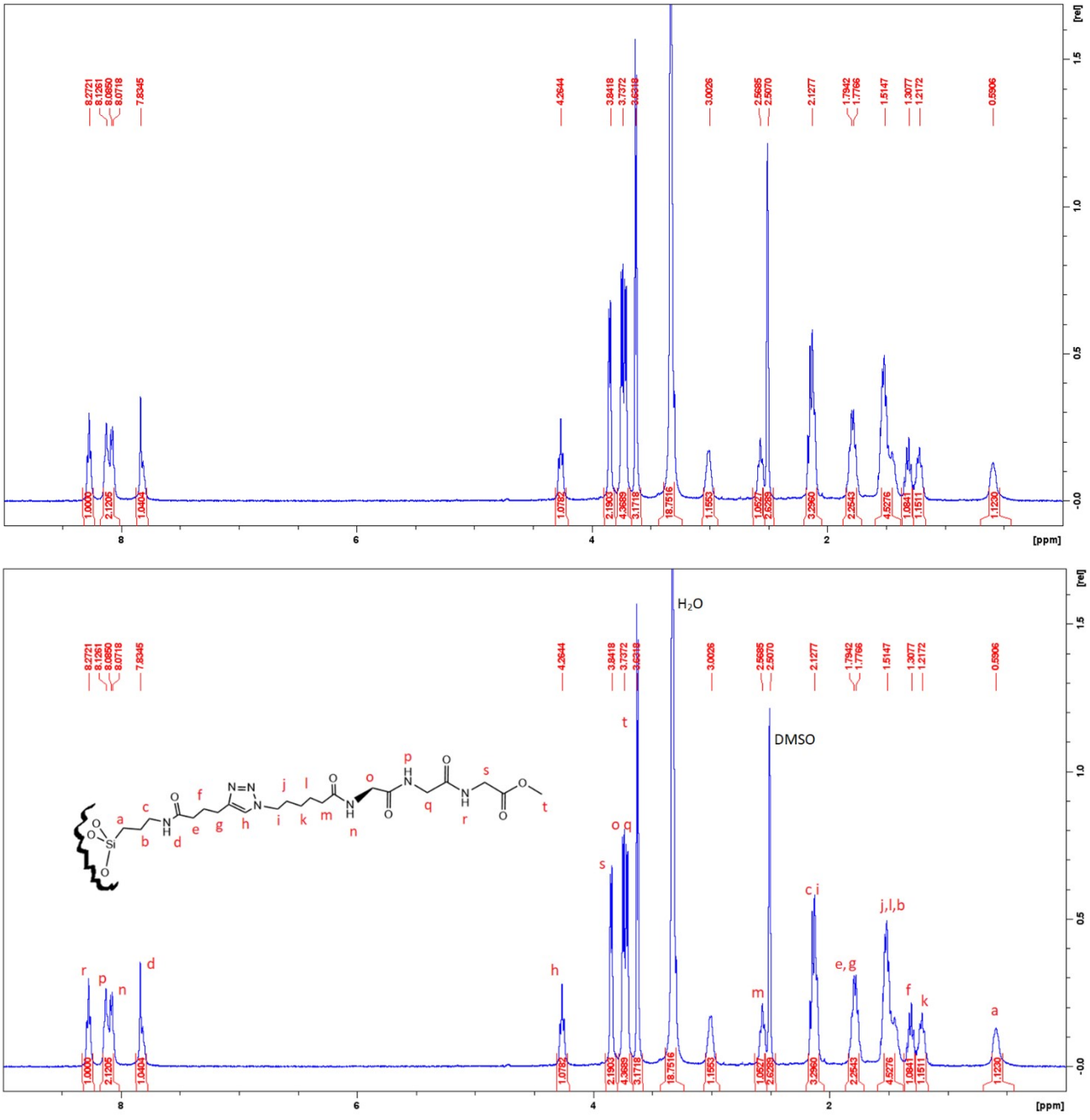

Figure S25 - NMR ^{1}H of (**5a**) (annotated – bottom, unannotated – top) (400 MHz, DMSO-d^{6}, δ, ppm): 8.27 (t, 1 H, Si-R-gly-gly-**NH**-CH_2-C(=O)-OMe), 8.13-8.09 (m, 2 x 1 H, Si-R-**NH**-CH_2-C(=O)-**NH**-CH_2-C(=O)-gly-OMe), 7.83 (s, 1H, Si-R-**NH**-C(=O)-R-triazole-R), 4.26 (t, 1 H, Si-R-triazole(=**CH**-N-R)-R), 3.84 (d, 2 H, Si-R-gly-gly-NH-**CH_2**-C(=O)-OMe), 3.74 (m, 2 x 2 H, Si-R-triazole-R-NH-**CH_2**-C(=O)-NH-**CH_2**-C(=O)-gly-OMe), 3.63 (s, 3 H, Si-R-gly-gly-gly-O-**CH_3**), 2.57 (t, 3 H, R-$(CH_2)_4$-**CH_2**-C(=O)-gly-gly-gly-OMe, 2.13 (m, 4 H, Si-$(CH_2)_2$-**CH_2**-NH-C(=O)-R-triazole-**CH_2**-R), 1.79-1.78 (m, 2 H, Si-$(CH_2)_3$-NH-C(=O)-**CH_2**-CH_2-**CH_2**-triazole-R), 1.51 (m, 6 H, Si-CH_2-**CH_2**-CH_2-R-triazole-CH_2-**CH_2**-CH_2-**CH_2**-CH_2-C(=O)-R), 1.31 (m, 2 H, Si-R-NH-C(=O)-CH_2-**CH_2**-CH_2-triazole-R), 1.22 (t, 2 H, Si-R-triazole-$(CH_2)_2$-**CH_2**-$(CH_2)_2$-C(=O)-R), 0.59 (t, 2 H, Si-**CH_2**-$(CH_2)_2$-R)

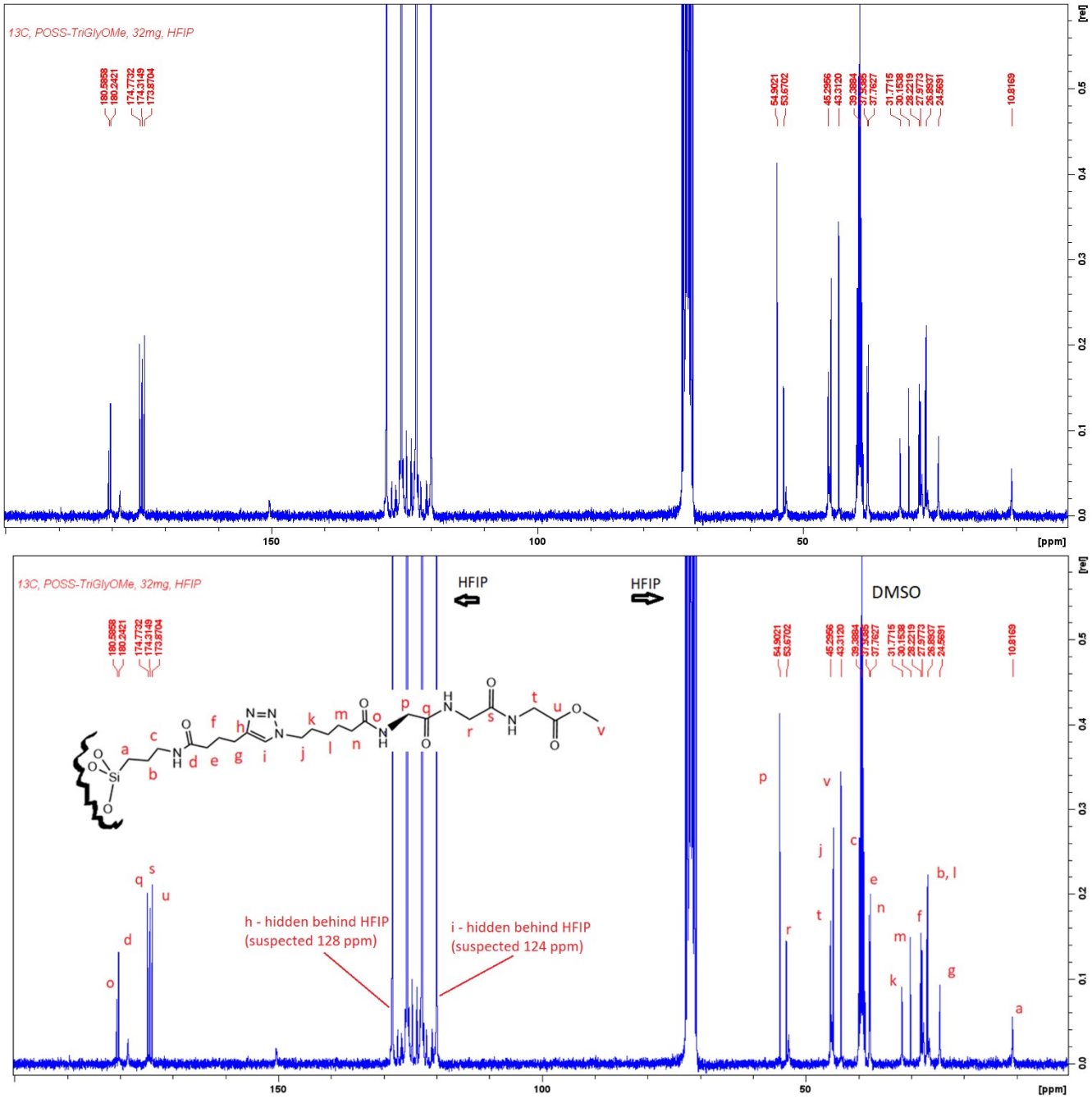

Figure S26 - NMR ^{13}C of (**5a**) (top – unannotated, bottom - annotated) (100 MHz, DMSO-d^{6}, δ, ppm): 180.59 (s, Si-R-triazole-$(CH_2)_5$-**C**(=O)-R), 180.24 (s, Si-$(CH_2)_3$-NH-**C**(=O)-R-triazole-R), 174.77 (s, Si-R-triazole-R-C(=O)NH-CH_2-**C**(=O)-gly-gly-OMe), 174.31 (s, Si-R-triazole-R-gly-NH-CH_2-**C**(=O)-gly-OMe), 173.87 (s, Si-R-triazole-R-gly-gly-NH-CH_2-**C**(=O)-OMe), 128.00-124.00 (predicted, (Si-$(CH_2)_2$-CH_2-NH-C(=O)-$(CH_2)_2$-**C**(-N=N-)=**C**-N(-N-)-R-OMe), 54.90 (s, Si-R-triazole-R-

NH-**C**H_2-C(=O)-gly-gly-OMe), 53.67 (s, Si-R-triazole-R-gly-NH-**C**H_2-C(=O)-gly-OMe), 45.30 (m, Si-R-NH-C(=O)-$(CH_2)_3$-triazole-**C**H_2-$(CH_2)_4$-C(=O)-gly-gly-NH-**C**H_2-C(=O)-OMe), 43.31 (s, Si-R-triazole-R-gly-gly-gly-O-**C**H_3), 40.49 (s, Si-$(CH_2)_2$-**C**H_2-R-OMe), 37.76 (s, (Si-$(CH_2)_2$-CH_2-NH-C(=O)-**C**H_2-$(CH_2)_2$-triazole-R), 37.76 (s, Si-R-triazole-$(CH_2)_4$-**C**H_2-C(=O)NH-R), 31.77 (s, Si-R-triazole-CH_2-**C**H_2-$(CH_2)_3$-C(=O)NH-R), 30.15 (s, Si-R-triazole-(CH_2)3-**C**H2-CH_2-C(=O)NH-R), 28.22 (s, Si-$(CH_2)_3$-NH-C(=O)-CH_2-**C**H_2-CH_2-triazole-R), 27.98 (s, Si-CH_2-**C**H_2-CH_2-R), 26.89 (s, Si-R-triazole-$(CH_2)_2$-**C**H_2-$(CH_2)_2$-R), 24.57 (s, Si-R-triazole-$(CH_2)_3$-**C**H_2-CH_2-R), 10.82 (s, Si-**C**H_2-$(CH_2)_2$-R).

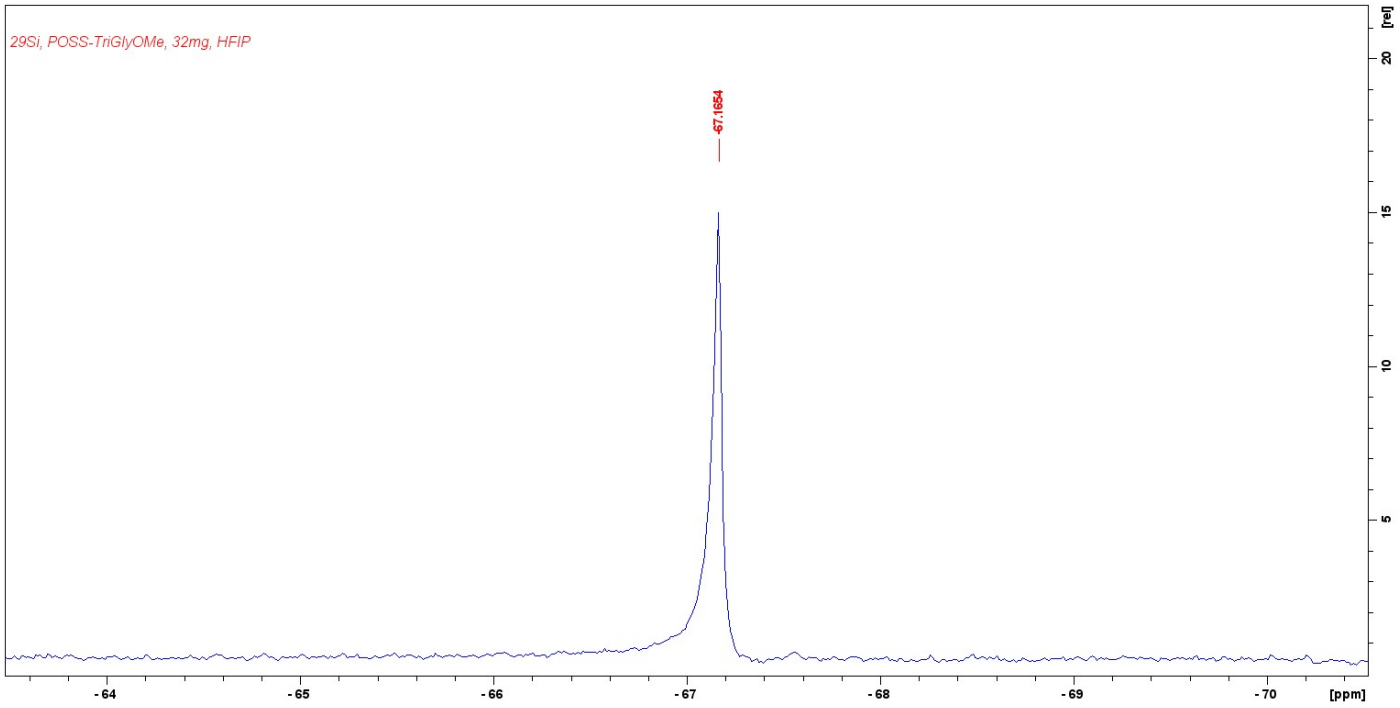

Figure S27 – NMR ^{29}Si of (**5a**) (105.7 MHz, DMSO-d^6, δ, ppm): -67.17

FTIR: Analysis confirms successful triazole formation between (**2a**) and (**4**) following CuAAC "click" reactions (**Figure S28**). The "click" product (**5a**) (**Figure S28** (**c**)), shows no bands relating to the azide group of (**2a**) at 2088.46 cm^{-1} (**Figure S28** (**b**)), nor the octa-alkyne terminus of (**4**) at 2117.46 cm^{-1} (**Figure S28** (**a**)).

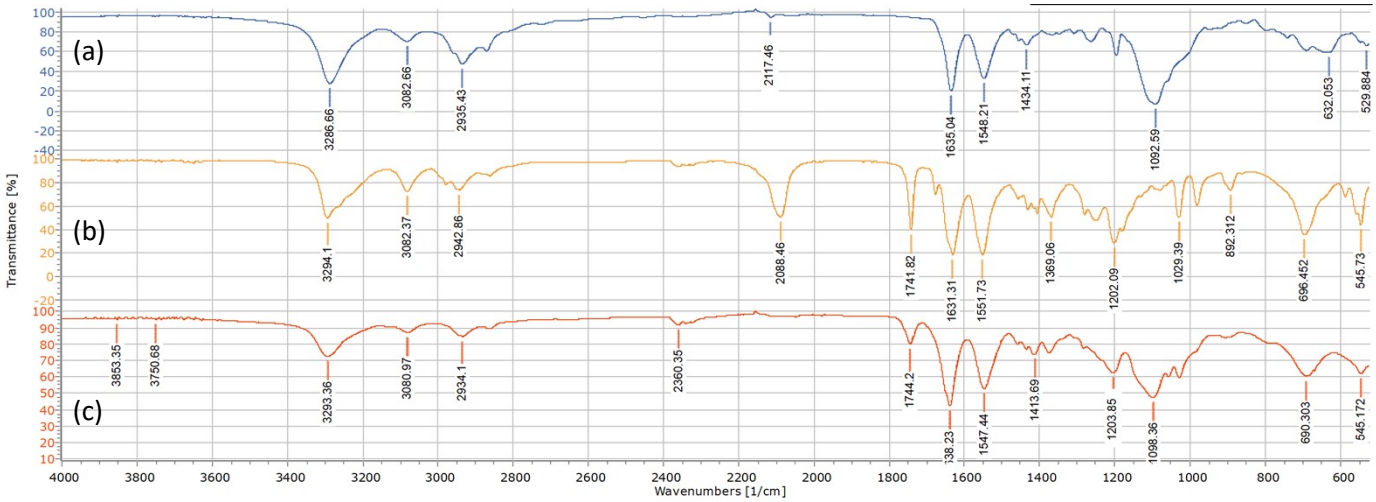

Figure S28 – FTIR of compound (**4**) (a), (**2a**) (b) & (**5a**) (c).

7. Synthesis of POSS-octa-trialanine methyl ester (T_8[(6-(4-(4-oxo-4-(propylamino)butyl)-1H-1,2,3-triazol-1-yl)hexanoyl)trialanine methyl ester]$_8$) nanocages through CuAAC "click" reaction (5b) – (Figures S29-S32)

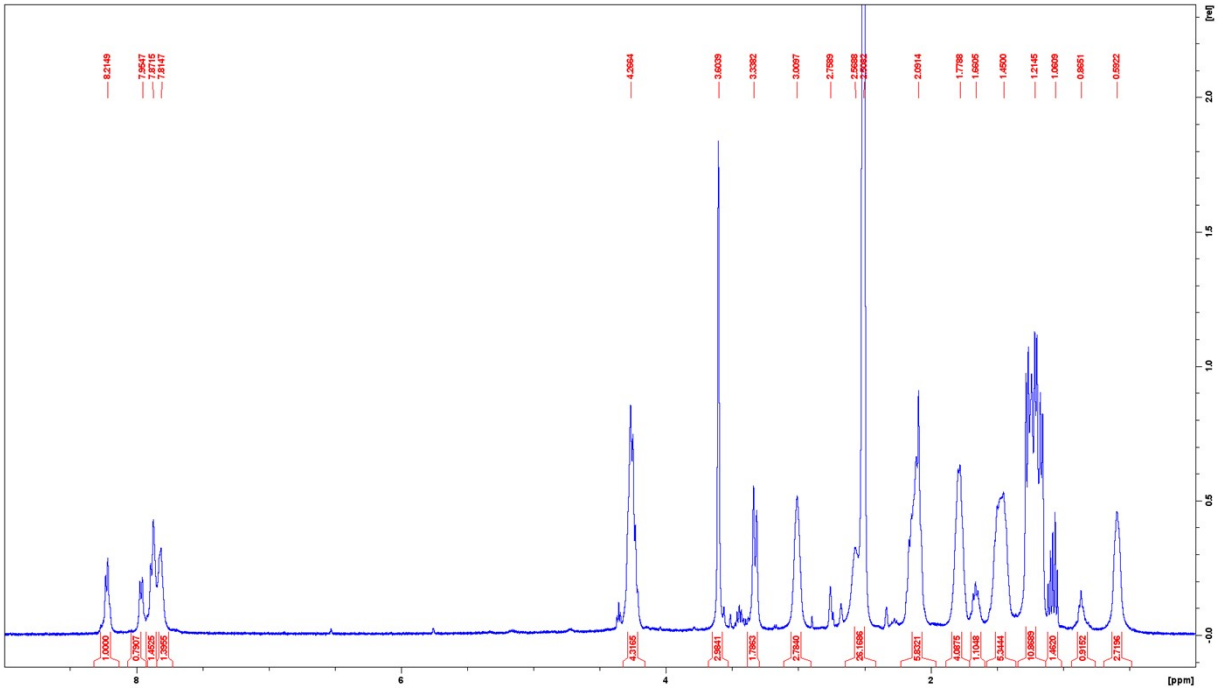

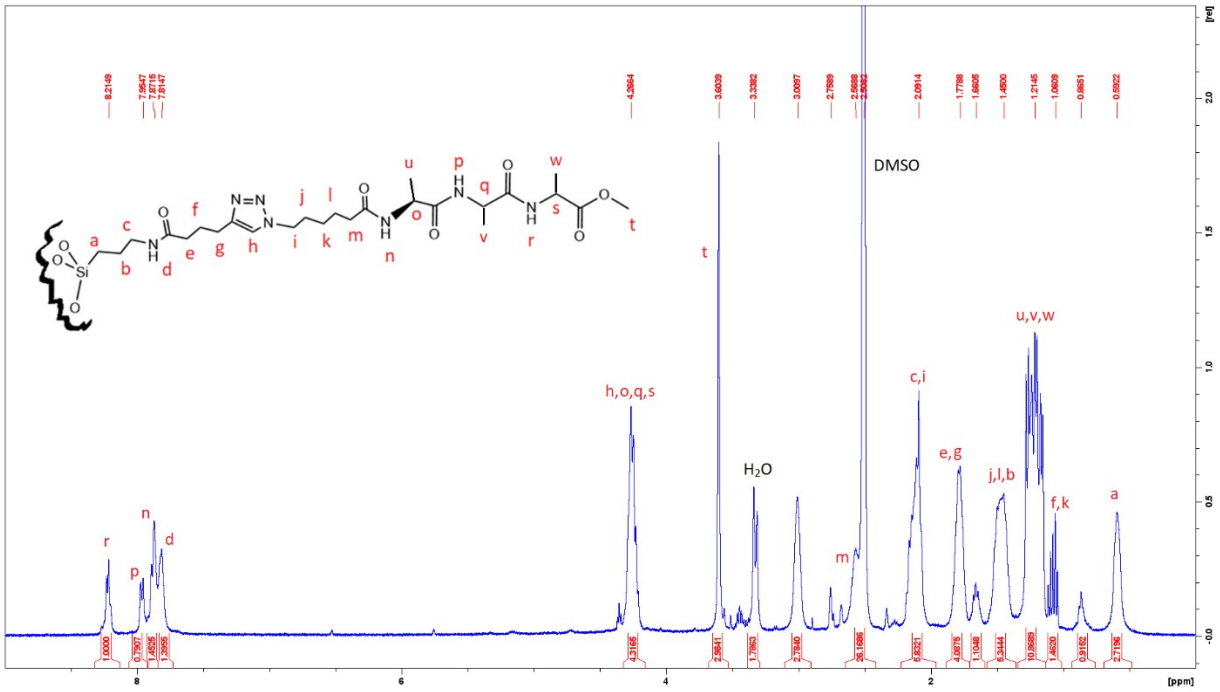

Figure S29 – NMR ^{1}H of (**5b**) (annotated – bottom, unannotated – top) (400 MHz, DMSO-d^{6}, δ, ppm): 8.21 (t, 1 H, Si-R-ala-ala-**NH**-CH(Me)-C(=O)-OMe), 7.95 (t, 1 H, Si-R-NH-ala-**NH**-CH(Me)-C(=O)-ala-OMe), 7.81-7.87 (m, 2 x 1H, Si-R-**NH**-C(=O)-R-triazole-R-**NH**-CH(Me)-C(=O)-ala-ala-OMe), 4.26 (m, 4 x 1 H, Si-R-triazole(=**CH**-N-R)-NH-**CH**(Me)-C(=O)-NH-**CH**(Me)-C(=O)-NH-**CH**(Me)-C(=O)-OMe), 3.60 (s, 3 H, Si-R-ala-ala-ala-O-**CH_3**), 2.57 (t, 2 H, R-$(CH_2)_4$-**CH_2**-C(=O)-ala-ala-ala-OMe), 2.09 (m, 6 H, Si-$(CH_2)_2$-**CH_2**-NH-C(=O)-R-triazole-**CH_2**-R), 1.78 (m, 4 H, Si-$(CH_2)_3$-NH-C(=O)-**CH_2**-CH_2-**CH_2**-triazole-R), 1.50 (m, 6 H, Si-CH_2-**CH_2**-CH_2-R-triazole-CH_2-**CH_2**-CH_2-**CH_2**-CH_2-C(=O)-R), 1.21 (m, 11 H, Si-R-NH-C(=O)-CH_2-**CH_2**-CH_2-triazole-ala(**Me**)-ala(**Me**)-ala(**Me**)-OMe), 1.10 (m, 2 H, Si-R-triazole-$(CH_2)_2$-**CH_2**-$(CH_2)_2$-C(=O)-R), 0.59 (t, 2 H, Si-**CH_2**-$(CH_2)_2$-R)

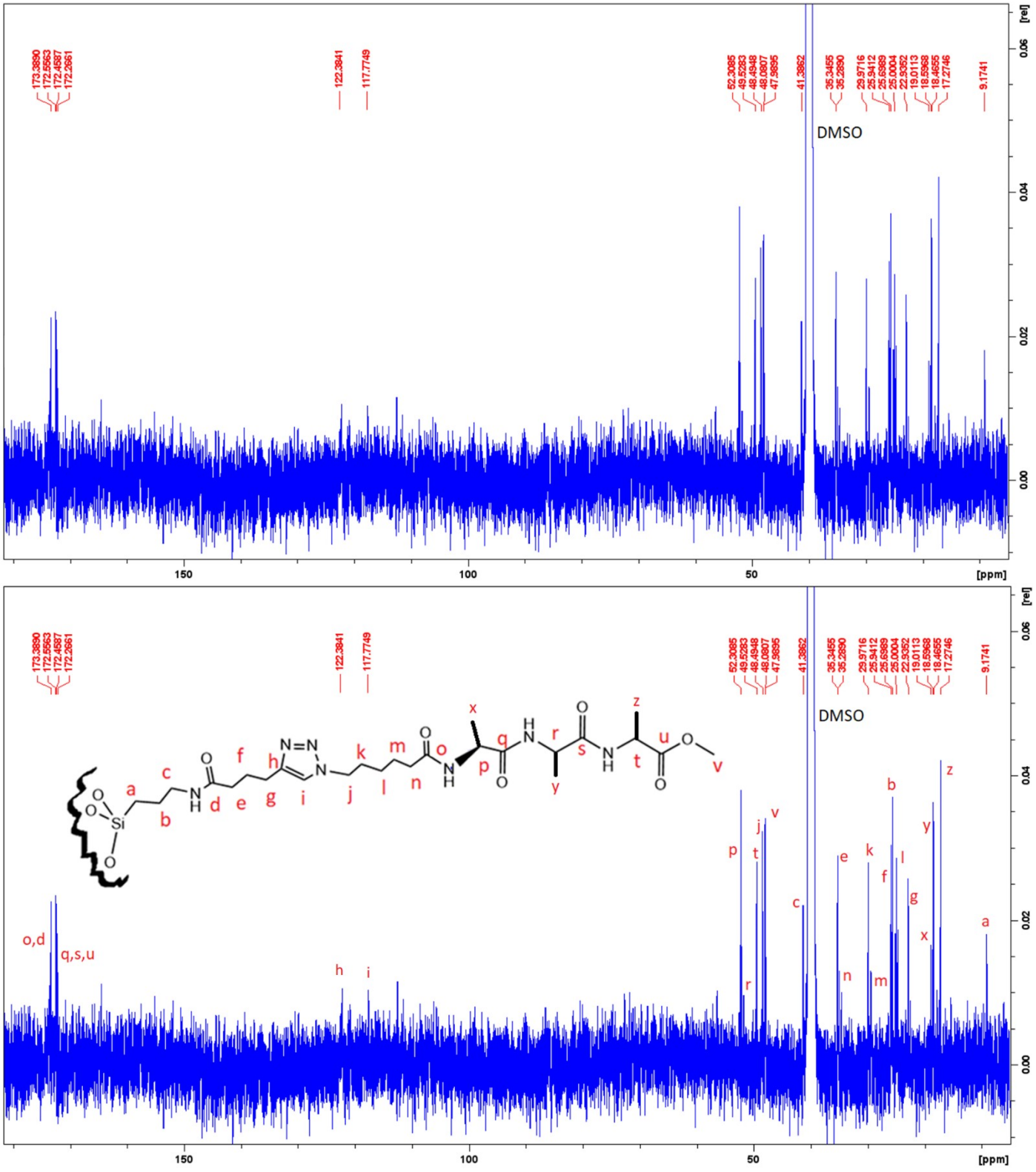

Figure S30 - NMR ^{13}C of (**5b**) (top – unannotated, bottom - annotated) (100 MHz, DMSO-d^6, δ, ppm): 173.39-172.56 (m, Si-$(CH_2)_3$-NH-**C**(=O)-R-triazole-$(CH_2)_5$-**C**(=O)-ala-ala-ala-OMe), 172.46-172.27 (m, Si-$(CH_2)_3$-NH-**C**(=O)-R-triazole-R-NH-CH(Me)-**C**(=O)NH-CH(Me)-**C**(=O)-NH-CH(Me)-**C**(=O)-OMe), 122.38 (s, Si-R-$(CH_2)_3$- **C**(-N=N-)=C-N(-N-)-R-OMe), 117.77 (s, Si-R-$(CH_2)_3$- C(-N=N-)=**C**-N(-N-)-R-OMe), 52.31 (m, Si-R-triazole-R-NH-**C**H(Me)-C(=O)-NH-**C**H(Me)-C(=O)-ala-OMe), 49.53 (s, Si-R-triazole-R-ala-ala-NH-**C**H_2-C(=O)-OMe), 48.49 (s, (Si-R-triazole-**C**H_2-$(CH_2)_4$-C(=O)-R), 47.99 (s, Si-R-triazole-R-ala-ala-ala-O-**C**H_3), 41.39 (s, Si-$(CH_2)_2$-**C**H_2-R-OMe), 35.35 (s, Si-$(CH_2)_3$-NH-C(=O)-**C**H_2-$(CH_2)_2$-triazole-R), 35.28 (s, Si-R-triazole-$(CH_2)_4$-**C**H_2-C(=O)NH-R), 29.97 (m, Si-R-triazole-CH_2-**C**H_2-CH_2-**C**H_2-CH_2-C(=O)NH-R), 25.70 (m, Si-CH_2-**C**H_2-CH_2-NH-C(=O)-CH_2-**C**H_2-CH_2-triazole-$(CH_2)_2$-**C**H_2-$(CH_2)_2$-R), 22.94 (s, Si-R-**C**H_2-triazole-R), 19.01-17.27 (3 s, Si-R-NH-CH(**Me**)-C(=O)NH-CH(**Me**)-C(=O)-NH-CH(**Me**)-C(=O)-OMe), 9.17 (s, Si-**C**H_2-$(CH_2)_2$-R).

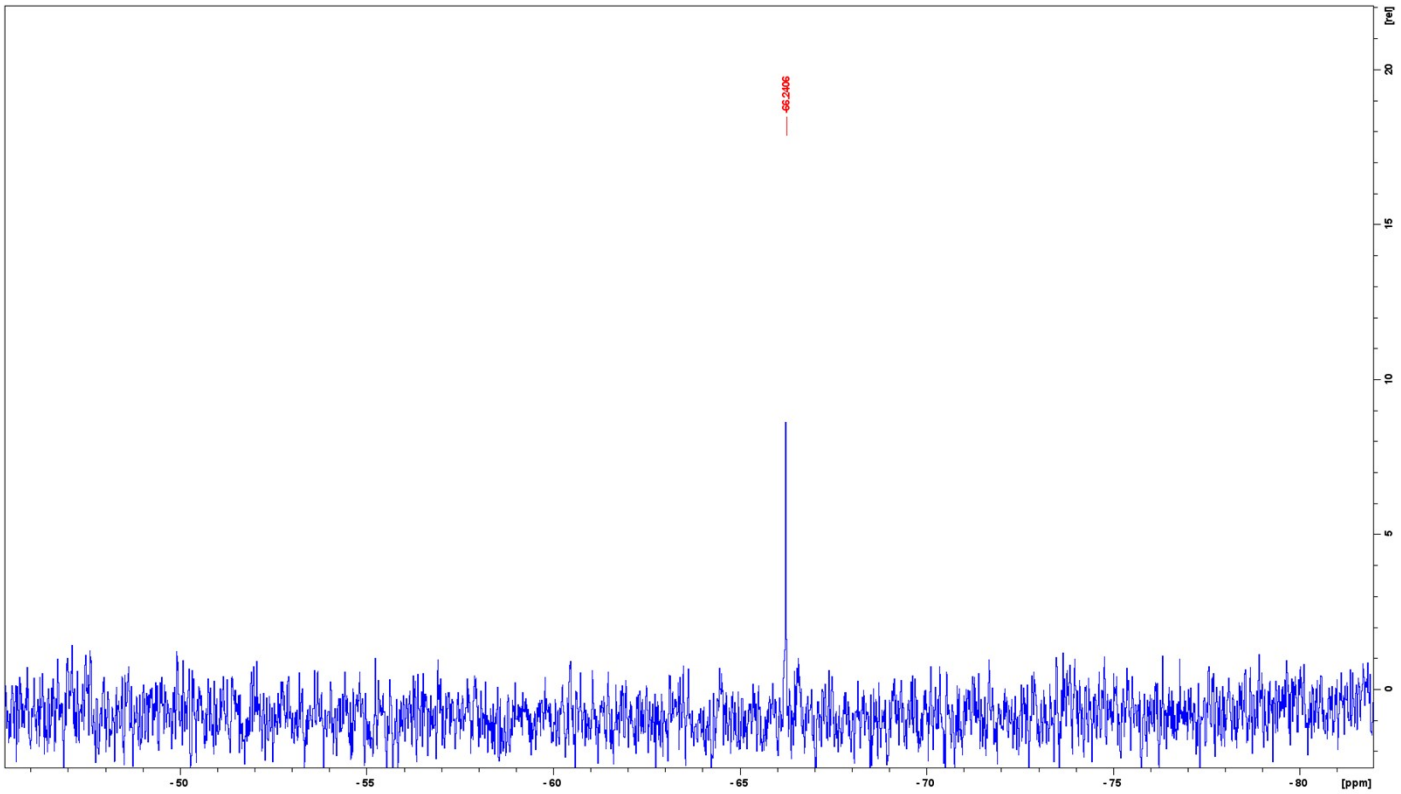

Figure S31 - NMR ^{29}Si of (**5b**) (105.7 MHz, DMSO-d^6, δ, ppm): -66.24

FTIR: Analysis confirms successful triazole formation between (**2b**) and (**4**) following CuAAC "click" reactions (**Figure S32**). The "click" product (**5b**) (**Figure S32** (**c**)), shows no bands relating to the azide group of (**2b**) at 2092.26 cm^{-1} (**Figure S32** (**b**)), nor the octa-alkyne terminus of (**4**) at 2117.46 cm^{-1} (**Figure S32** (**a**)).

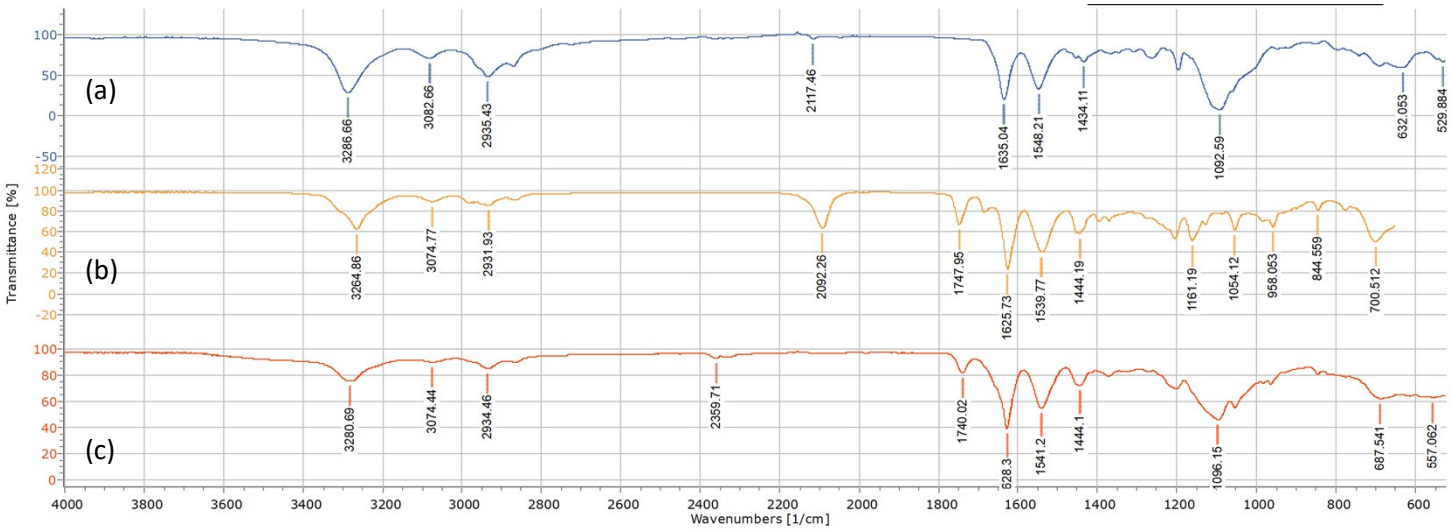

Figure S32 – FTIR of compound (**4**) (a), (**2b**) (b) & (**5b**) (c).

8. Synthesis of 1-azidohexane– (Figures S33-S34)

yield: 86%

NMR: Confirmation of 1-azidohexane synthesis was established through NMR ^{1}H and ^{13}C, **Figures S33** & **S34**, respectively.

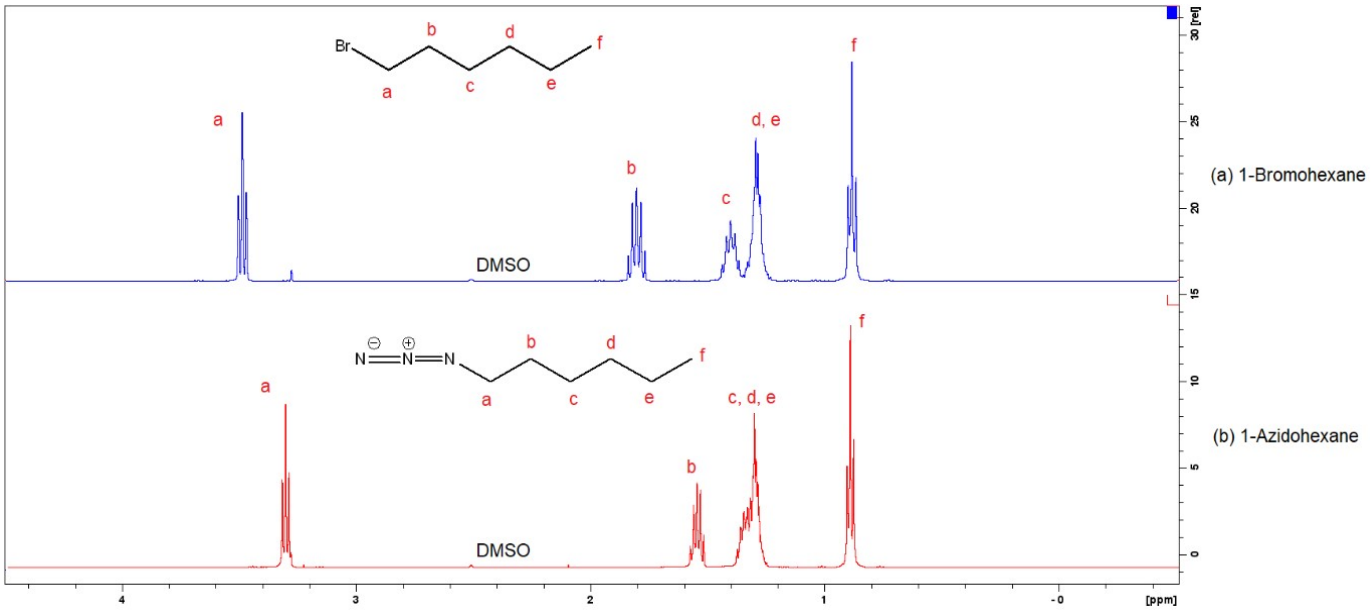

Figure S33 - ^{1}H NMR of 1-Bromohexane (a) and 1-Azidohexane (b) following substitution reaction. NMR ^{1}H of 1-azidohexane (400 MHz, DMSO-d^6, δ, ppm): 3.30 (t, 3 H, N_3-**CH_2**-$(CH_2)_4$-CH_3), 1.54 (p, 2 H, N_3-CH_2-**CH_2**-$(CH_2)_3$-CH_3), 1.31-1.30 (m, 6 H, N_3-$(CH_2)_2$-**$(CH_2)_3$**-CH_3), 0.89 (t, 3 H, N_3-$(CH_2)_5$-**CH_3**).

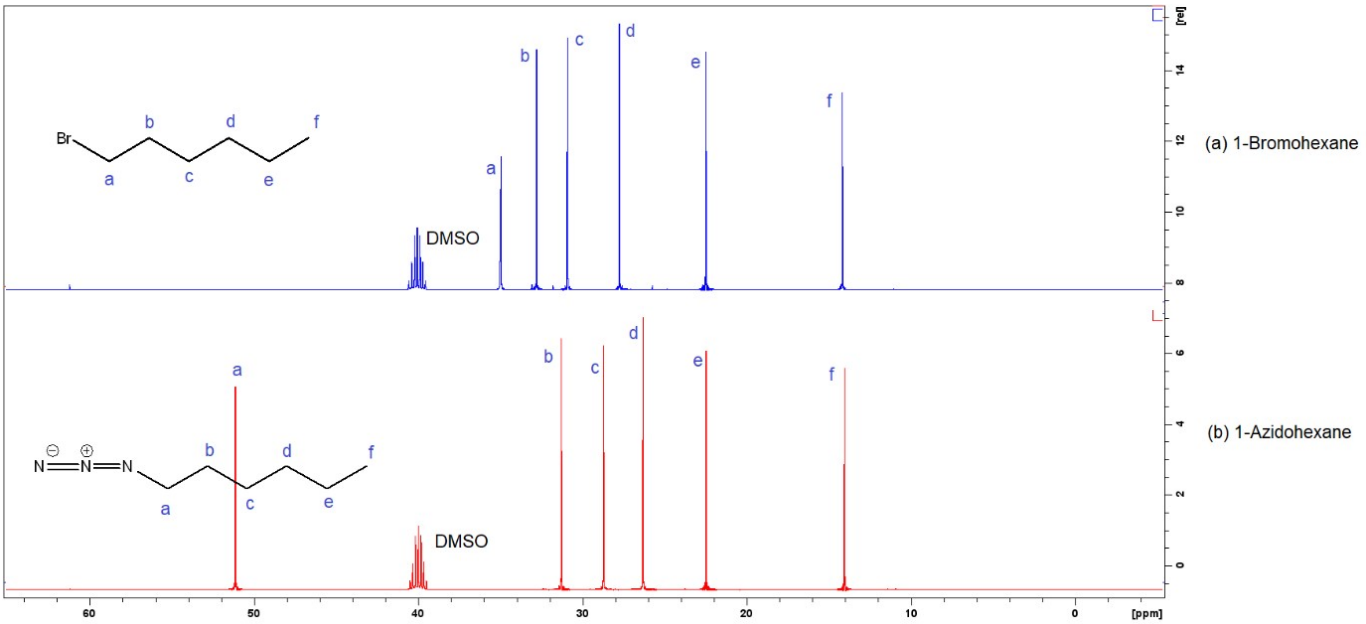

Figure S34 - ^{13}C NMR of 1-Bromohexane (a) and 1-Azidohexane (b) following substitution reaction. NMR ^{13}C of 1-azidohexane (100 MHz, DMSO-d^6, δ, ppm): 51.13 (s, N_3-**C**H_2-$(CH_2)_4$-CH_3), 31.29 (s, N_3-CH_2-**C**H_2-$(CH_2)_3$-CH_3), 28.72 (s, N_3-$(CH_2)_2$-**C**H_2-$(CH_2)_2$-CH_3), 26.31 (s, N_3-$(CH_2)_3$-**C**H_2-CH_2-CH_3), 22.47 (s, N_3-$(CH_2)_4$-**C**H_2-CH_3), 14.05 (s, N_3-$(CH_2)_5$-**C**H_3).

9. The effect of $CuSO_4$ concentration on CuAAC "click" reactions between (2a) and (4) – (Figures S35-S39)

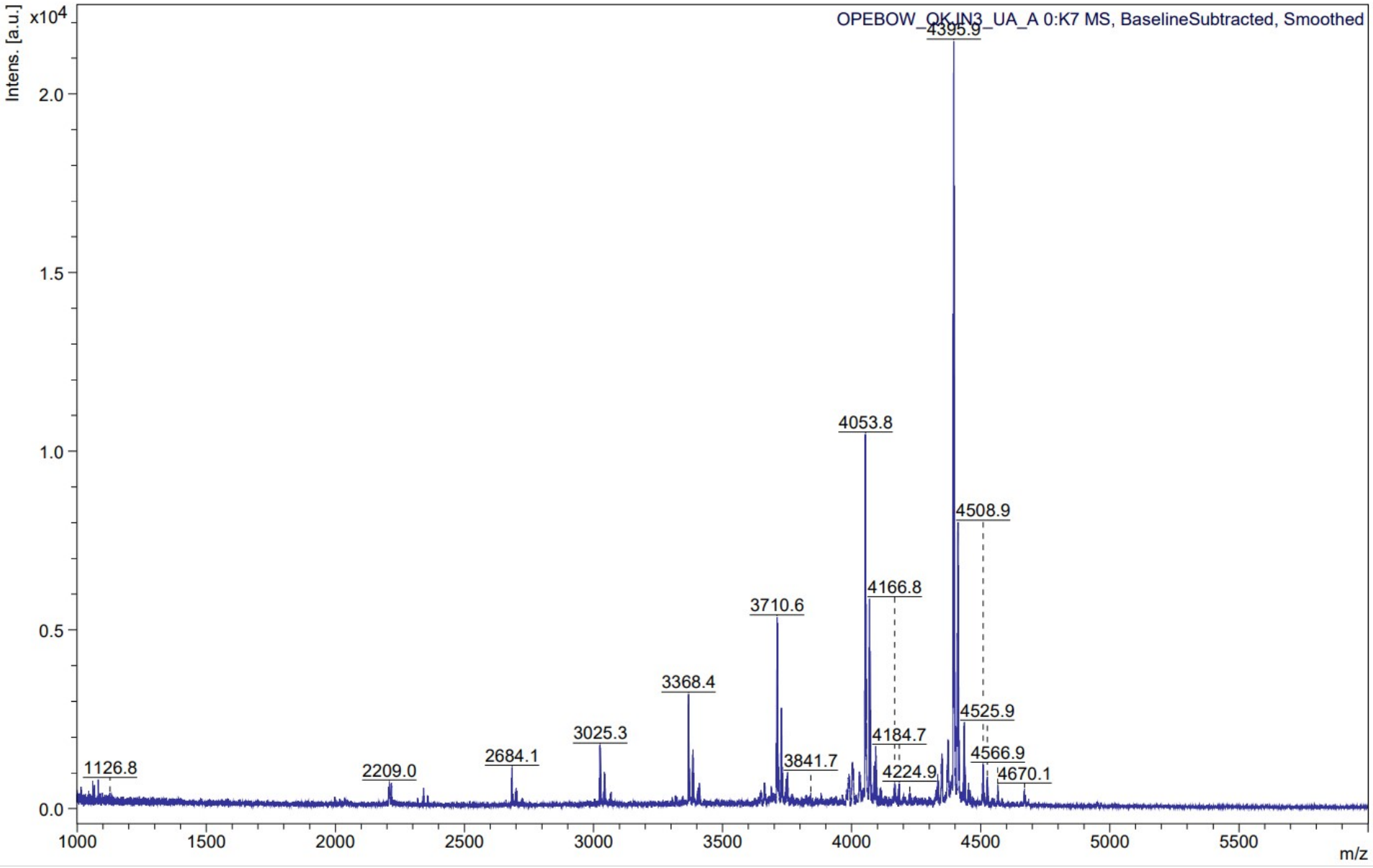

Figure S35 – MALDI-ToF mass spectrum of product (**5a**) formation at 72-hrs. Reaction conditions: **Table 1 A**

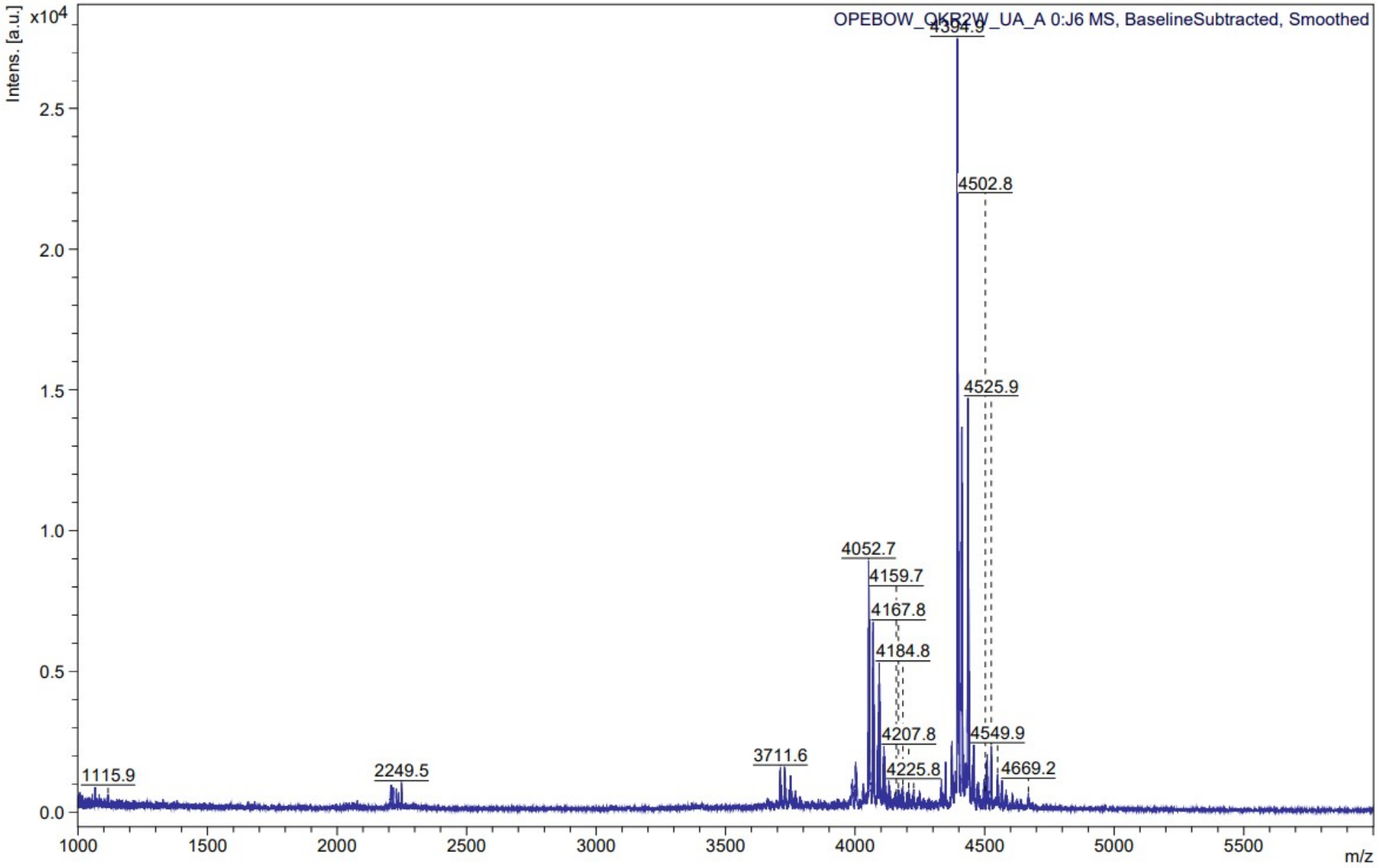

Figure S36 – MALDI-ToF mass spectrum of product (**5a**) formation at 72-hrs. Reaction conditions: **Table 1 B**

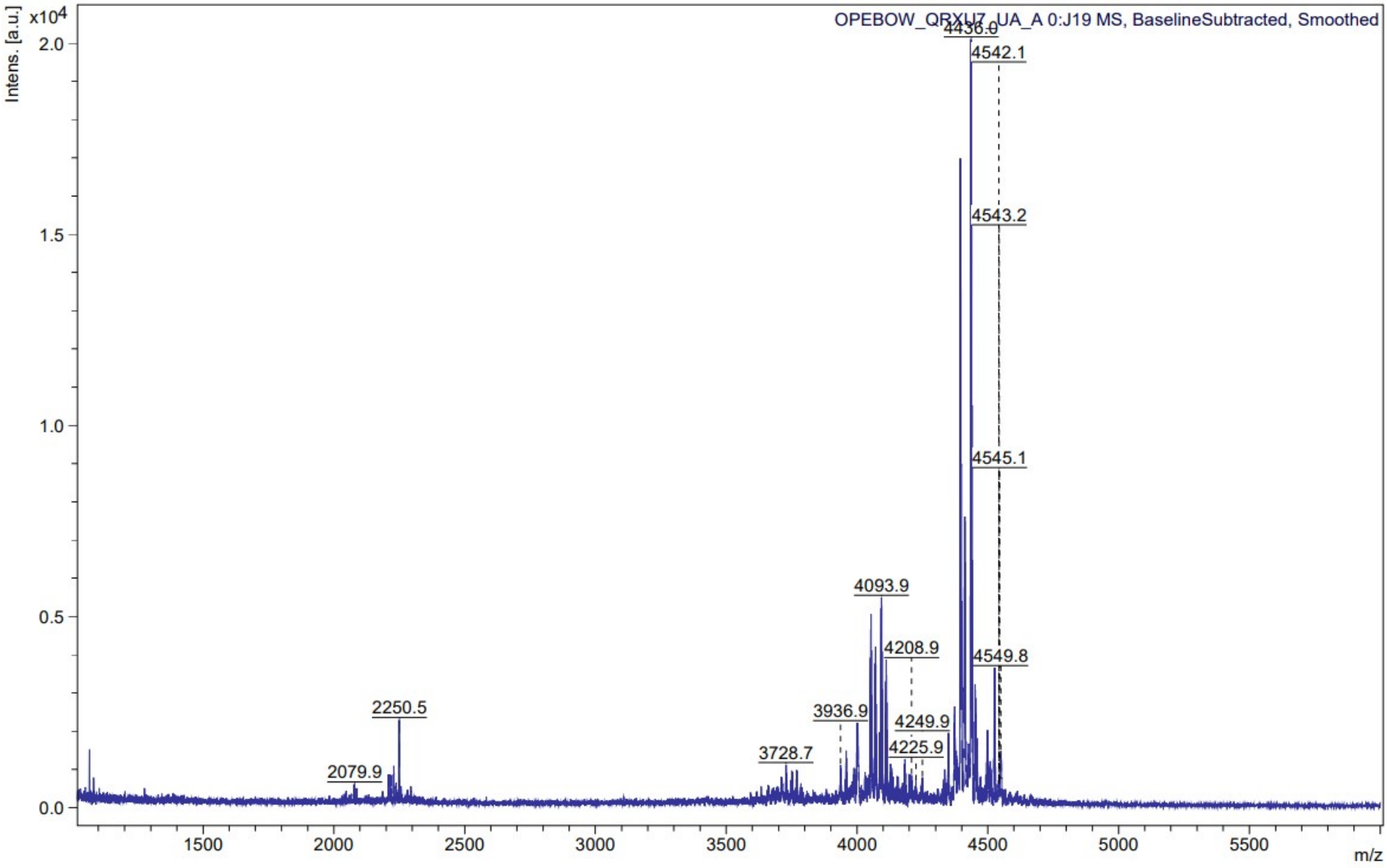

Figure S37 – MALDI-ToF mass spectrum of product (**5a**) formation at 72-hrs. Reaction conditions: **Table 1 C**

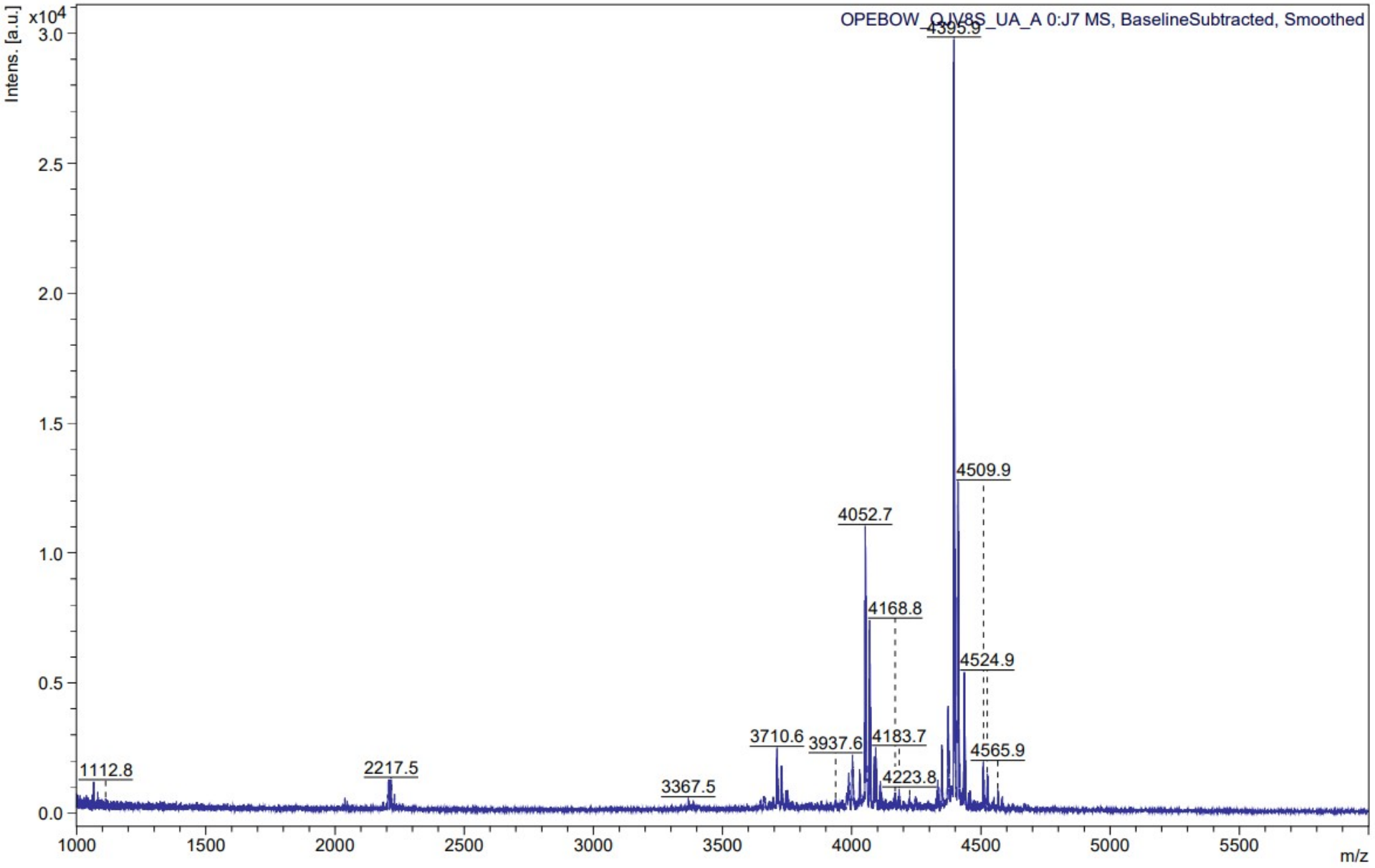

Figure S38 – MALDI-ToF mass spectrum of product (**5a**) formation at 72-hrs. Reaction conditions: **Table 1 D**

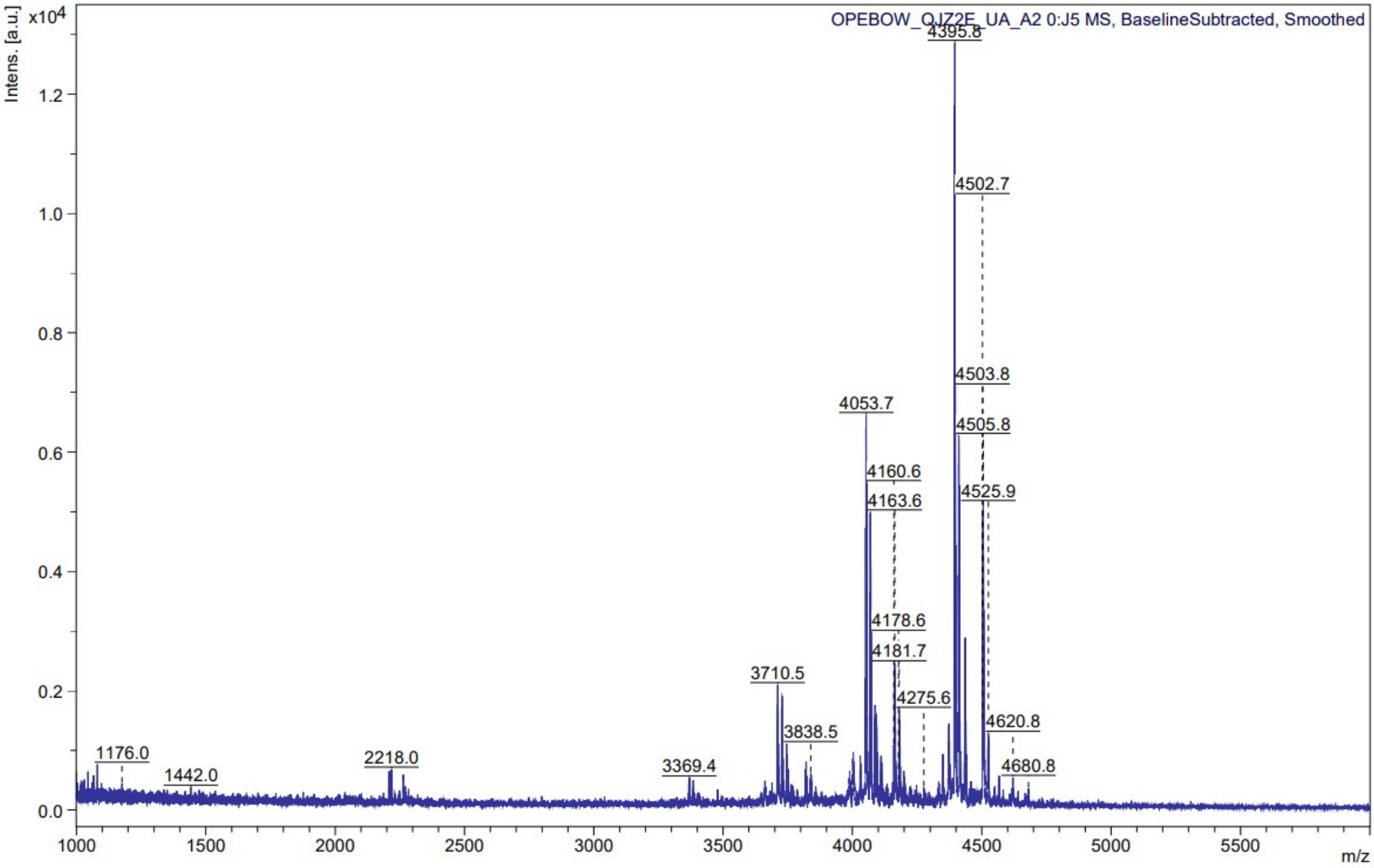

Figure S39 – MALDI-ToF mass spectrum of product (**5a**) formation at 72-hrs. Reaction conditions: **Table 1 E**

10. The effect of temperature on CuAAC "click" reactions between (2a) and (4), in addition to product formations relative to time – (Figures S40-S51)

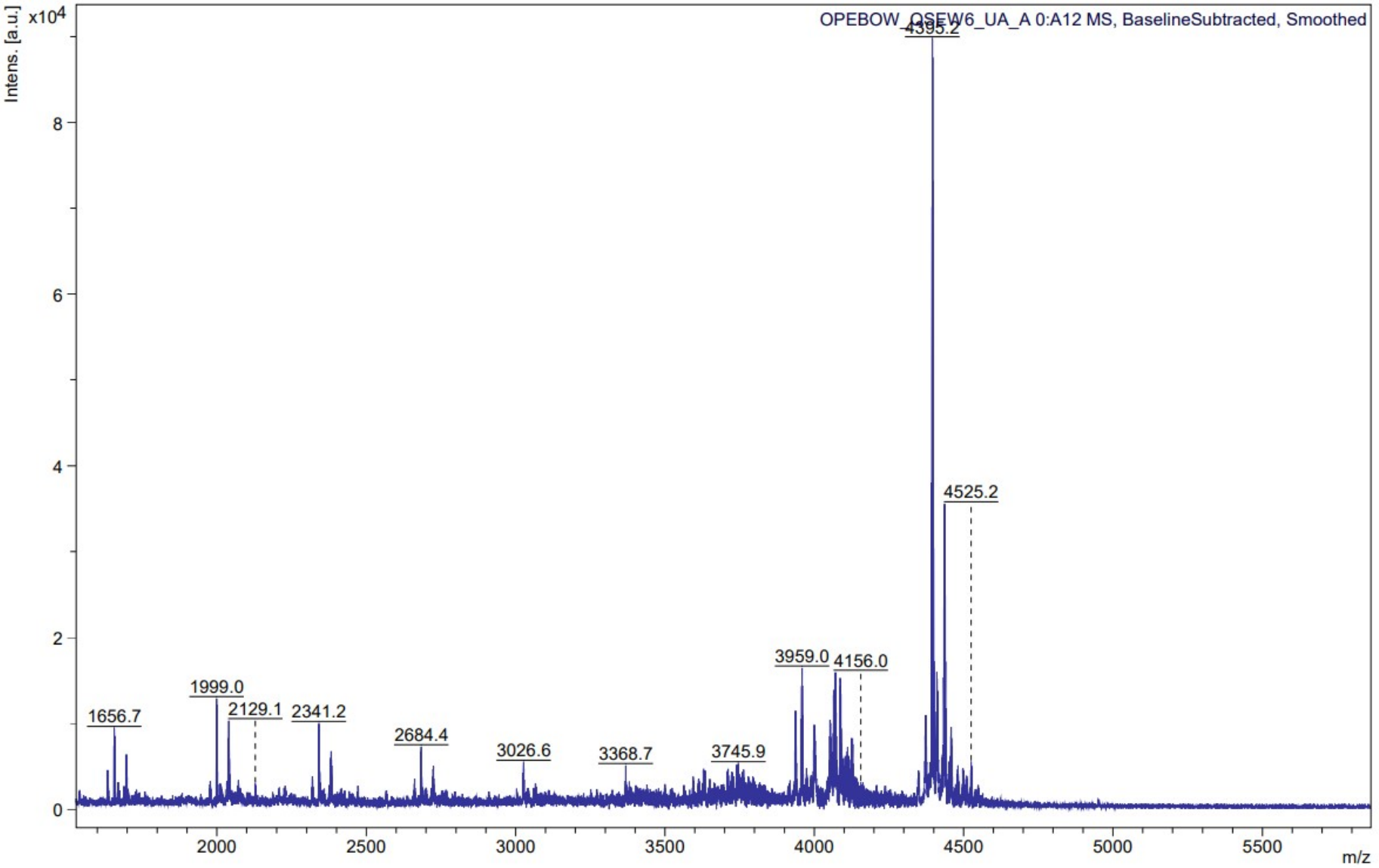

Figure S40 – MALDI-ToF mass spectrum of product (**5a**) formation at 2-hrs. Reaction conditions: (**4**):(**2a**):**$CuSO_4$**:**NaAscorbate 1:16:4:4.4.** 25°C.

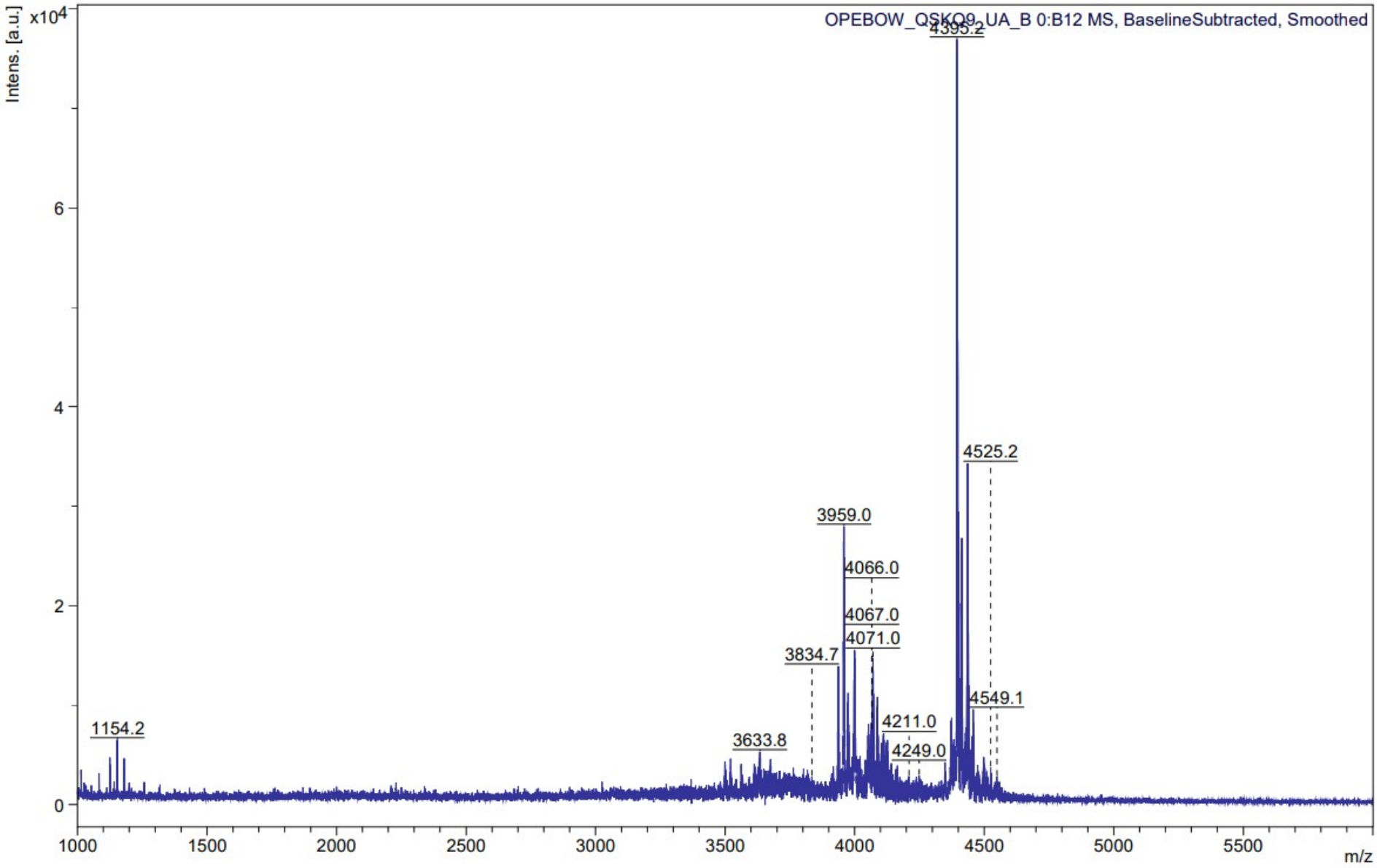

Figure S41 – MALDI-ToF mass spectrum of product (**5a**) formation at 5-hrs. Reaction conditions: (**4**):(**2a**):**$CuSO_4$**:**NaAscorbate 1:16:4:4.4.** 25°C.

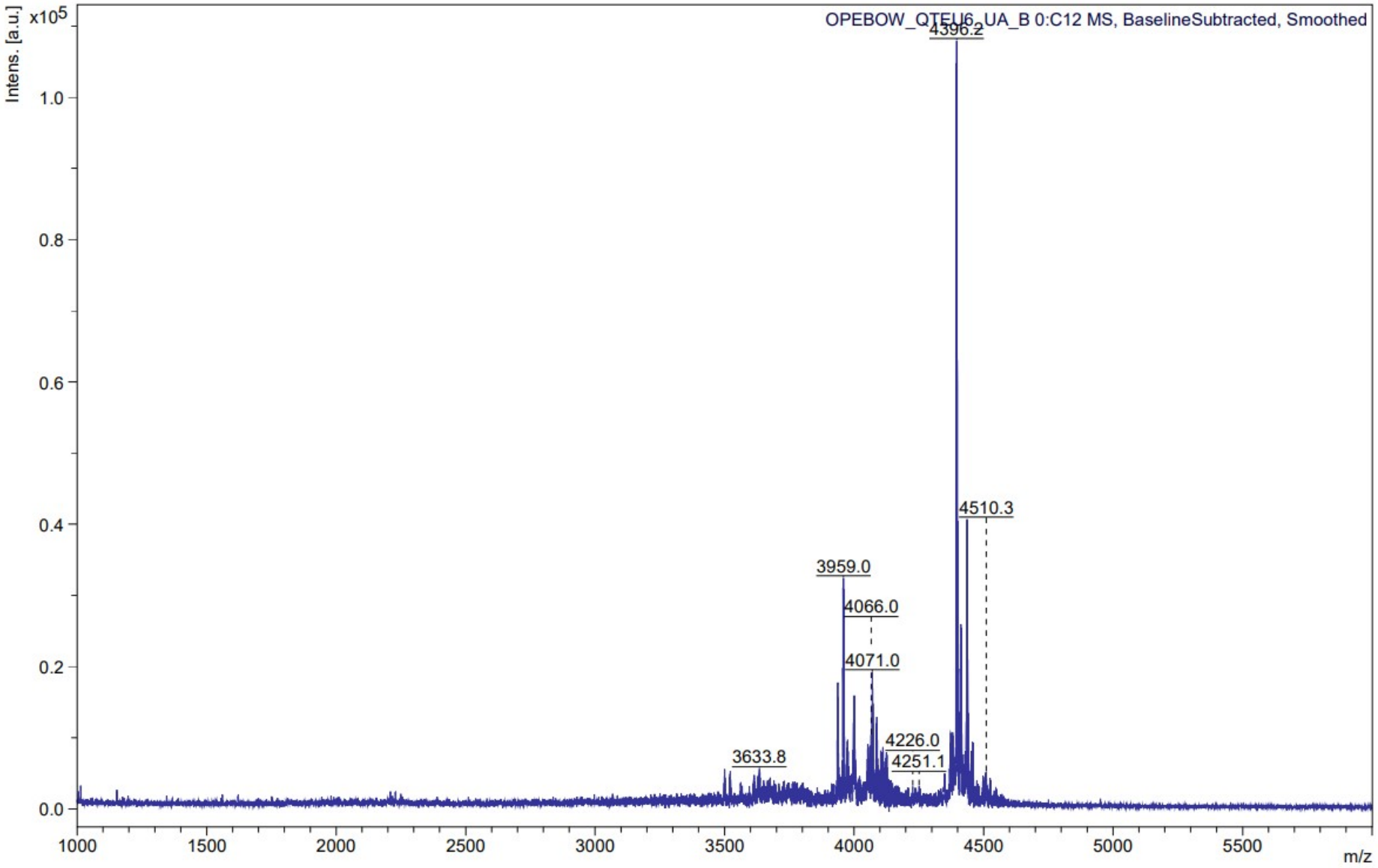

Figure S42 – MALDI-ToF mass spectrum of product (**5a**) formation at 21-hrs. Reaction conditions: (**4**):(**2a**):**$CuSO_4$**:**NaAscorbate 1:16:4:4.4.** 25°C.

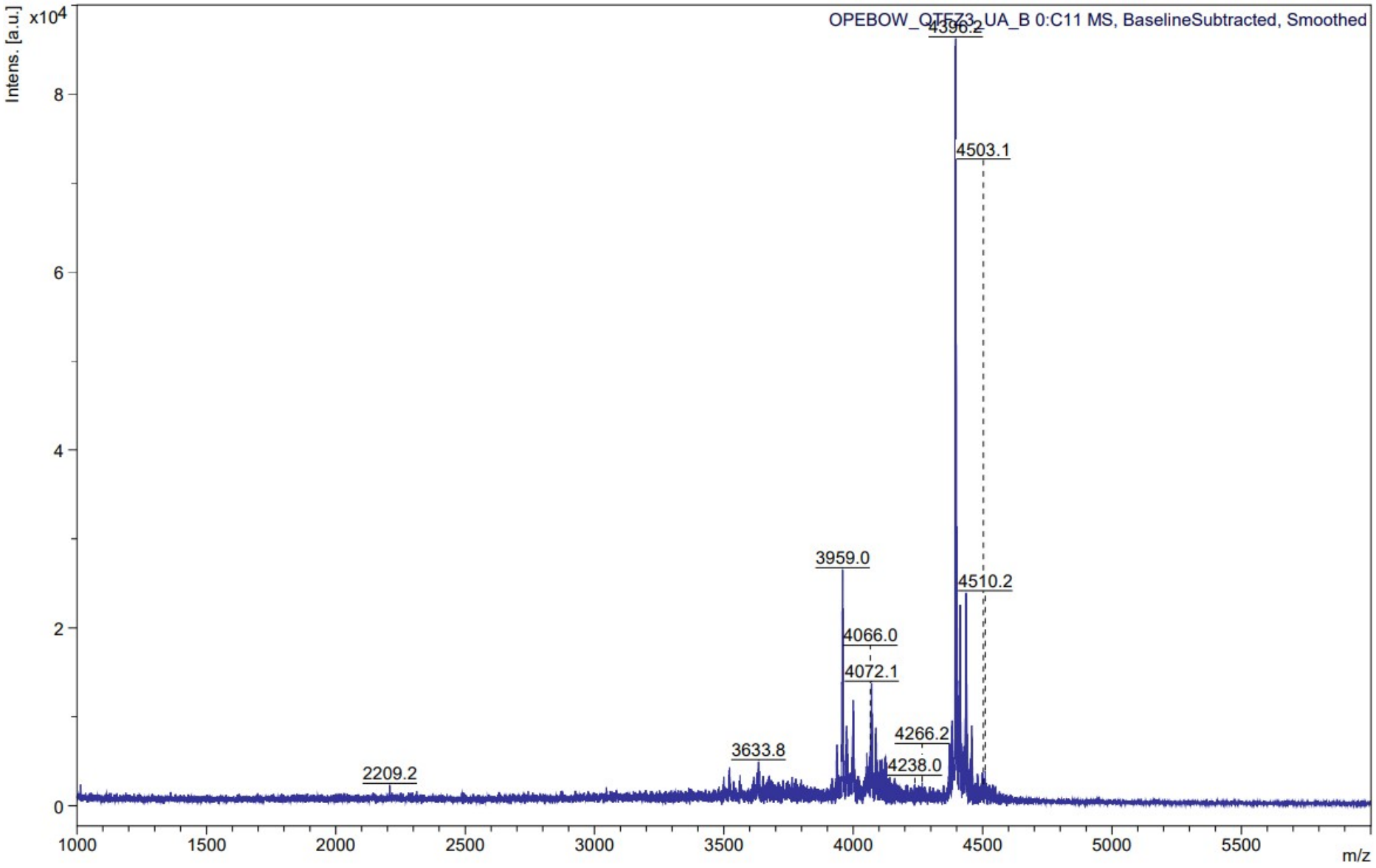

Figure S43 – MALDI-ToF mass spectrum of product (**5a**) formation at 27-hrs. Reaction conditions: (**4**):(**2a**):**$CuSO_4$**:**NaAscorbate 1:16:4: 4.4.** 25°C.

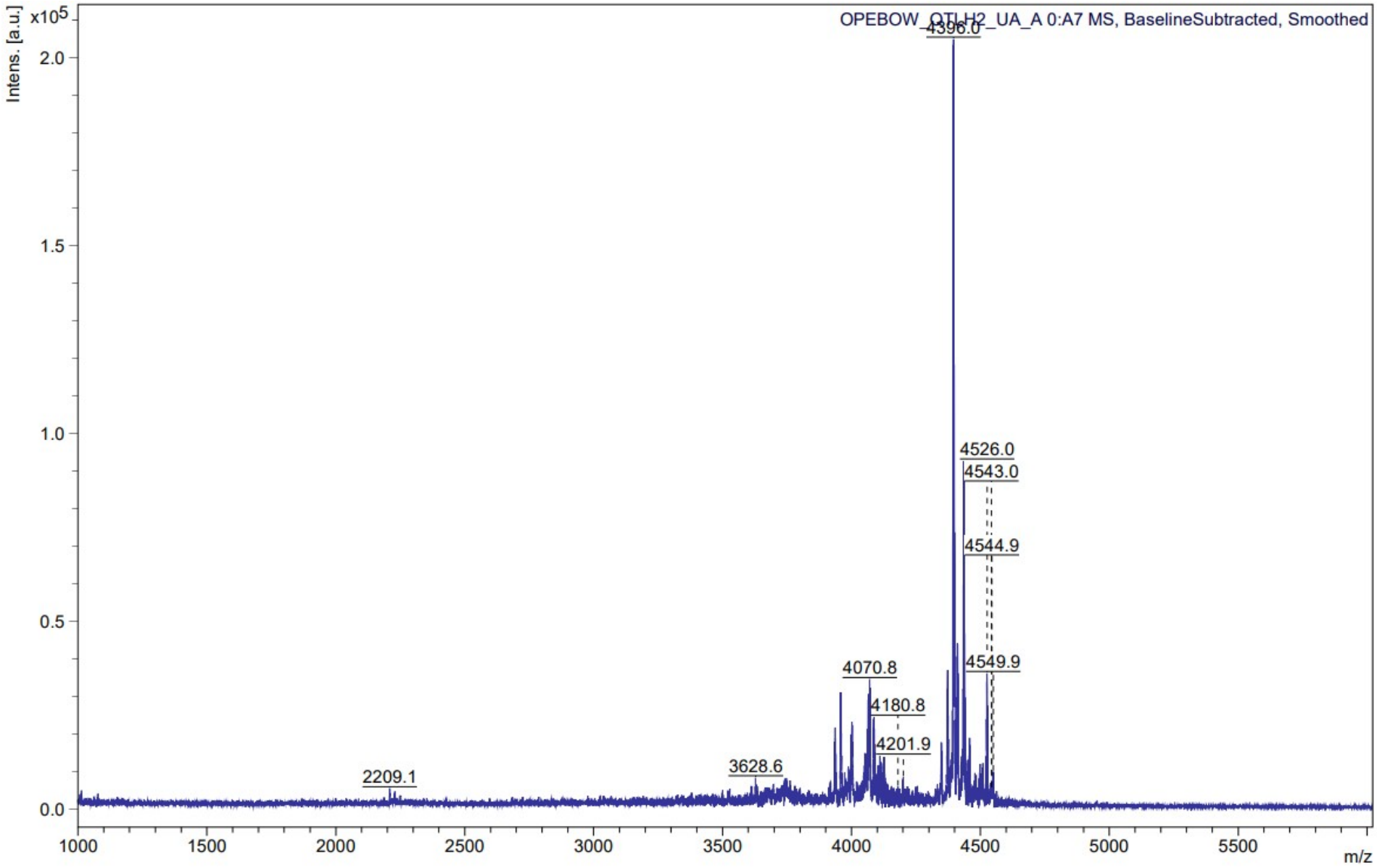

Figure S44 – MALDI-ToF mass spectrum of product (**5a**) formation at 42-hrs. Reaction conditions: (**4**):(**2a**):**$CuSO_4$**:**NaAscorbate 1:16:4:4.4.** 25°C.

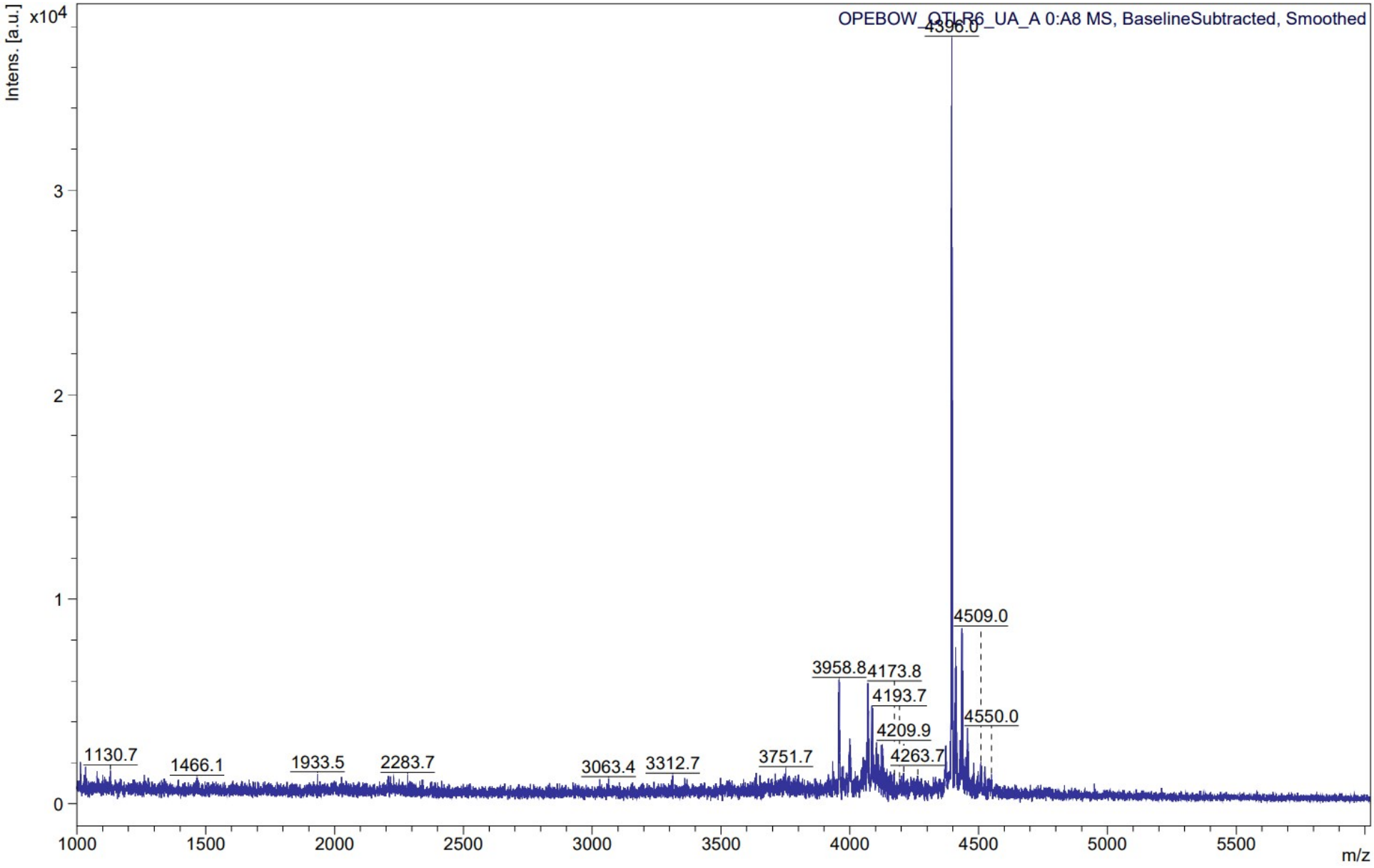

Figure S45 – MALDI-ToF mass spectrum of product (**5a**) formation at 52-hrs. Reaction conditions: (**4**):(**2a**):**$CuSO_4$**:**NaAscorbate 1:16:4:4.4.** 25°C.

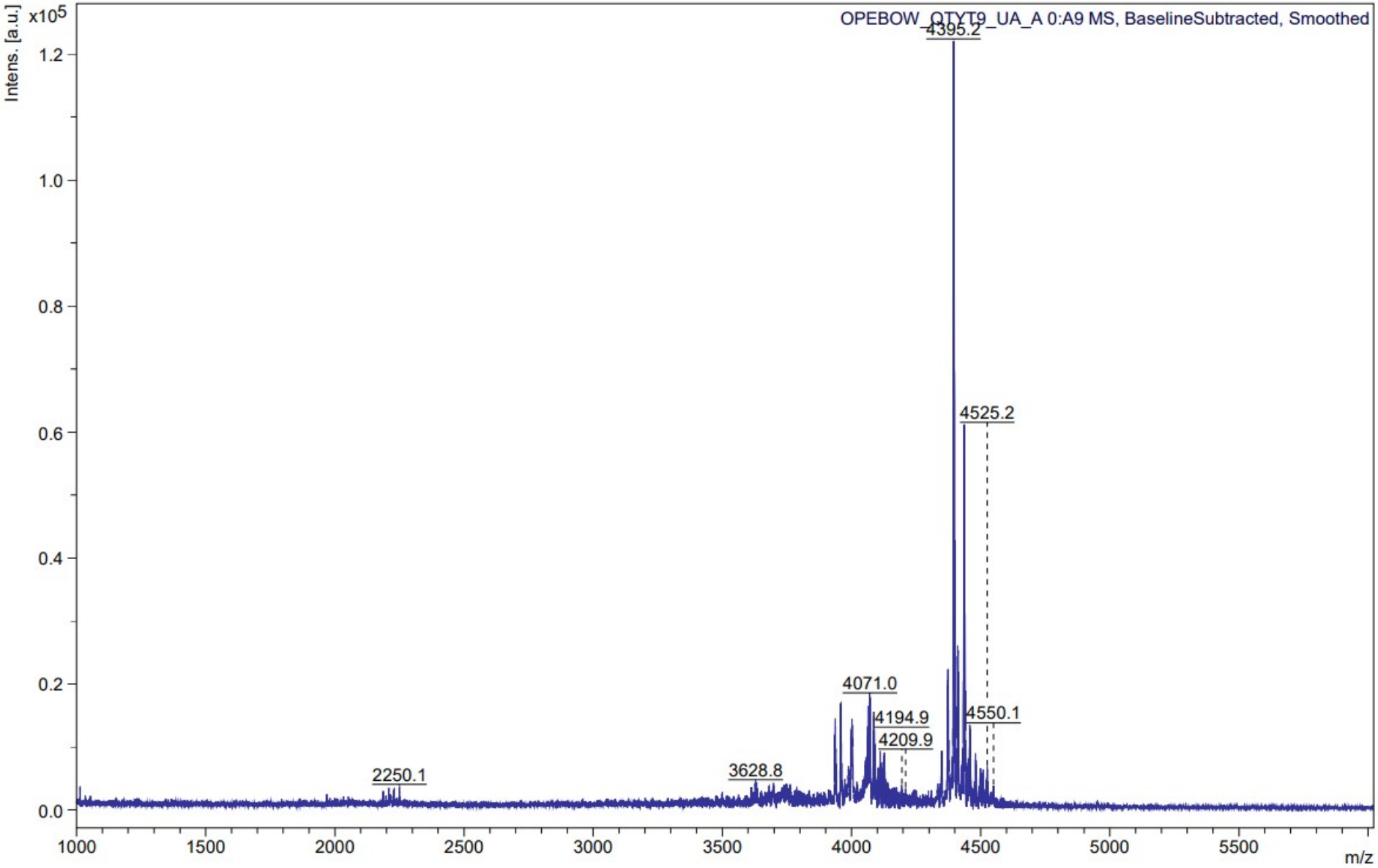

Figure S46 – MALDI-ToF mass spectrum of product (**5a**) formation at 72-hrs. Reaction conditions: (**4**):(**2a**):**$CuSO_4$**:**NaAscorbate 1:16:4:4.4.** 25°C.

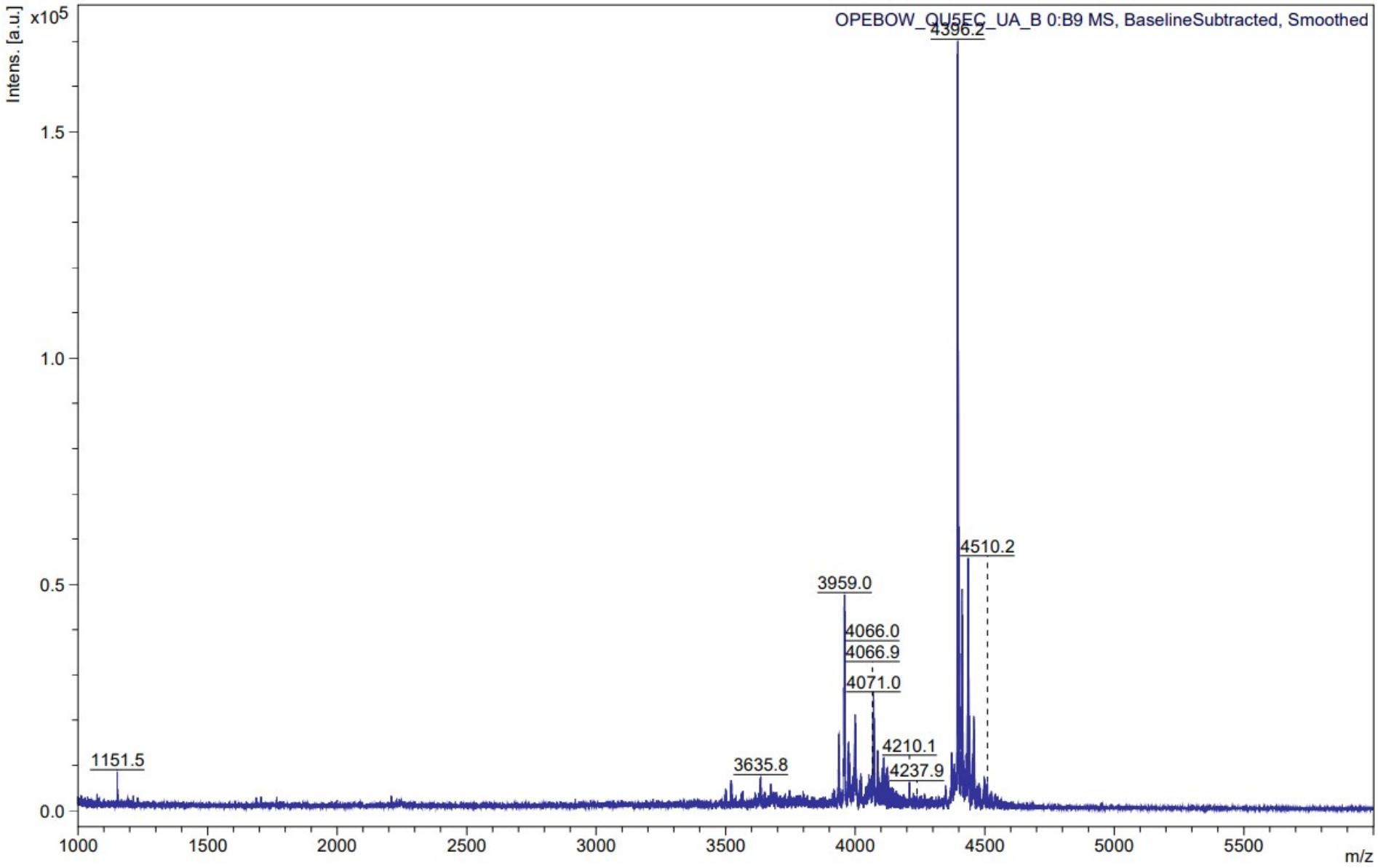

Figure S47 – MALDI-ToF mass spectrum of product (**5a**) formation at 144-hrs. Reaction conditions: (**4**):(**2a**):**$CuSO_4$**:**NaAscorbate 1:16:4:4.4.** 25°C.

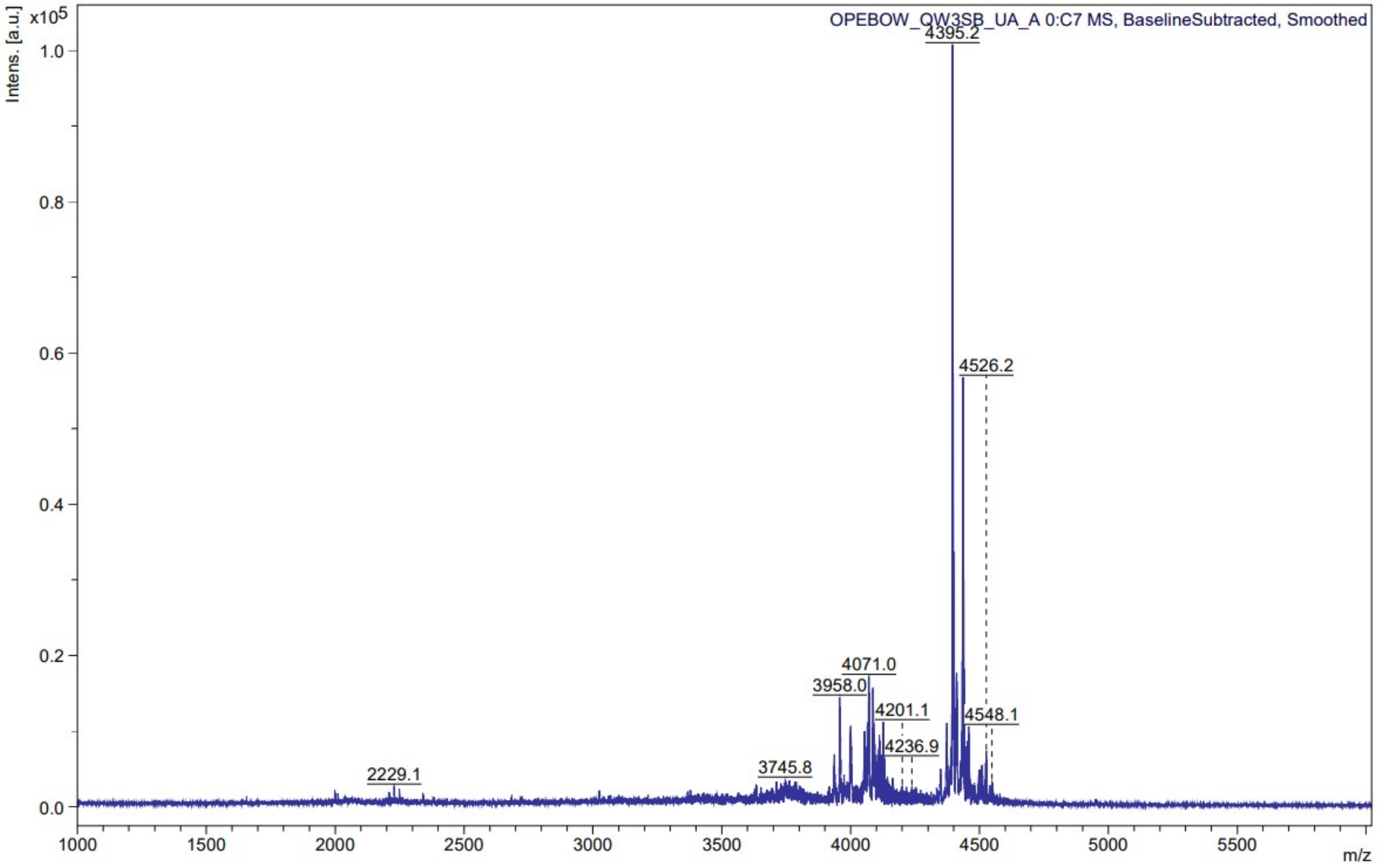

Figure S48 – MALDI-ToF mass spectrum of product (**5a**) formation at 5-hrs. Reaction conditions: (**4**):(**2a**):**$CuSO_4$**:**NaAscorbate 1:16:4:4.4.** 15°C.

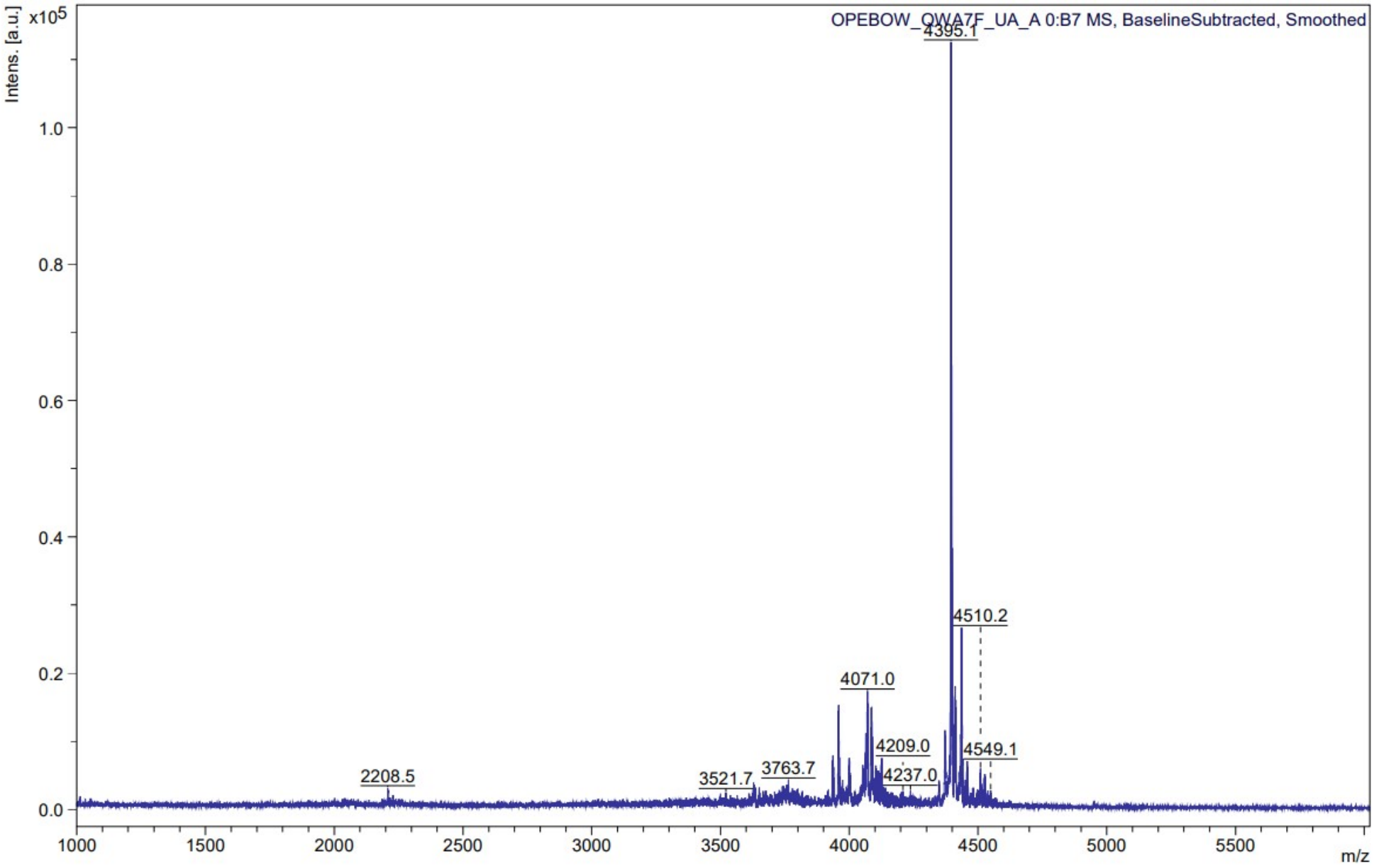

Figure S49 – MALDI-ToF mass spectrum of product (**5a**) formation at 42-hrs. Reaction conditions: (**4**):(**2a**):**$CuSO_4$**:**NaAscorbate 1:16:4:4.4.** 15°C.

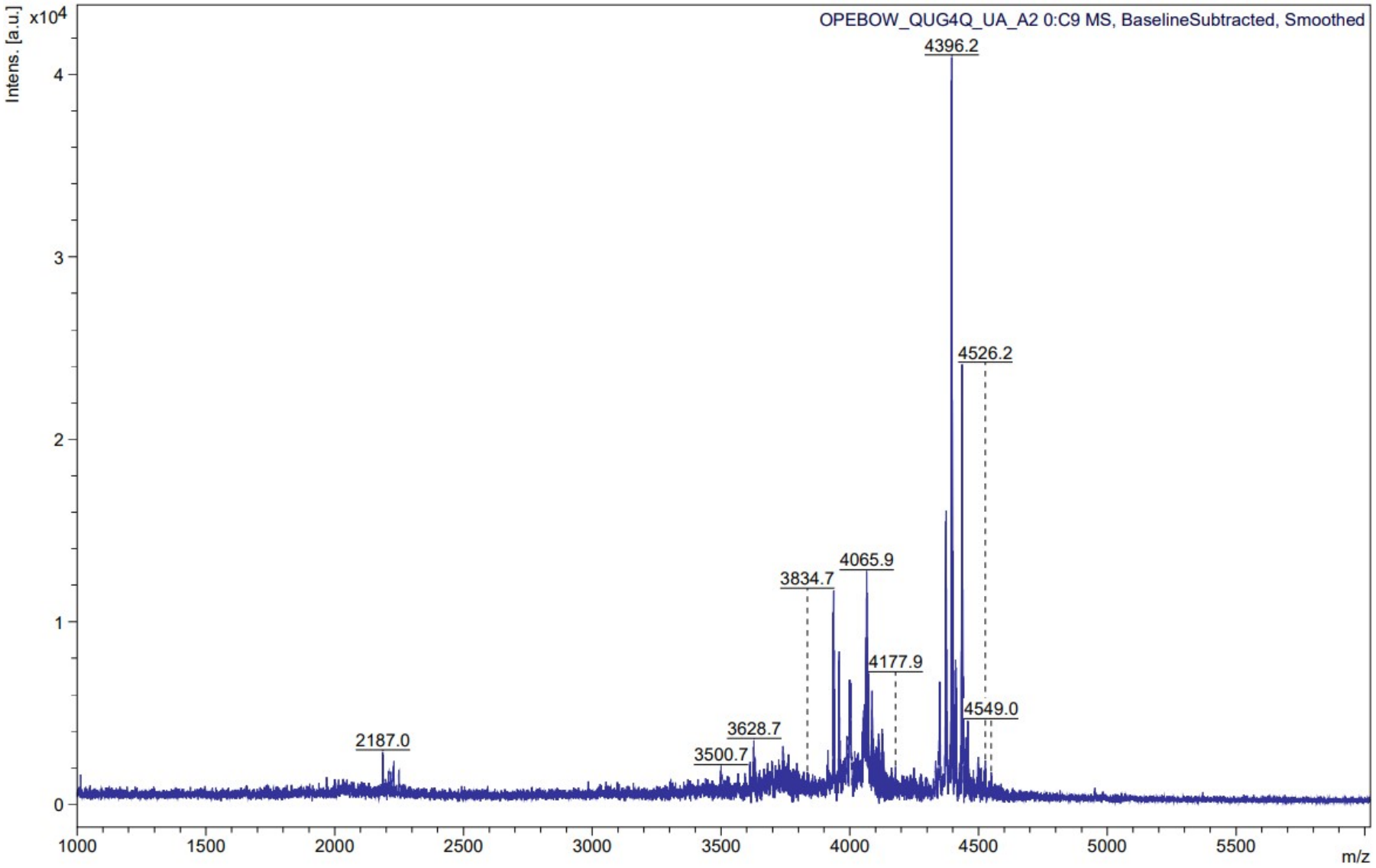

Figure S50 – MALDI-ToF mass spectrum of product (**5a**) formation at 5-hrs. Reaction conditions: (**4**):(**2a**):**$CuSO_4$**:**NaAscorbate 1:16:4:4.4.** 35°C.

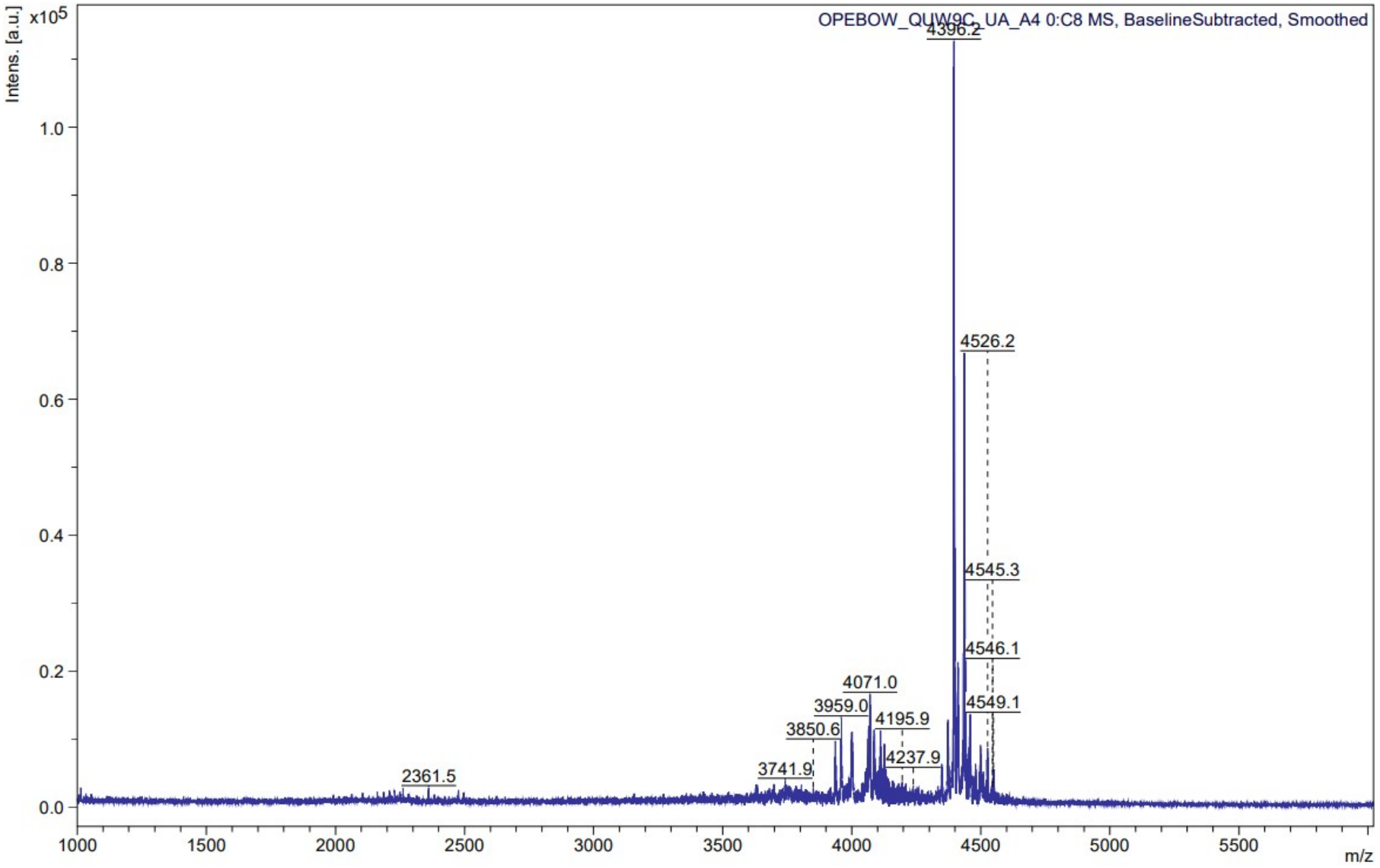

Figure S51 – MALDI-ToF mass spectrum of product (**5a**) formation at 42-hrs. Reaction conditions: (**4**):(**2a**):**$CuSO_4$**:**NaAscorbate 1:16:4:4.4.** 35°C.

11. ESI-QToF MS of (2a) pre- and post- addition of $CuSO_4$ – (Figure S52)

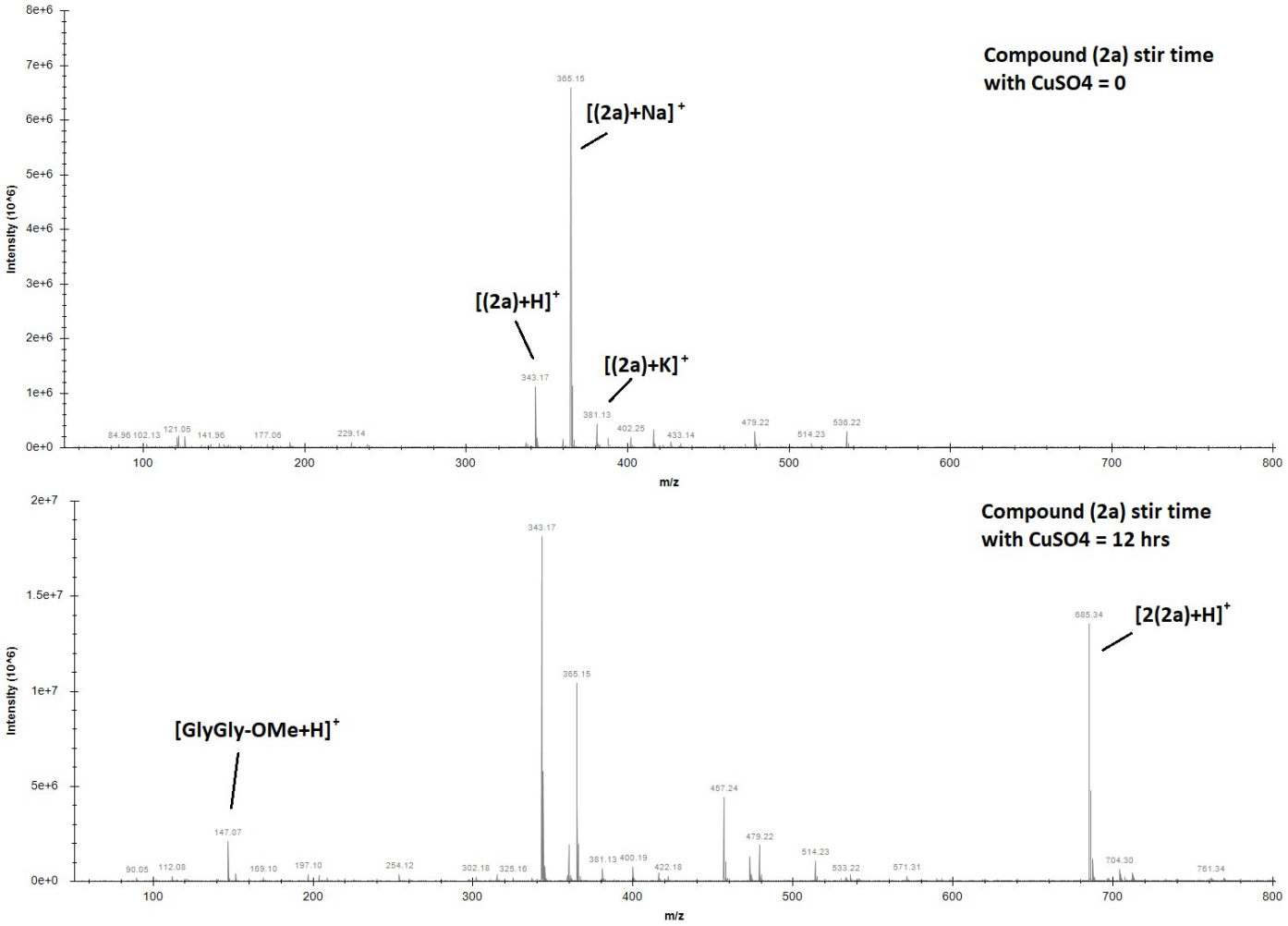

Figure S52 – ESI-QTOF MS of (**2a**) before addition of $CuSO_4$ (top spectra) and after 12 hours of stirring (under N_2) with 4 eq $CuSO_4$.

12. HRAM nanoESI of (5a) – (Figures S53-S55)

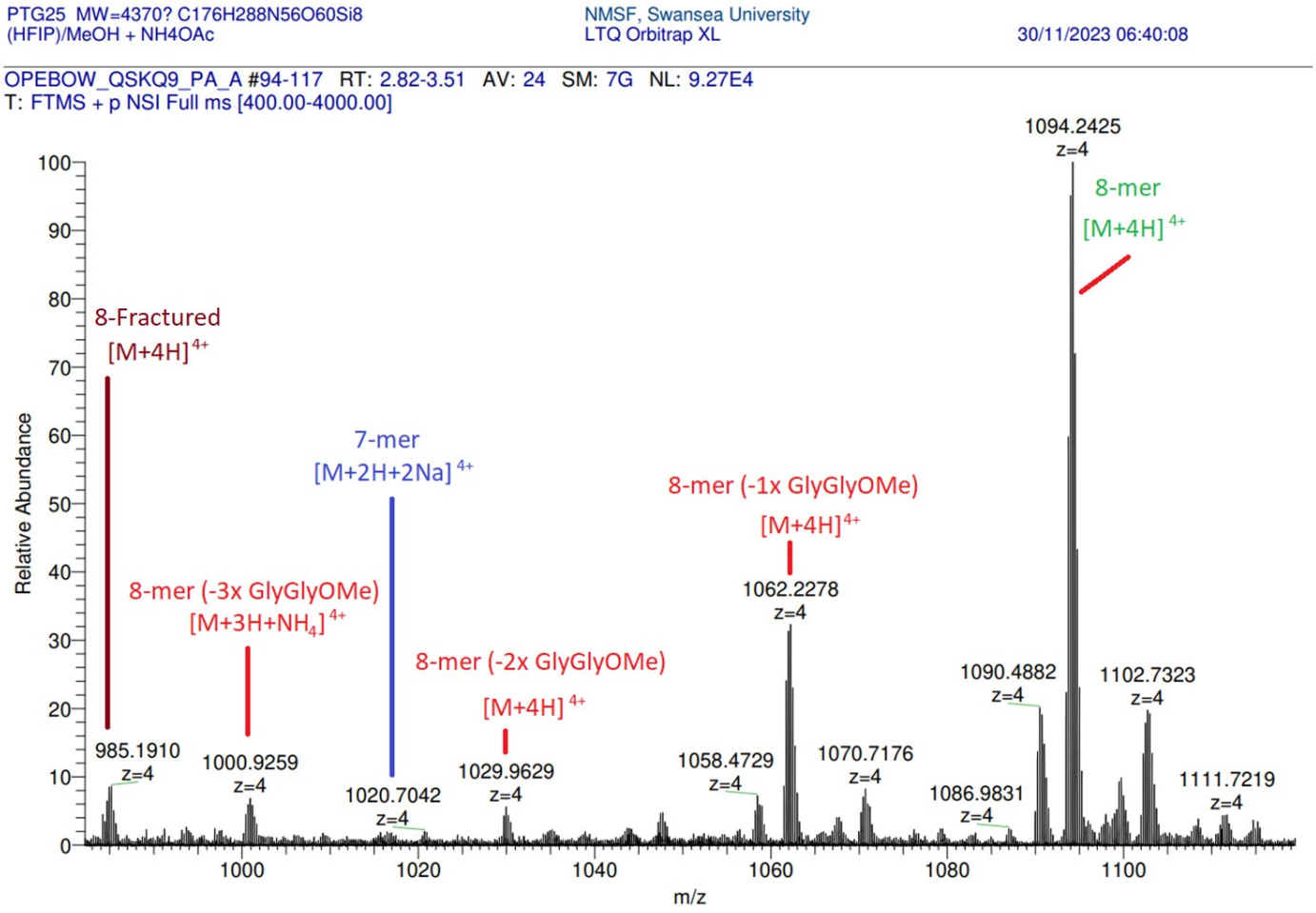

Figure S53 – nanoESI m/z range 980 – 1120 of product (**5a**) formation at 72-hrs. Reaction conditions: (**4**):(**2a**):**$CuSO_4$**:**NaAscorbate 1:16:4:4.4.** 25°C.

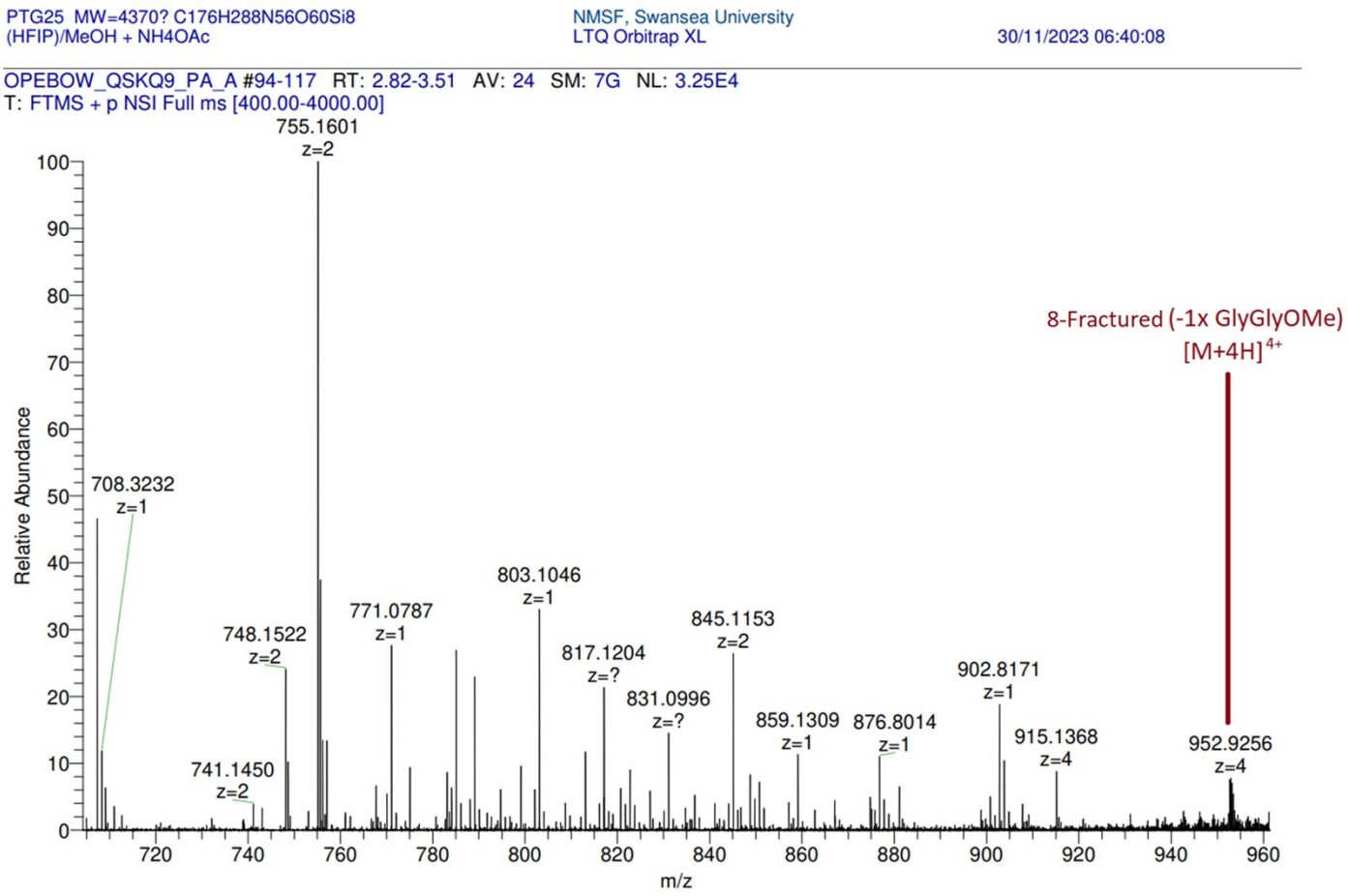

Figure S54 – nanoESI m/z range 700 – 960 of product (**5a**) formation at 72-hrs. Reaction conditions: (**4**):(**2a**):**$CuSO_4$**:**NaAscorbate 1:16:4:4.4.** 25°C.

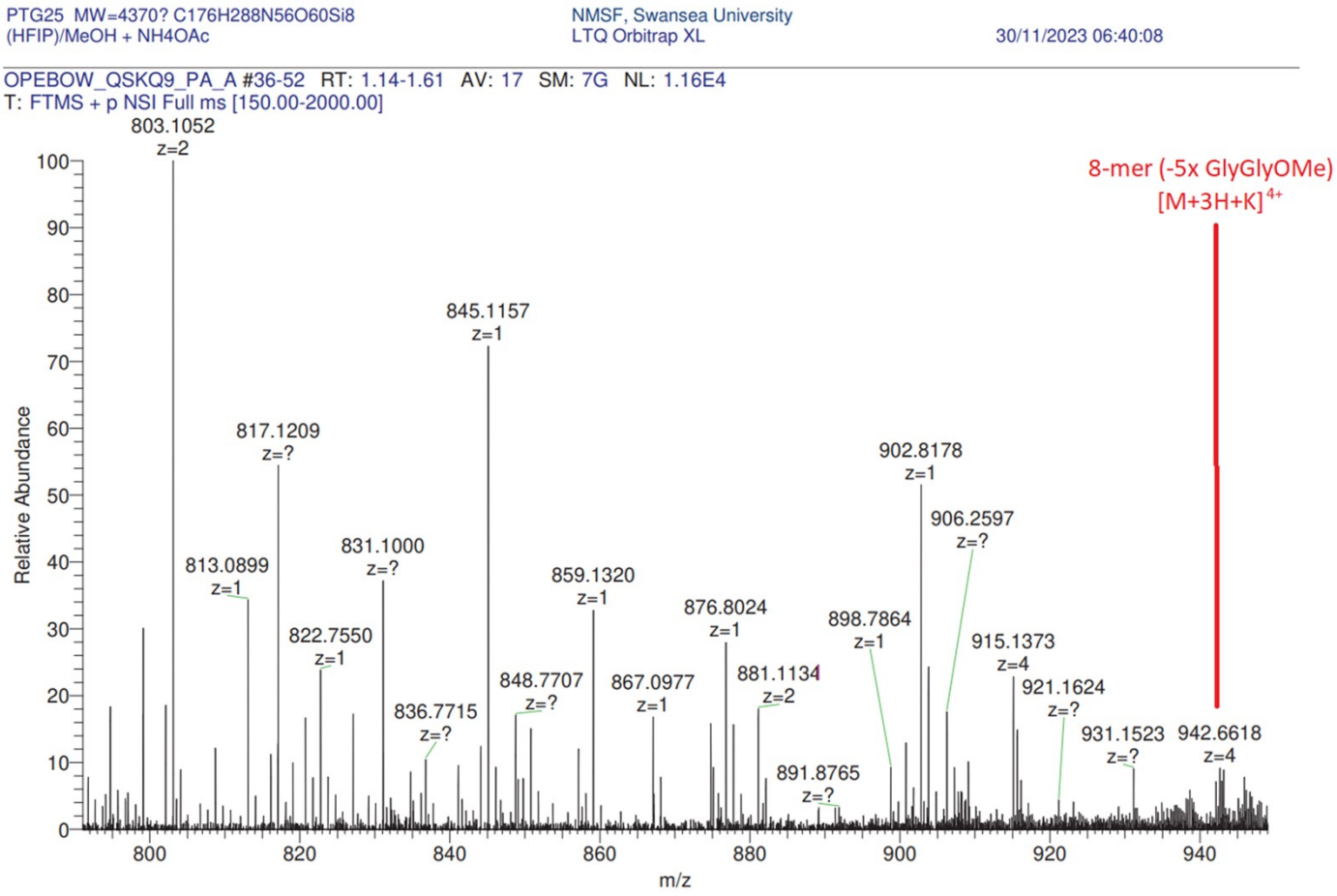

Figure S55 – nanoESI m/z range 780 – 950 of product (**5a**) formation at 72-hrs. Reaction conditions: (**4**):(**2a**):**$CuSO_4$**:**NaAscorbate 1:16:4:4.4.** 25°C.

13. Double and triple CuAAC “clicks” of pre-formed (5a) – (Figures S56-S57)

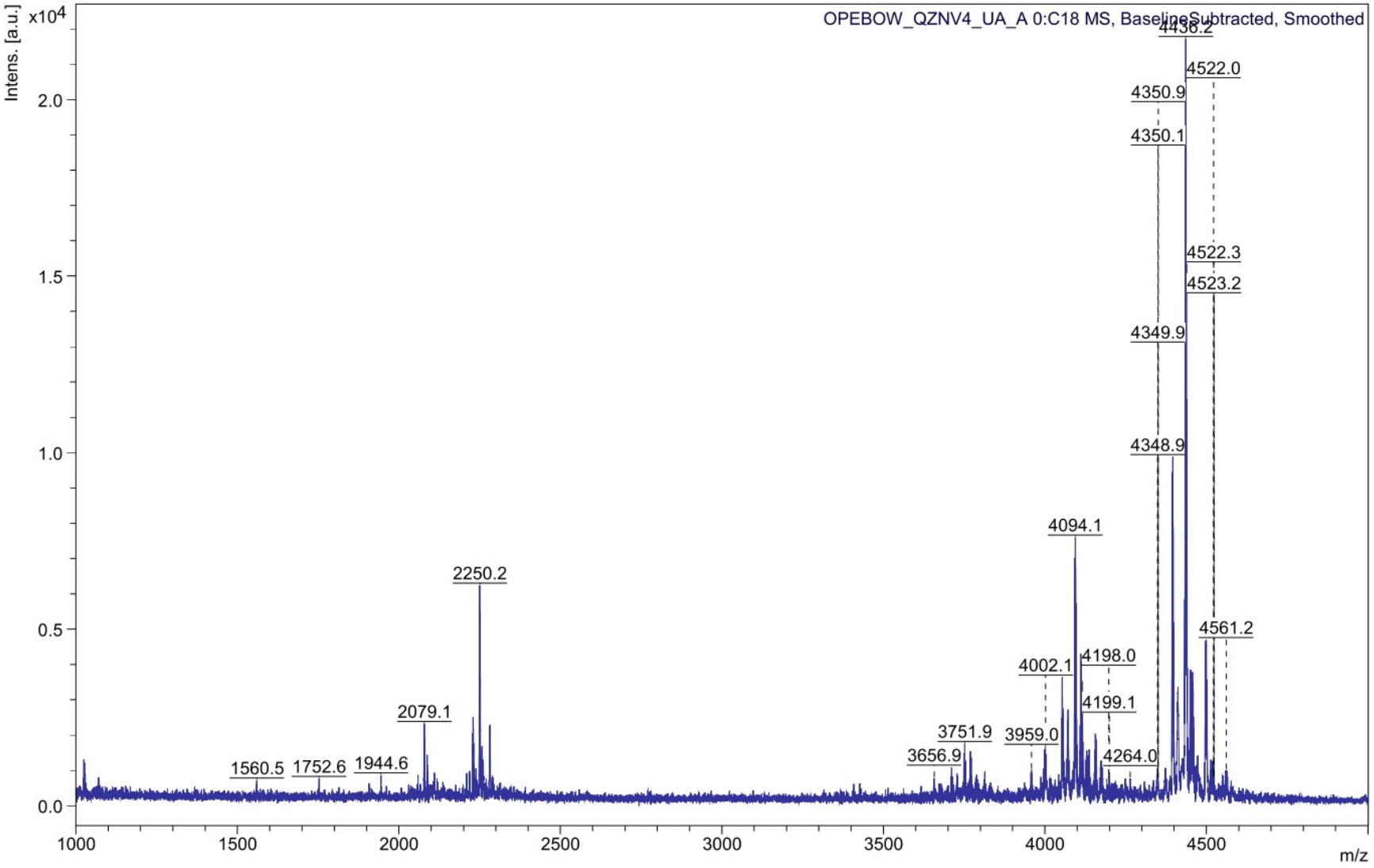

Figure S56 – MALDI-ToF mass spectrum of product (**5a**) formation at 42-hrs after double CuAAC “click” with previously formed (**5a**). Reaction conditions: (**5a**):(**2a**):**$CuSO_4$**:**NaAscorbate 1:16:4:4.4.** 25°C.

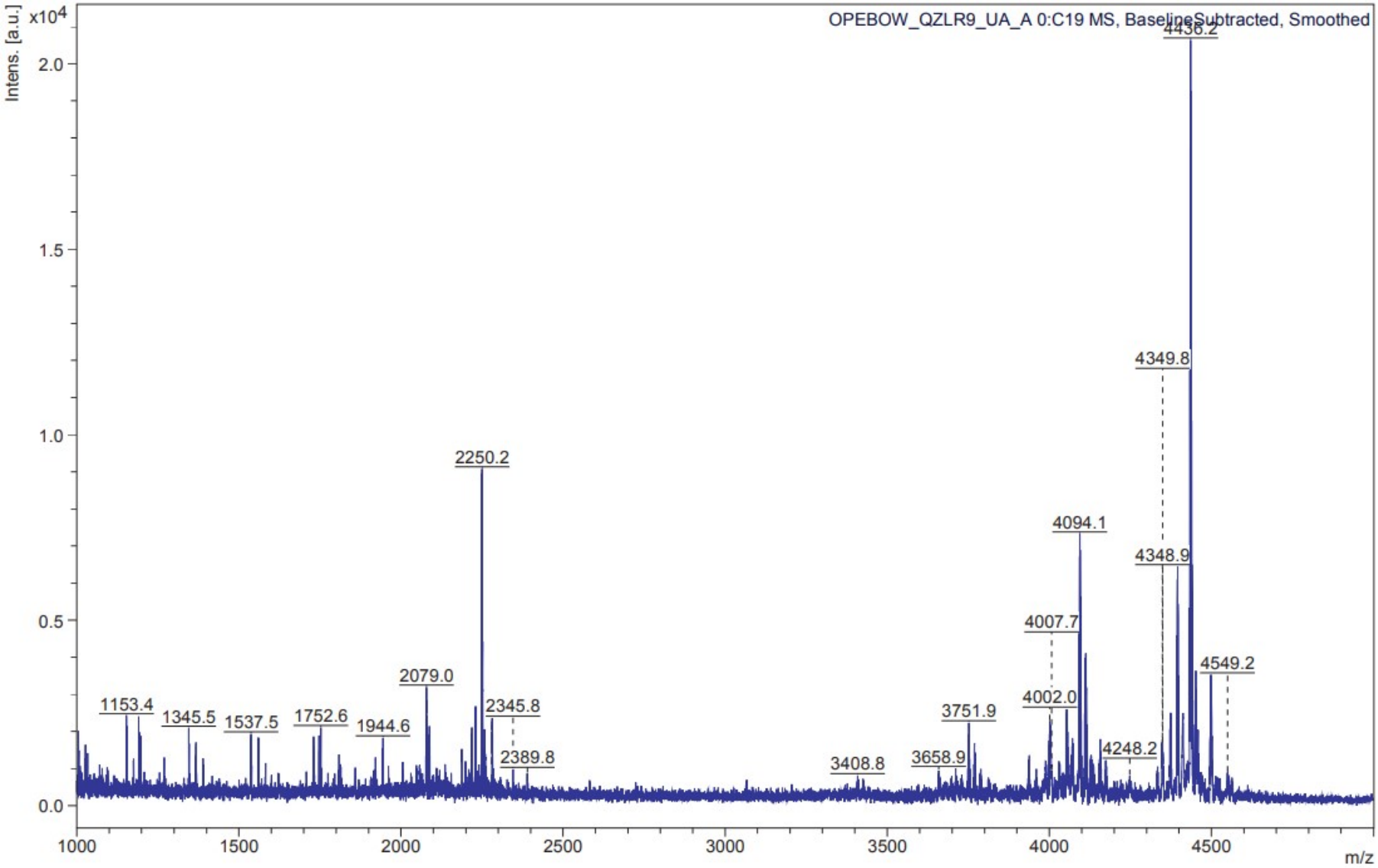

Figure S57 – MALDI-ToF mass spectrum of product (**5a**) formation at 42-hrs after triple CuAAC "click" with previously formed (**5a**). Reaction conditions: (**5a**):(**2a**):**$CuSO_4$**:**NaAscorbate 1:16:4:4.4.** 25°C.

14. CuAAC “clicks” of pre-formed (5a) with 1-azidohexane – (Figures S58-S62)

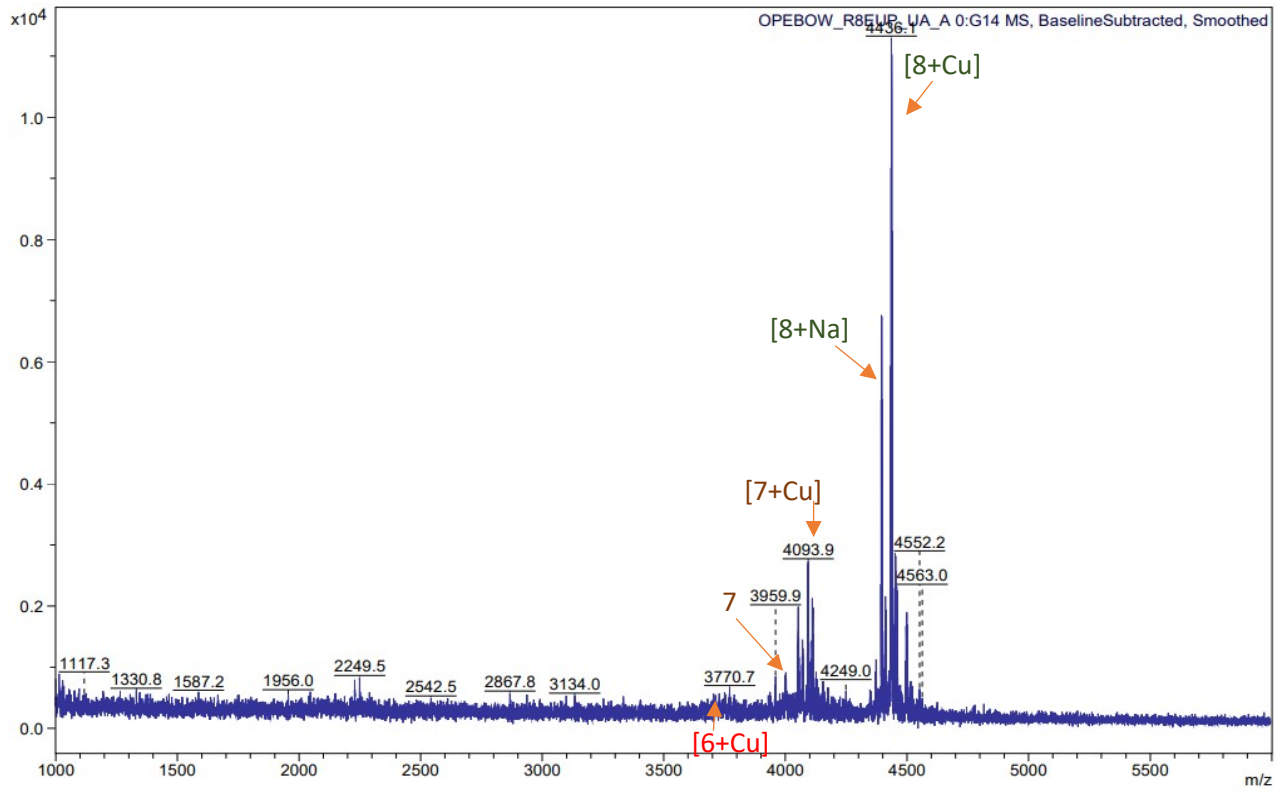

Figure S58 – MALDI-ToF mass spectrum of product (**5a**) formation at 72-hrs.

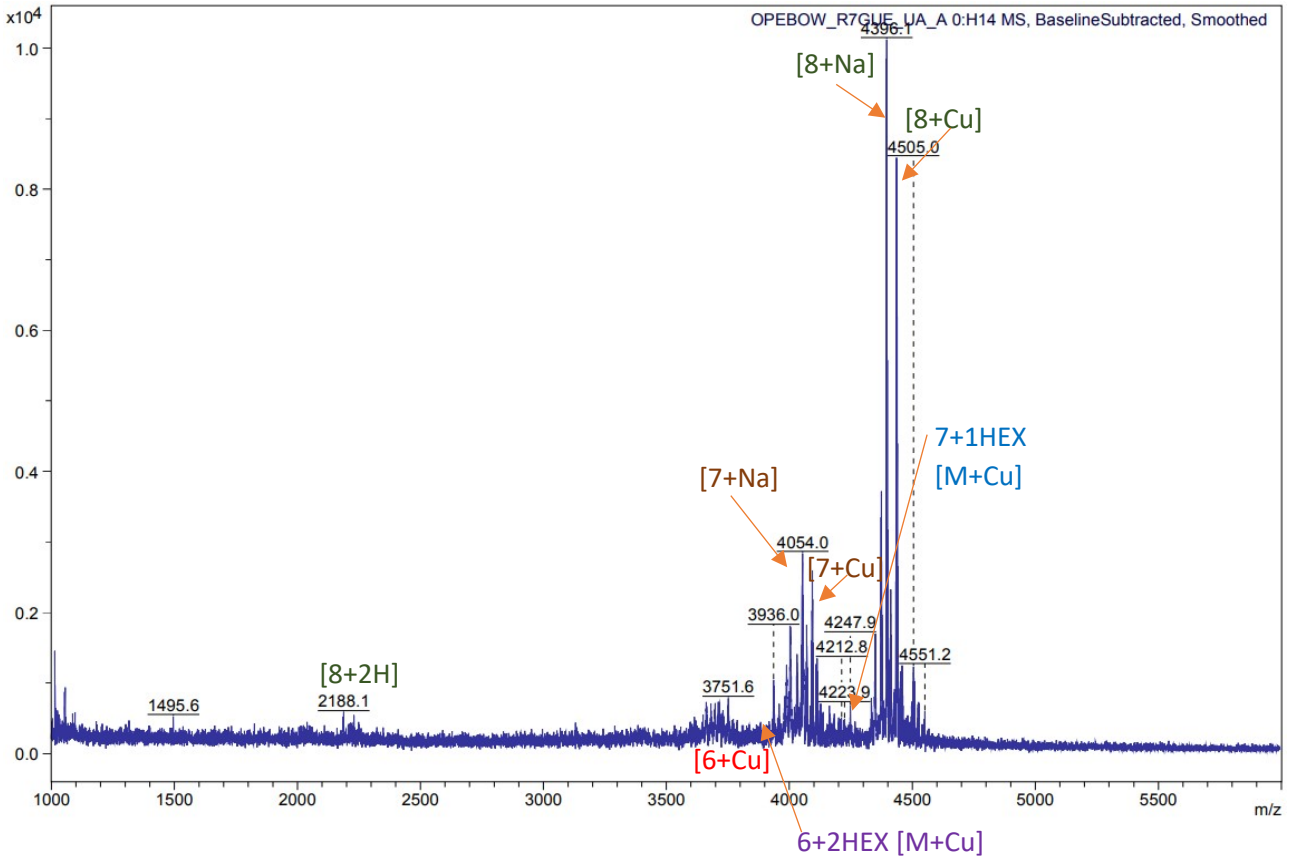

Figure S59 – MALDI-ToF mass spectrum of product (**5a**) formation at 24-hrs during CuAAC “click” of 1-azidohexane with previously formed (**5a**). Reaction conditions: (**5a**):(**1-azidohexane**):**$CuSO_4$**:**NaAscorbate 1:16:4:4.4.** 25°C.

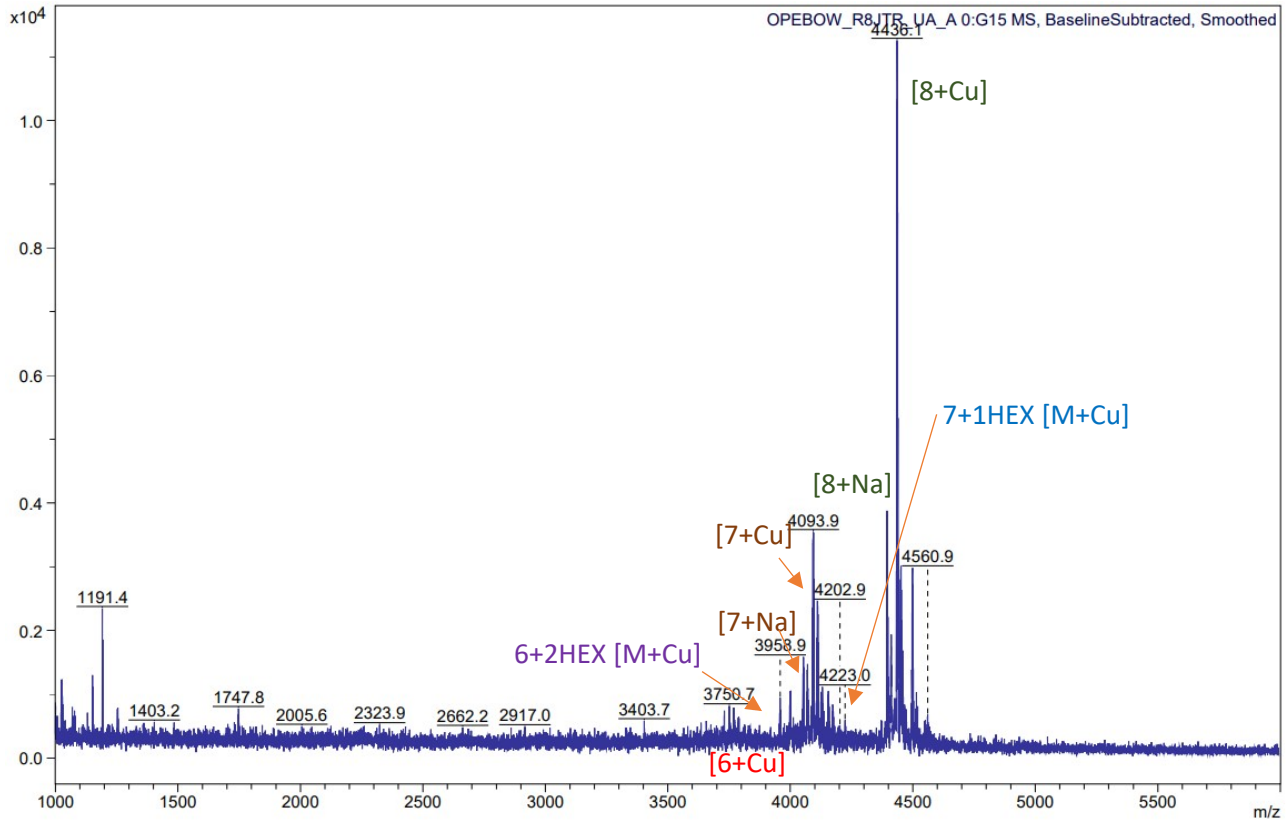

Figure S60 – MALDI-ToF mass spectrum of product (**5a**) formation at 48-hrs CuAAC "click" of 1-azidohexane with previously formed (**5a**). Reaction conditions: (**5a**):(**1-azidohexane**):**$CuSO_4$**:**NaAscorbate 1:16:4:4.4.** 25°C.

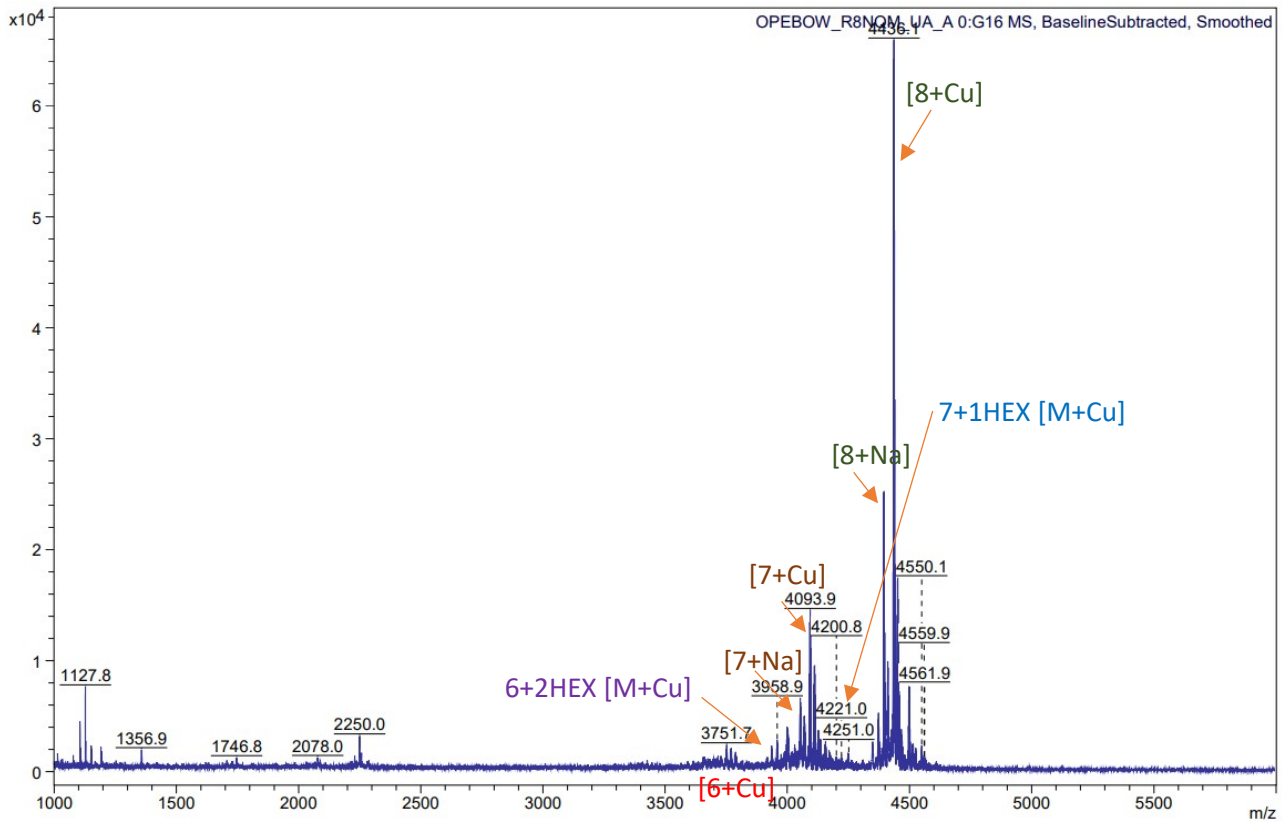

Figure S61 – MALDI-ToF mass spectrum of product (**5a**) formation at 72-hrs CuAAC "click" of 1-azidohexane with previously formed (**5a**). Reaction conditions: (**5a**):(**1-azidohexane**):**$CuSO_4$**:**NaAscorbate 1:16:4:4.4.** 25°C.

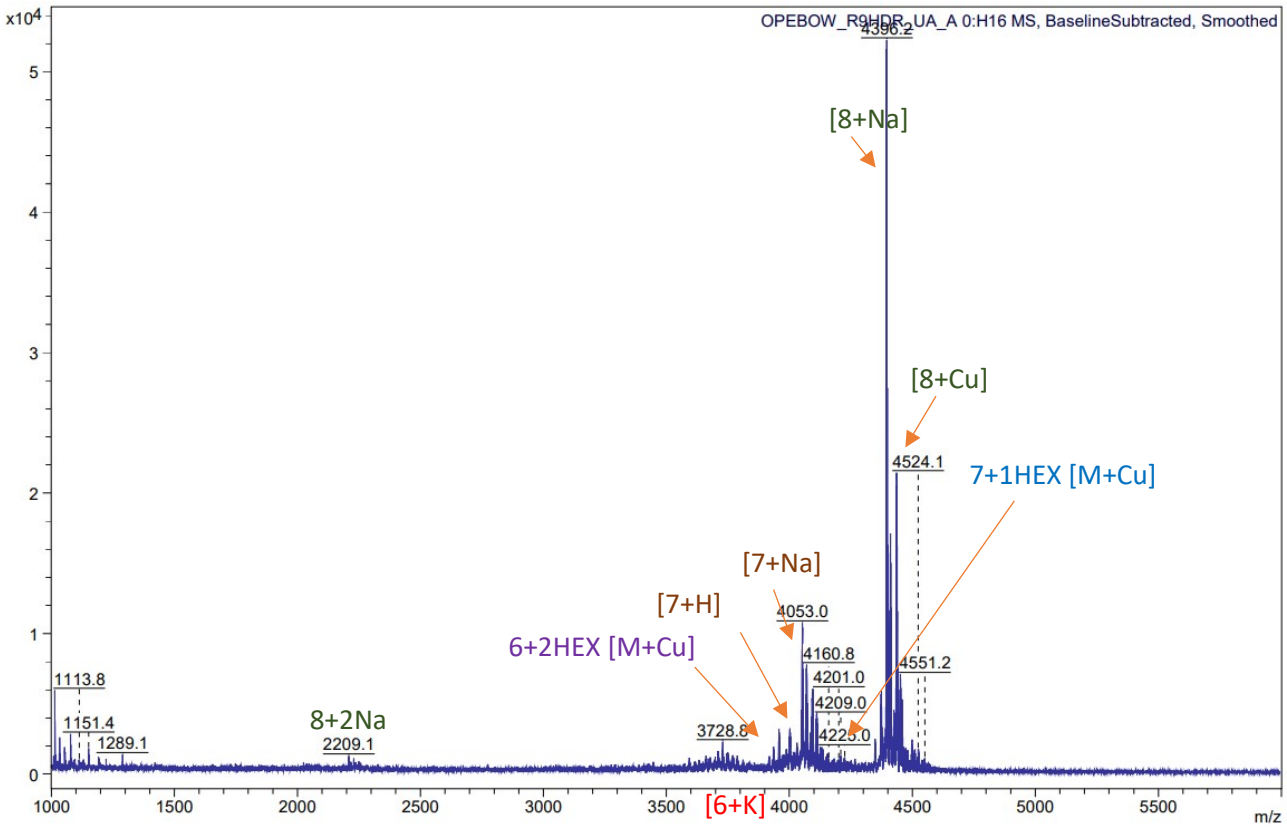

Figure S62 – MALDI-ToF mass spectrum of product (**5a**) formation at 144-hrs CuAAC "click" of 1-azidohexane with previously formed (**5a**). Reaction conditions: (**5a**):(**1-azidohexane**):**$CuSO_4$**:**NaAscorbate 1:16:4:4.4.** 25°C.

15. Cu catalyst effect on POSS-Alkyne (4) – (Figures S63-S66)

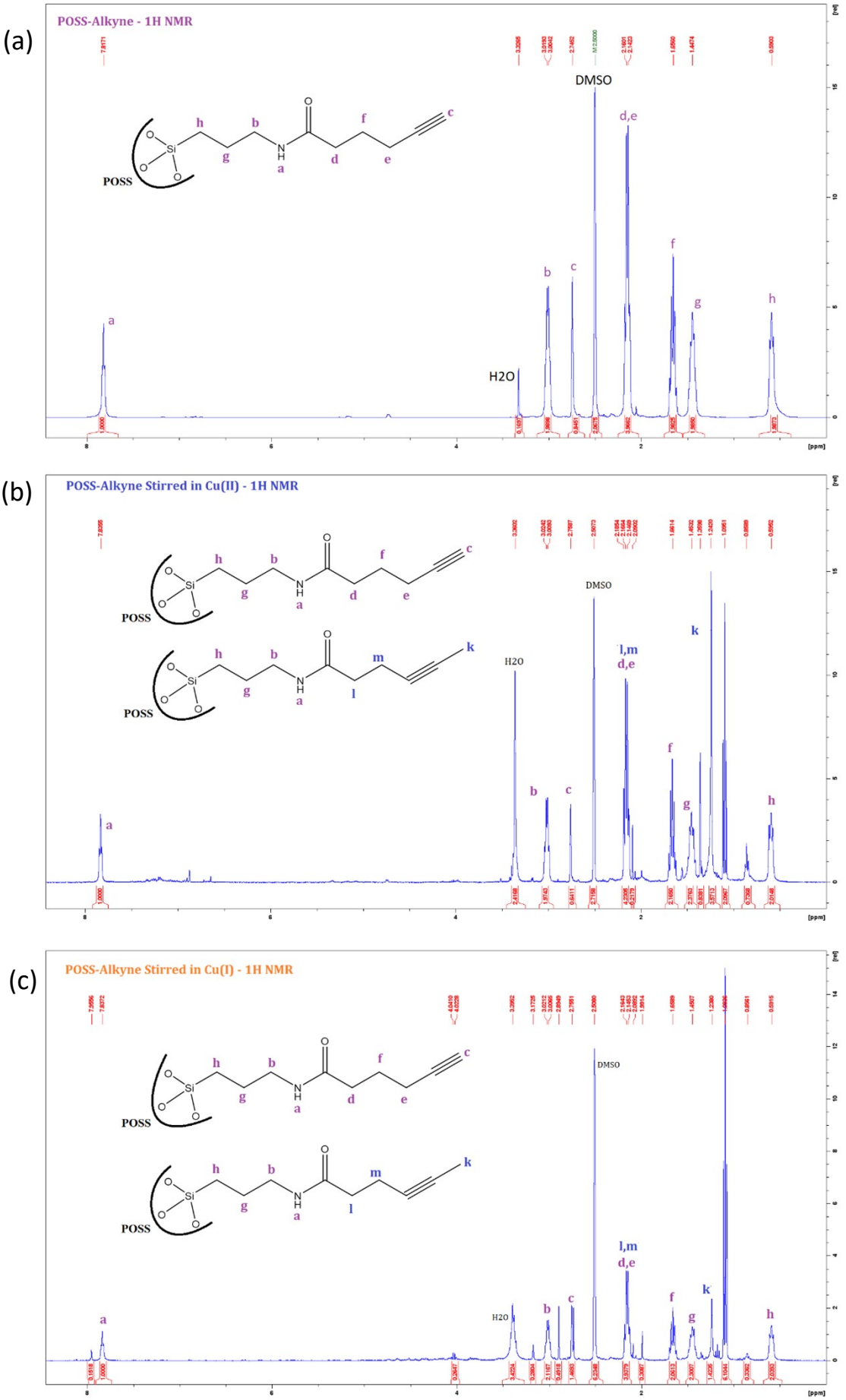

Figure S63 – ^{1}H NMR of POSS-Alkyne (**4**) (a), post-stirring within Cu(II) solution (b) and post-stirring within Cu(I) solution (c).

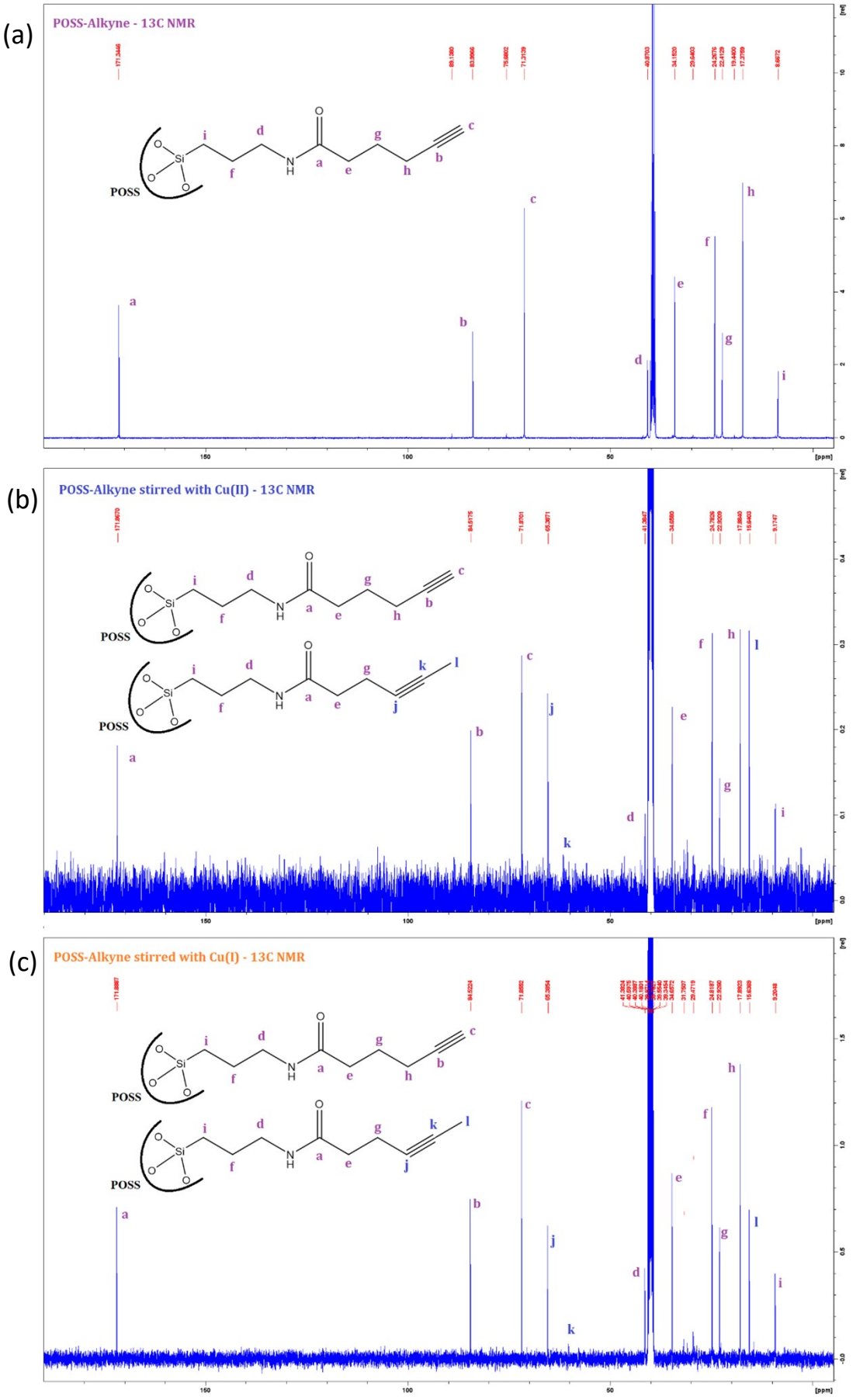

Figure S64 – ^{13}C NMR of POSS-Alkyne (**4**) (a), post-stirring within Cu(II) solution (b) and post-stirring within Cu(I) solution (c).

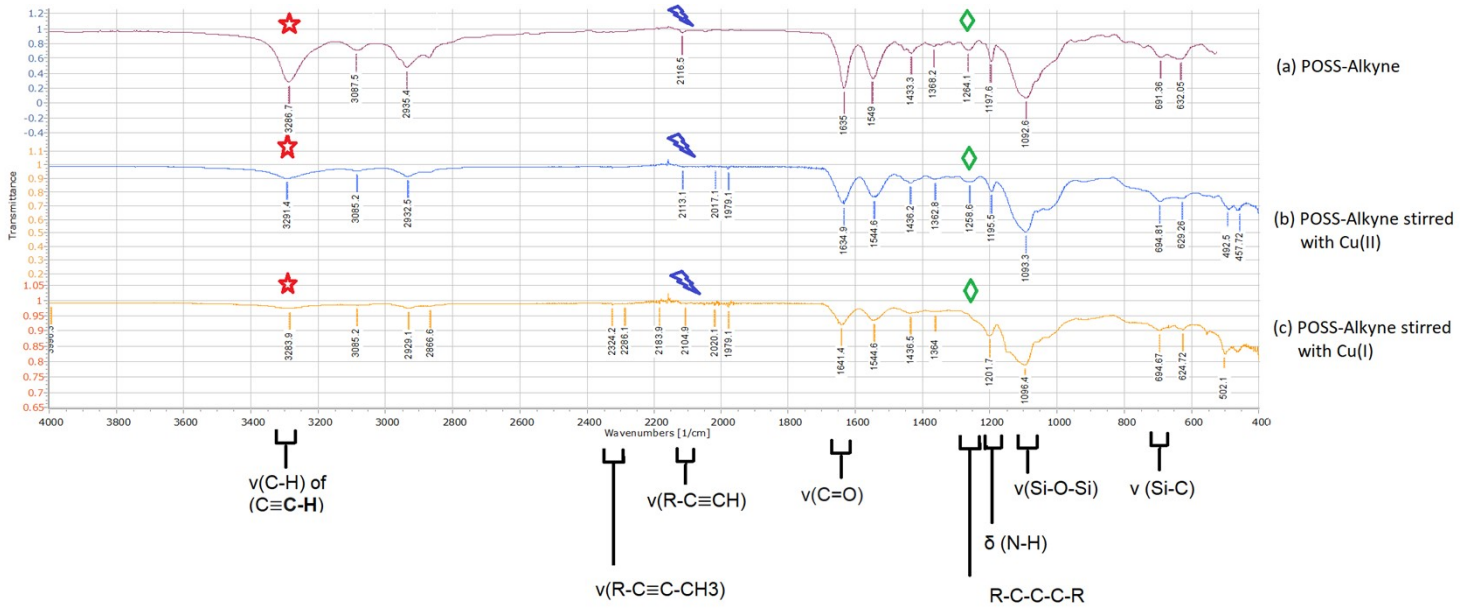

Figure S65 – FTIR of POSS-Alkyne (**4**) (a), post-stirring within Cu(II) solution (b) and post-stirring within Cu(I) solution (c).

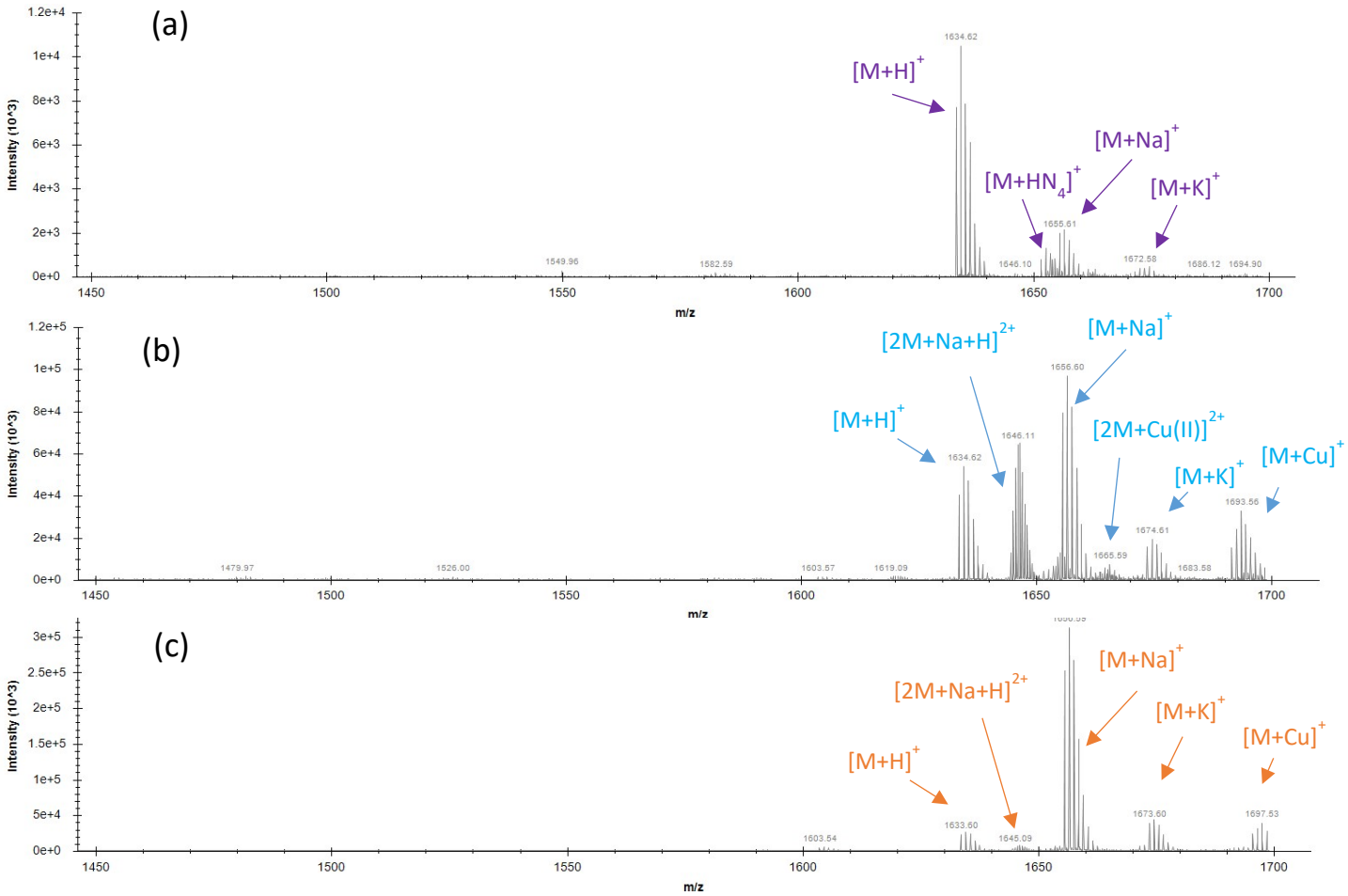

Figure S66 – ESI-TOF MS of POSS-Alkyne (**4**) (a), post-stirring within Cu(II) solution (b) and post-stirring within Cu(I) solution (c).

16. CuAAC “click” reactions between (2b) and (4) relative to time – (Figures S67-S71)

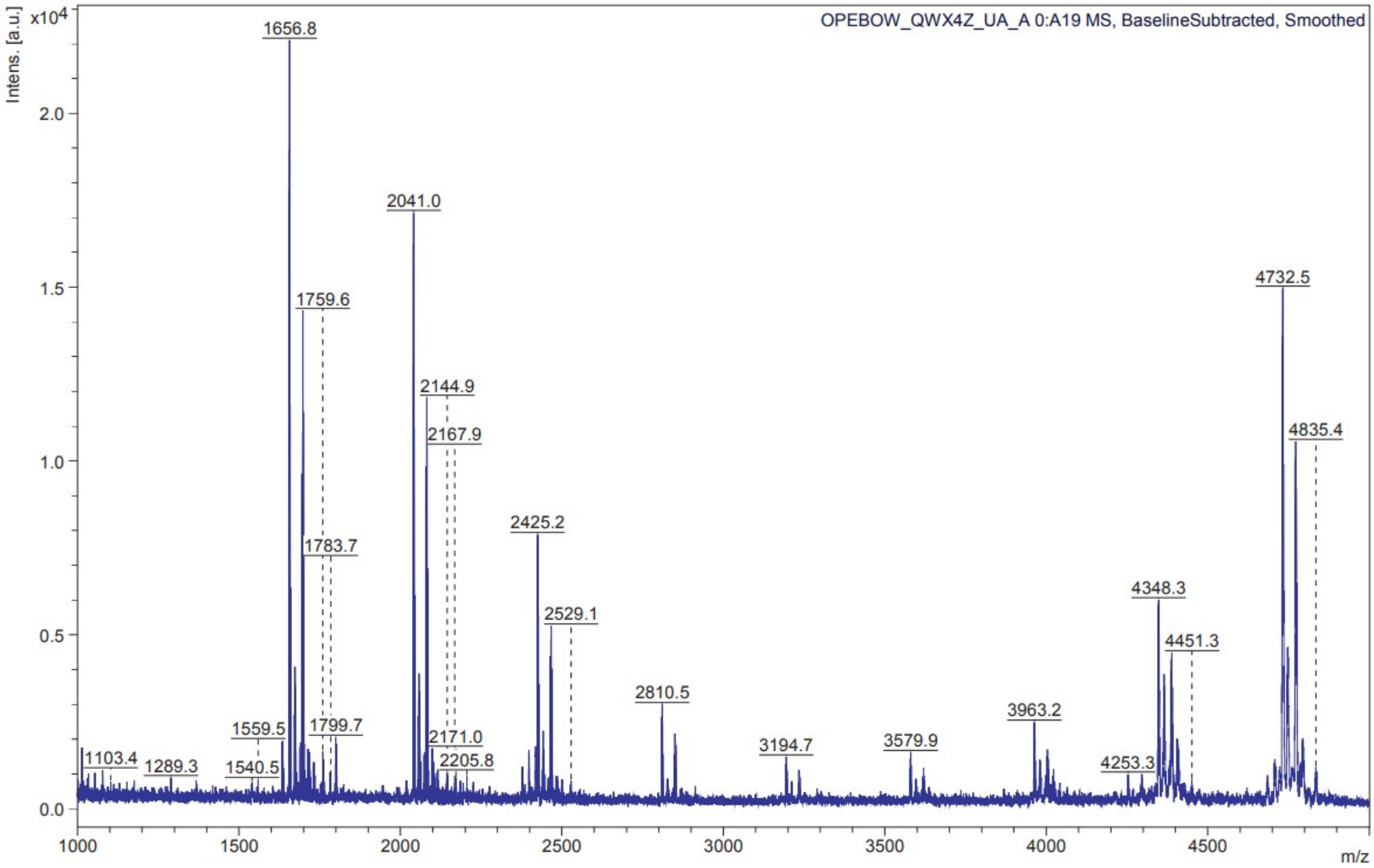

Figure S67 – MALDI-ToF mass spectrum of product (**5b**) formation at 2-hrs. Reaction conditions: (**4**):(**2b**):**$CuSO_4$**:**NaAscorbate 1:16:4:4.4.** 25°C.

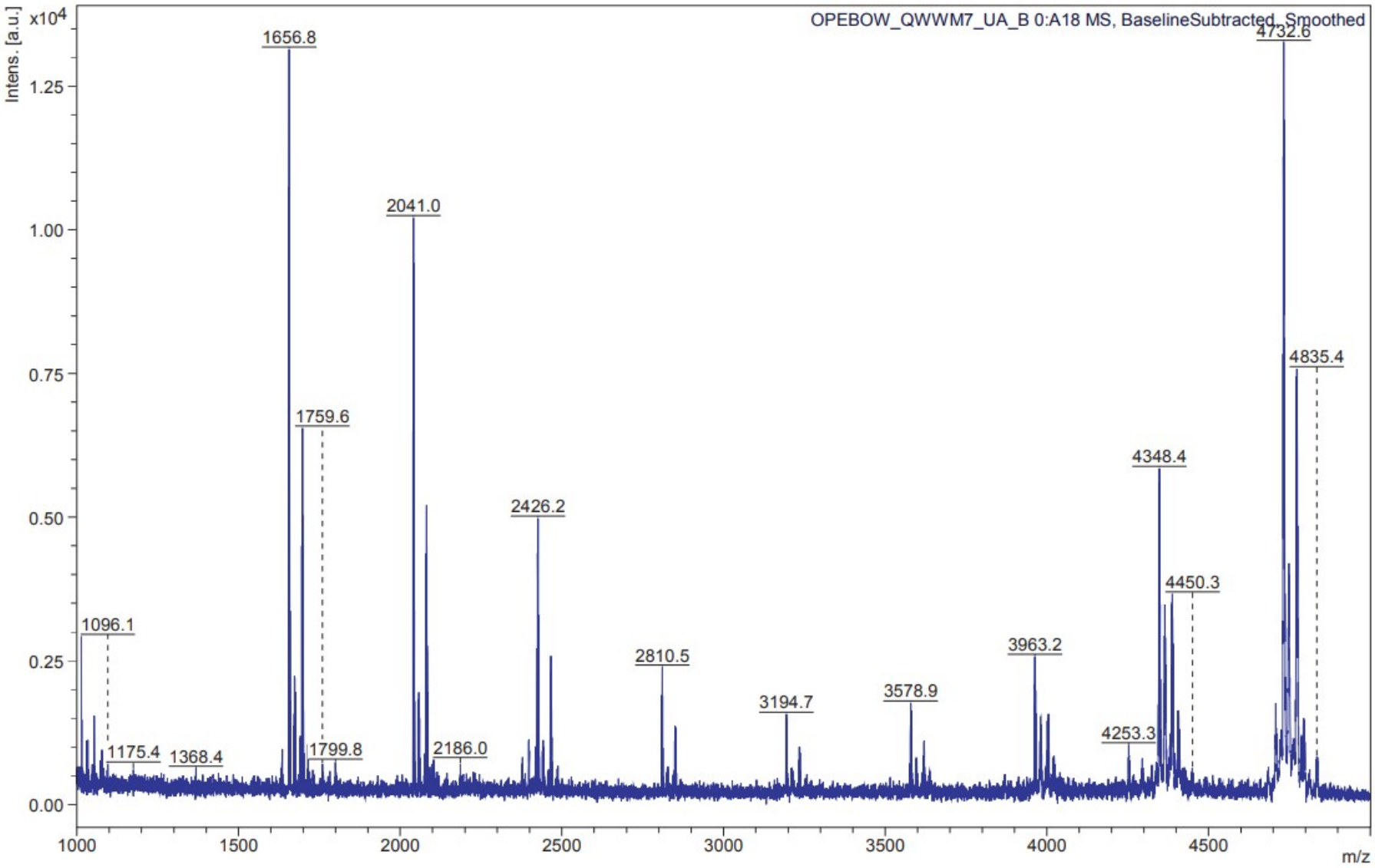

Figure S68 – MALDI-ToF mass spectrum of product (**5b**) formation at 5-hrs. Reaction conditions: (**4**):(**2b**):**$CuSO_4$**:**NaAscorbate 1:16:4:4.4.** 25°C.

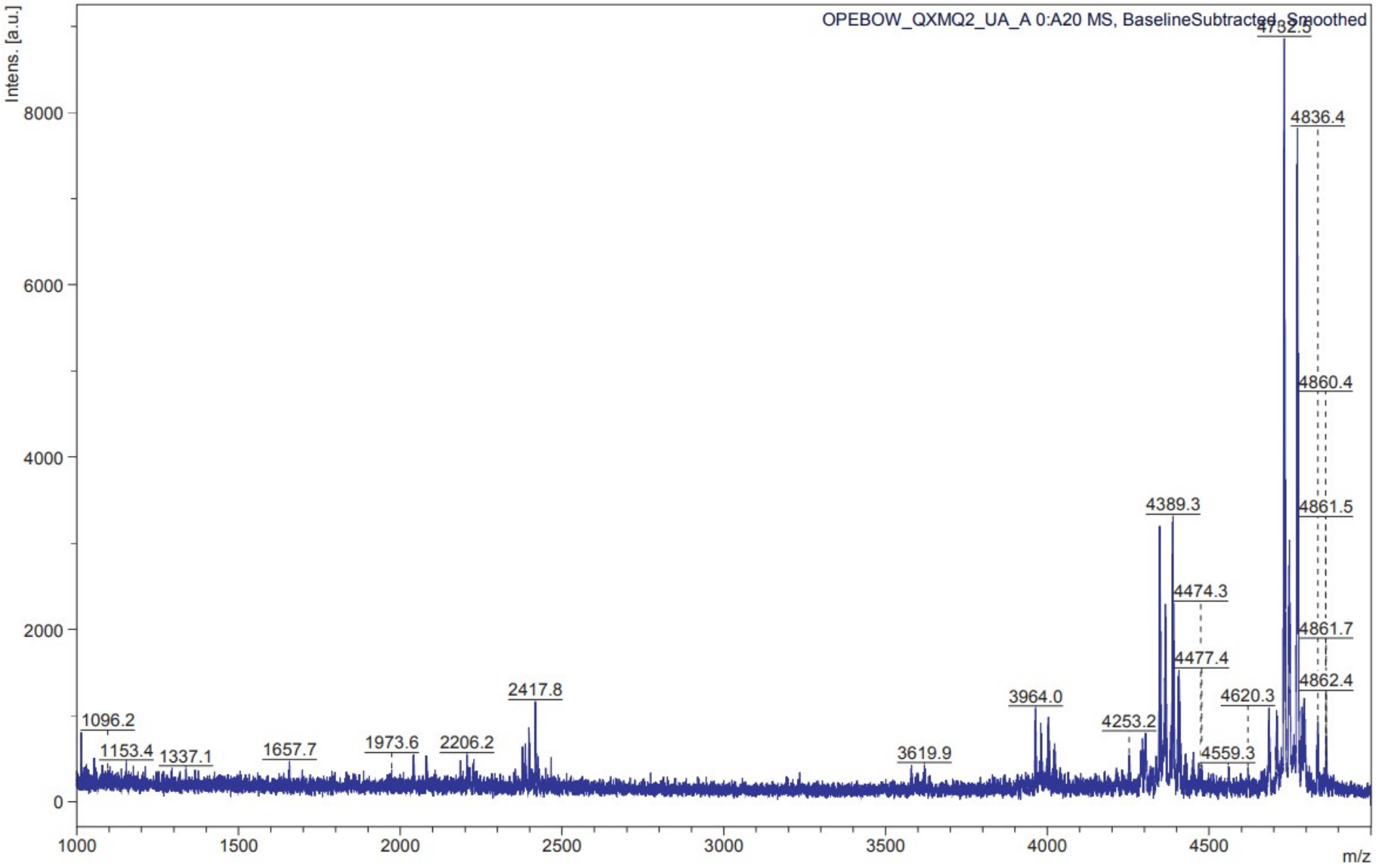

Figure S69 – MALDI-ToF mass spectrum of product (**5b**) formation at 21-hrs. Reaction conditions: (**4**):(**2b**):**$CuSO_4$**:**NaAscorbate 1:16:4:4.4.** 25°C.

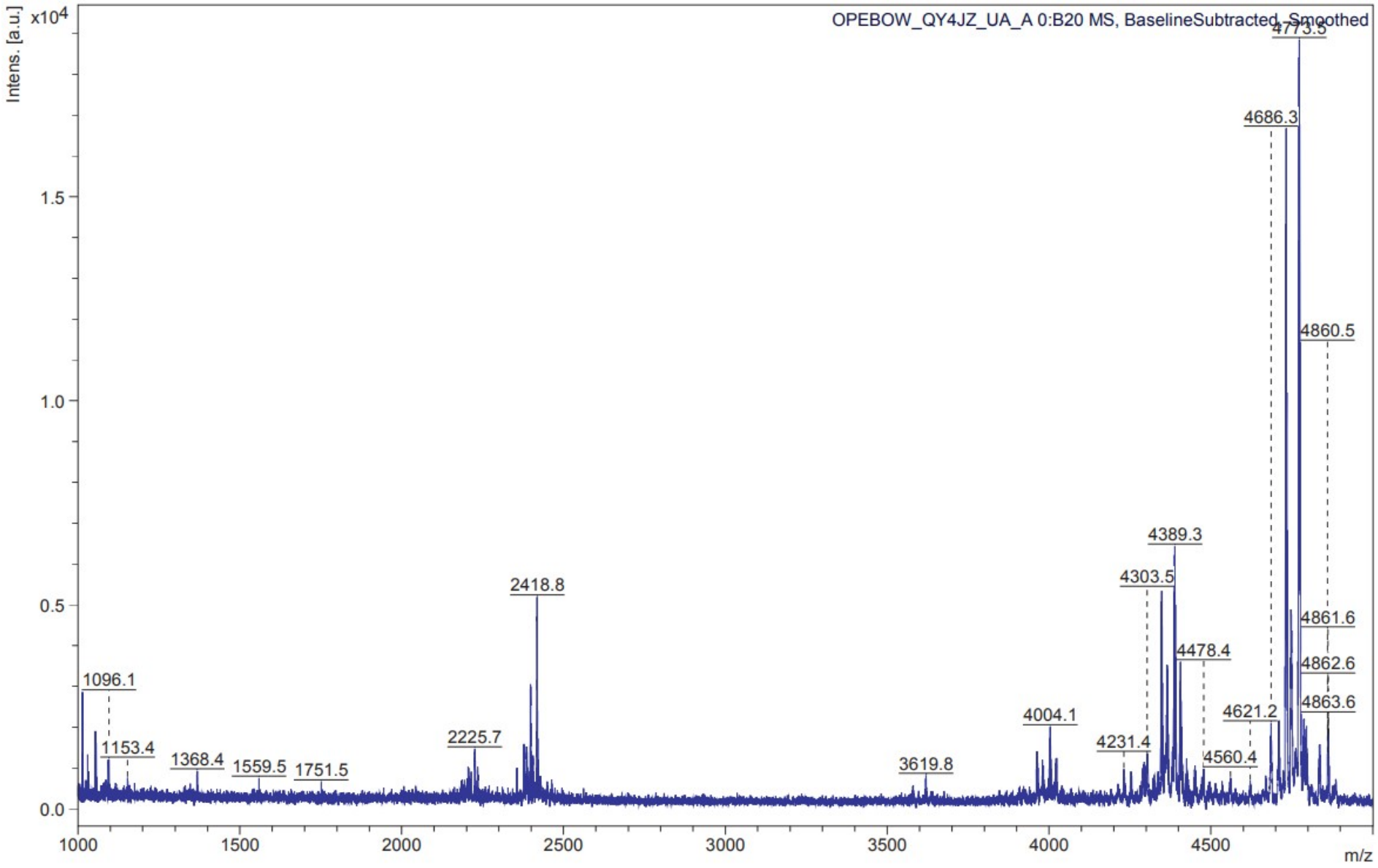

Figure S70 – MALDI-ToF mass spectrum of product (**5b**) formation at 52-hrs. Reaction conditions: (**4**):(**2b**):**$CuSO_4$**:**NaAscorbate 1:16:4:4.4.** 25°C.

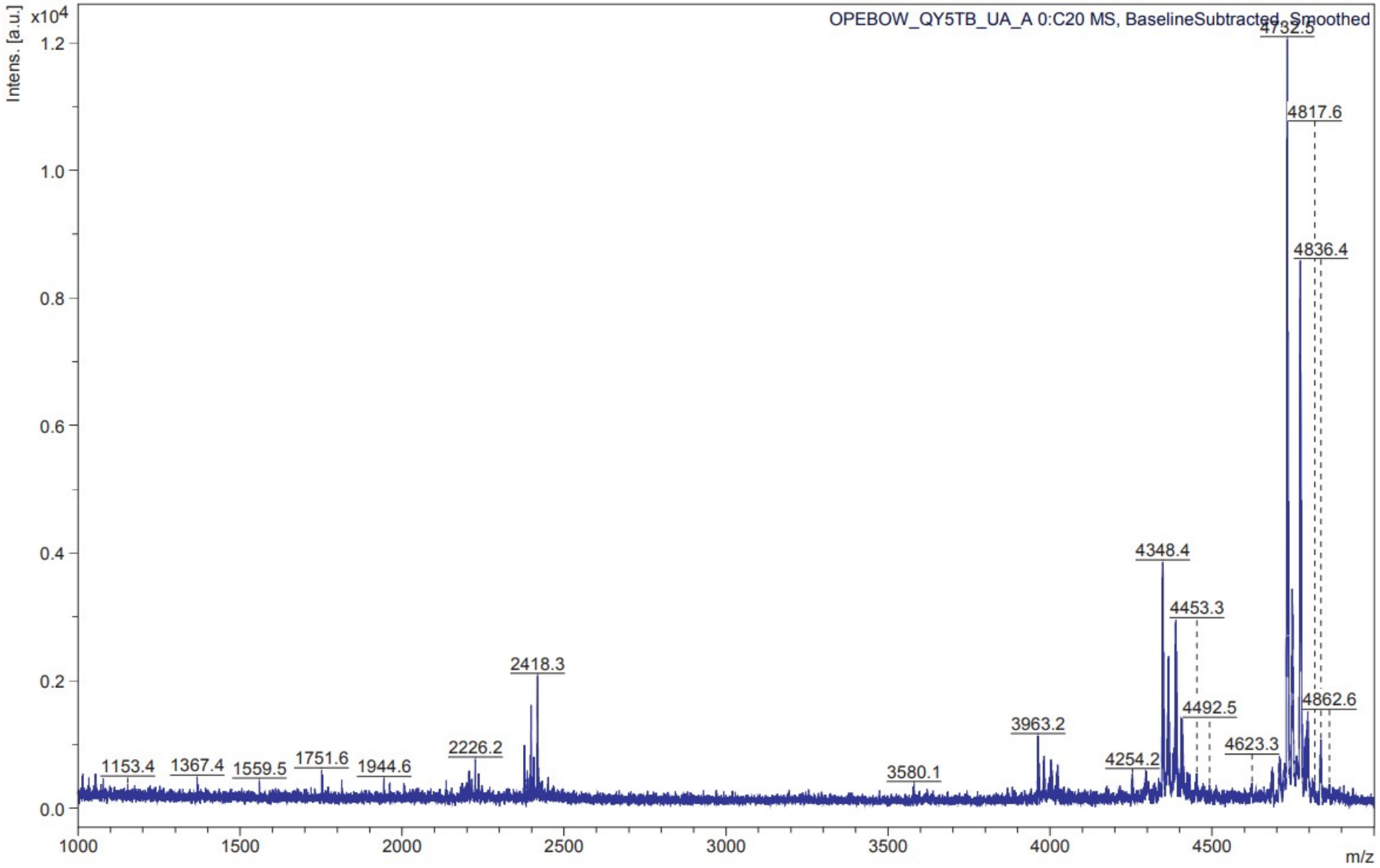

Figure S71 – MALDI-ToF mass spectrum of product (**5b**) formation at 144-hrs. Reaction conditions: (**4**):(**2b**):**$CuSO_4$**:**NaAscorbate 1:16:4:4.4.** 25°C.

17. Supplementary catalyst addition to pre-"clicked" 5a and 5b – (Figures S72-S73)

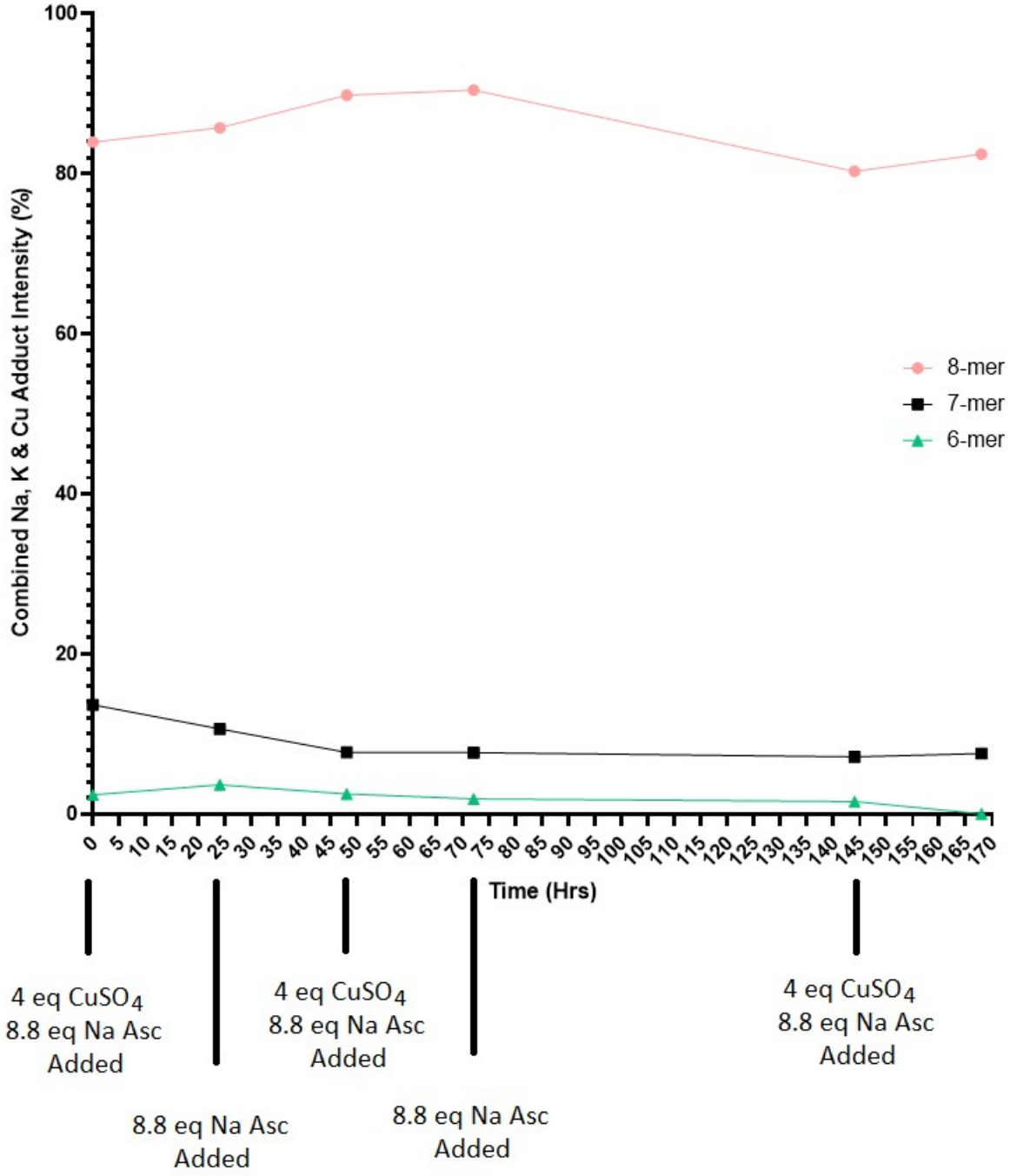

Figure S72 – Plot of MALDI-ToF MS Na, K and Cu adduct intensities (combined) during secondary "clicks" of (**5a**) with supplementary $CuSO_4$ and/or Na Ascorbate during the reaction where illustrated.

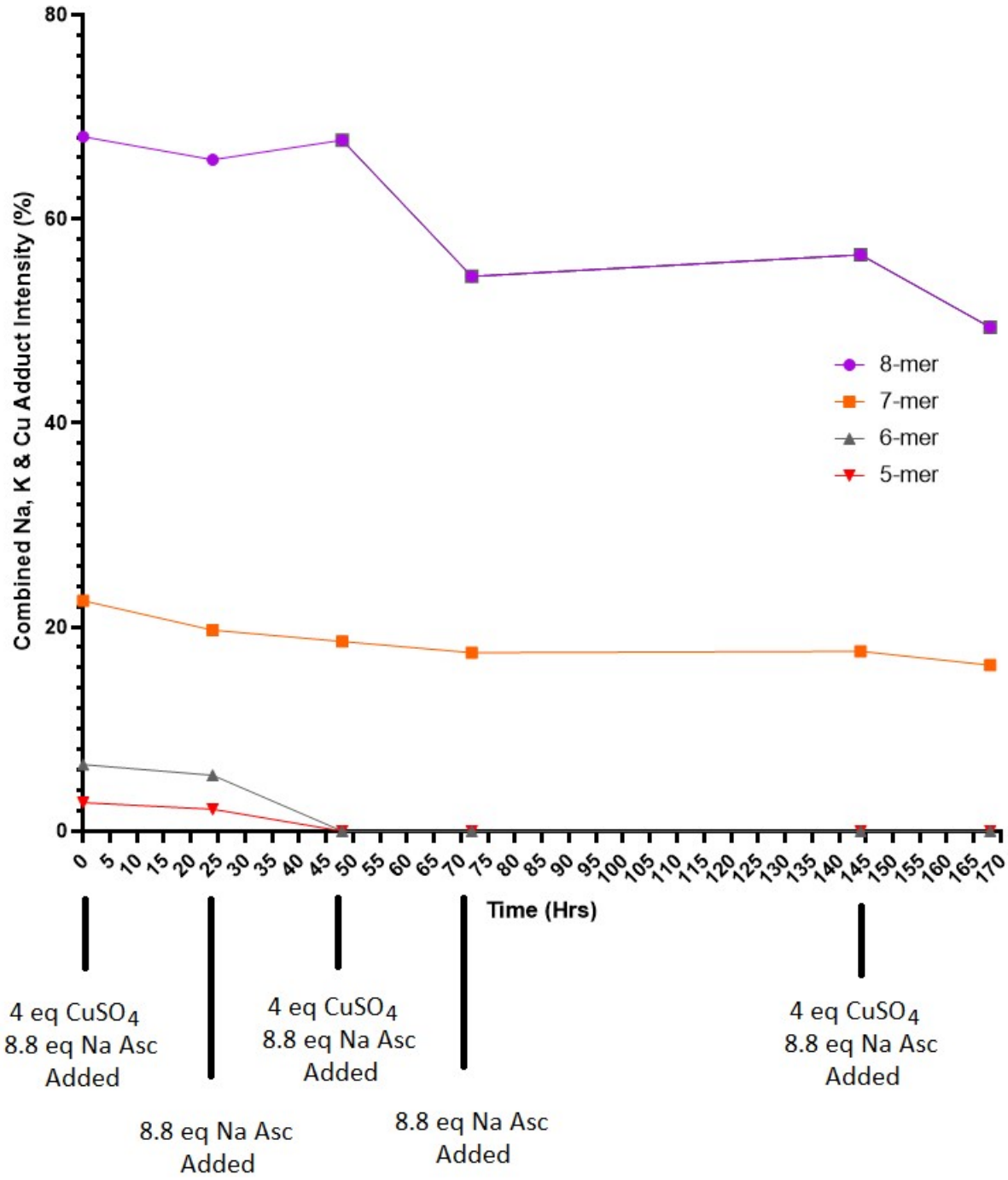

Figure S73 – Plot of MALDI-ToF MS Na, K and Cu adduct intensities (combined) during secondary "clicks" of (**5b**) with supplementary $CuSO_4$ and/or Na Ascorbate during the reaction where illustrated.

18. Double CuAAC “click” reactions of (5a) with periodic catalyst supplementation – (Figures S74-S75)

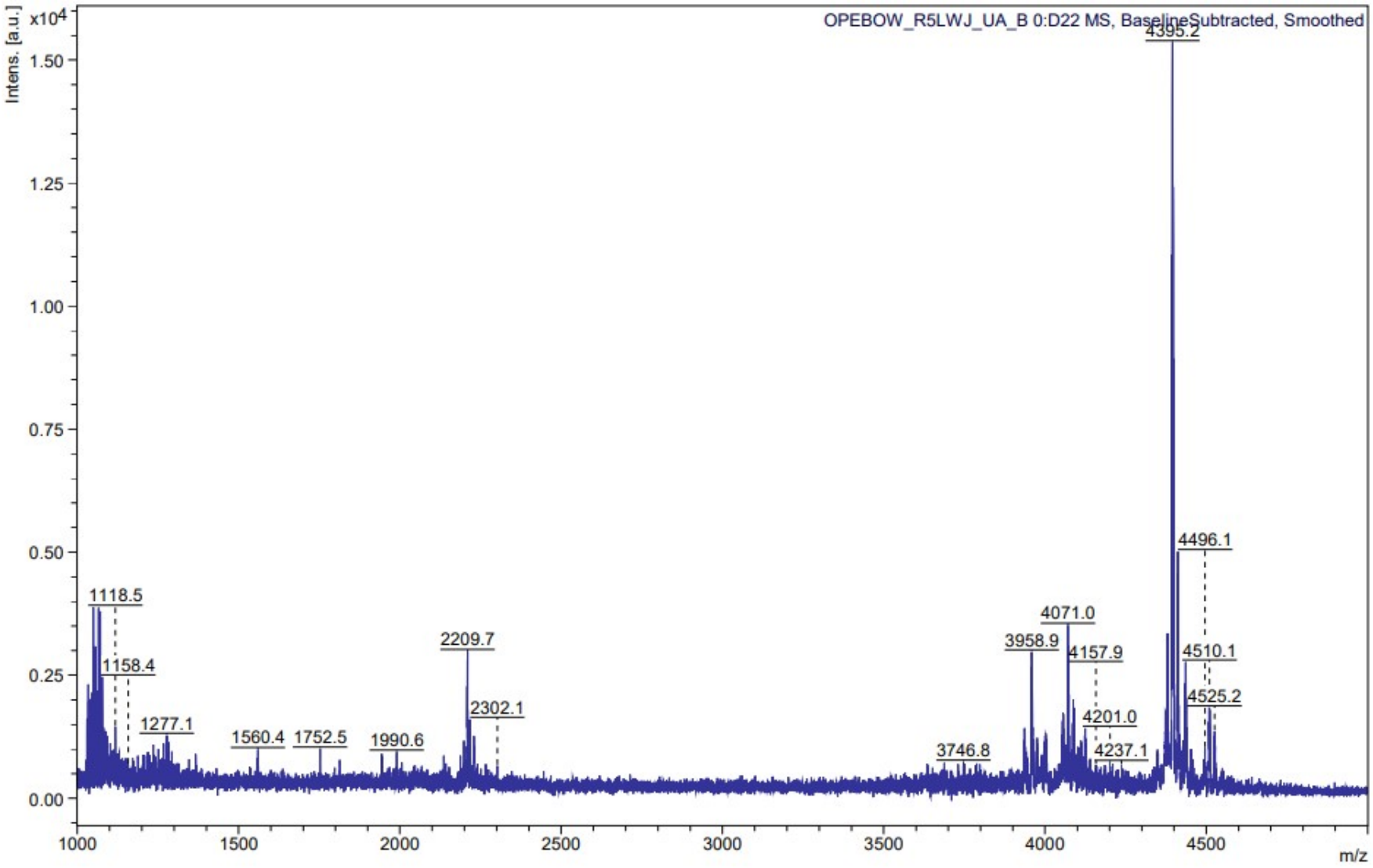

Figure S74 – MALDI-ToF mass spectrum of (**5a**) at 144-hrs during secondary ”clicks” of with supplementary $CuSO_4$ and/or Na Ascorbate during illustrating the product breakdown.

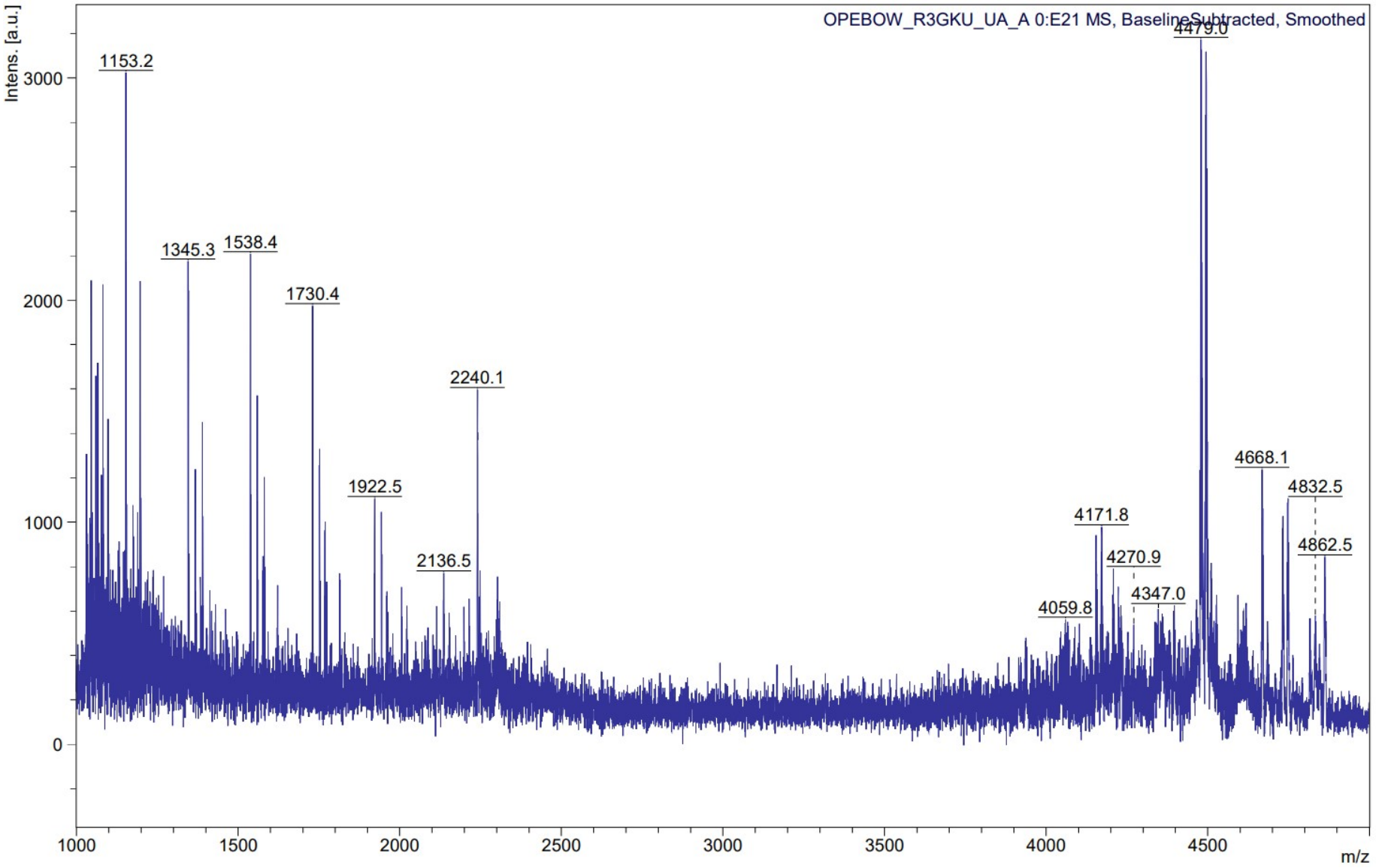

Figure S75 – MALDI-ToF mass spectrum of (**5b**) at 72-hrs during secondary “clicks” of with supplementary $CuSO_4$ and/or Na Ascorbate during illustrating the product breakdown.

19. EDS of crude products (5a) and (5b) – Pre-EDTA column filtration – (Tables S1-S2)

Table S1 - EDS summary table of elemental intensities from product (**5a**) pre-EDTA column filtration

Label	C	N	O	Na	Si	S	Cu	Total
Spectrum 1	50.02	20.48	16.95	1.44	4.70	1.97	4.43	100
Spectrum 2	47.76	20.98	24.82	1.27	2.63	0.60	1.95	100
Spectrum 3	54.75	22.44	17.92	0.46	2.36	0.58	1.49	100
Spectrum 4	51.90	16.96	17.00	1.33	5.44	1.88	5.49	100
Spectrum 5	64.31	14.91	13.51	0.69	2.90	1.15	2.52	100
Spectrum 6	47.37	20.57	23.97	1.78	2.96	1.18	2.17	100
Spectrum 7	48.03	19.83	23.17	1.87	3.14	1.31	2.64	100
Spectrum 8	48.87	19.69	22.20	2.00	3.24	1.31	2.69	100
Spectrum 9	49.00	18.35	22.22	2.12	3.66	1.52	3.13	100
Spectrum 10	47.70	19.71	24.13	1.76	3.12	1.23	2.34	100
Statistic	C	N	O	Na	Si	S	Cu	
Max	64.31	22.44	24.82	2.12	5.44	1.97	5.49	
Min	47.37	14.91	13.51	0.46	2.36	0.58	1.49	
Average	50.97	19.39	20.59	1.47	3.41	1.27	2.89	
Standard Deviation	5.22	2.16	3.90	0.55	0.95	0.46	1.21	

(m)**Label**	**C**	**N**	**O**	**Na**	**Al**	**Si**	**S**	**K**	**Fe**	**Ni**	**Cu**	**Total**

Spectrum 11	44.30	15.19	26.36	2.33	0.49	1.92	3.13	0.47	0.34	0.77	4.71	100.00
Spectrum 12	42.55	16.62	31.79	3.97	0.13	2.09	1.99	0.18	0.05	0.08	0.55	100.00
Spectrum 13	39.97	18.84	34.71	3.35	0.09	0.95	1.10	0.07	0.27	0.57	0.10	100.00
Spectrum 14	47.19	14.36	22.93	1.90	0.67	6.62	2.42	0.29	0.10		3.51	100.00
Spectrum 15	45.69	16.33	28.04	2.37	0.07	2.75	2.36	0.21			2.18	100.00
Spectrum 16	46.75	23.42	27.98	0.26		0.89	0.19	0.01	0.16	0.30	0.03	100.00
Spectrum 17	44.53	18.33	30.30	3.97	0.07	1.68	0.85	0.05	0.05	0.08	0.09	100.00
Spectrum 18	45.17	21.71	29.95	0.36	0.14	1.54	0.34	0.04	0.15	0.37	0.22	100.00
Spectrum 19	42.54	24.87	30.67	0.25		1.19	0.27	0.02	0.05	0.07	0.07	100.00
Spectrum 20	43.99	22.63	31.29	0.20	0.05	1.36	0.25	0.02	0.03	0.04	0.14	100.00
Statistic	C	N	O	Na	Al	Si	S	K	Fe	Ni	Cu	
Max	47.19	24.87	34.71	3.97	0.67	6.62	3.13	0.47	0.34	0.77	4.71	
Min	39.97	14.36	22.93	0.20	0.05	0.89	0.19	0.01	0.03	0.04	0.03	
Average	44.27	19.23	29.40	1.90	0.21	2.10	1.29	0.14	0.14	0.28	1.16	
Standard Deviation	2.16	3.70	3.25	1.55	0.23	1.69	1.09	0.15	0.11	0.27	1.71	

Table S2 - EDS summary table of elemental intensities from product (**5b**) pre-EDTA column filtration

20. Residual Cu and Na concentrations within (5a) & (5b) – (Figure S76)

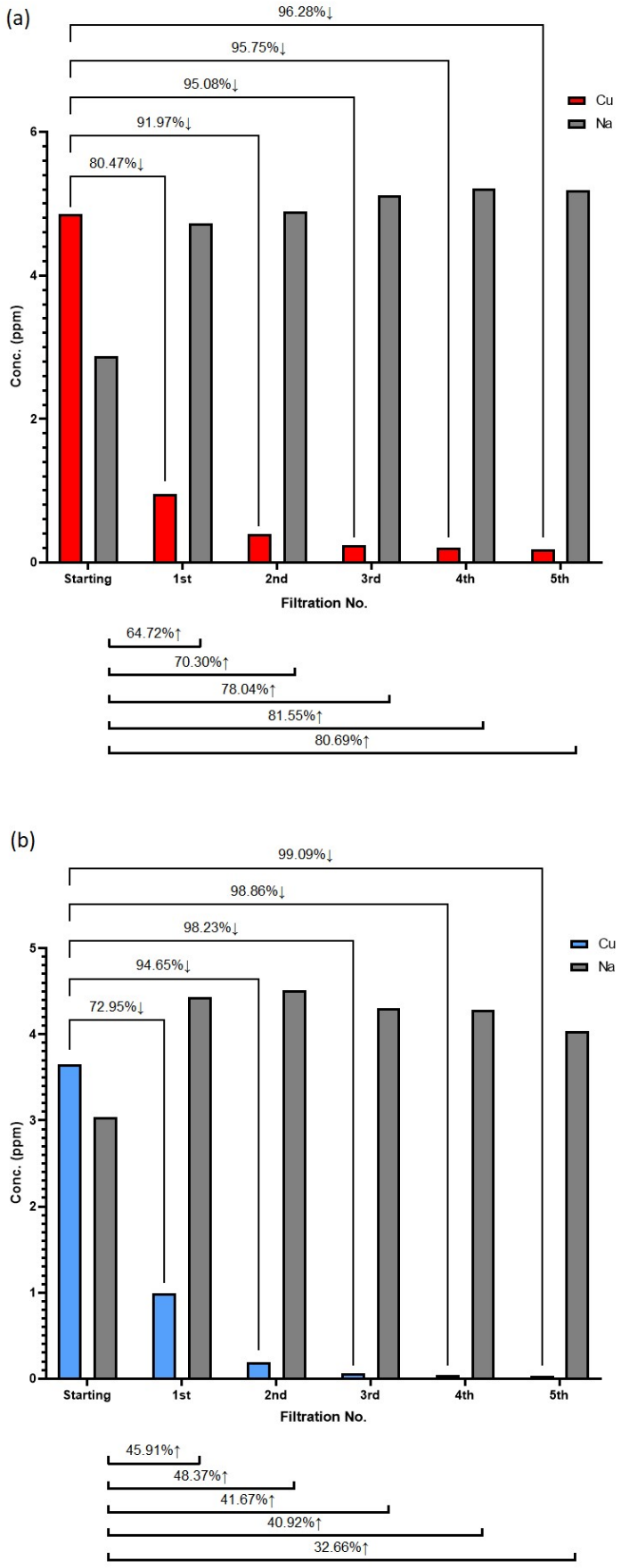

Figure S76 - ICP-OES measurement of residual Cu and Na concentration (ppm) within impure products (**5a**)(a) and (**5b**)(b), with subsequent Cu and Na concentrations following passage through EDTA-modified Amberlite® columns.